THE
PHYSICAL REVIEW
A Journal of Experimental and Theoretical Physics, Established by E. L. Nichols in 1893
VOL. 49, NO. 6 MARCH 15, 1936 SECOND SERIES

Cloud Chamber Photographs of Counter Selected Cosmic-Ray Showers

E. C. STEVENSON AND J. C. STREET, *Research Laboratory of Physics, Harvard University*
(Received January 24, 1936)

A detailed discussion is given of the appearance of cosmic-ray showers from a lead plate 1.3 cm thick in a large cloud chamber controlled by three G–M counters, one above and two below the chamber. Showers of photons were responsible for about half the triple coincident counts, but sprays of electrons from the lead accounted for the tripping of the lower counters in most of the other cases. Three-quarters of the single-centered electron shower sprays were due to electrons which traversed the upper counter and struck the lead from above. The remainder were due to nonionizing rays, presumably photons. Twenty-three photographs out of a total of a hundred seventy-four showed complex phenomena. The distributions of the showers according to size and the shower electrons according to angular spread are given.

WE have described in the form of a letter[1] some preliminary observations on the appearance of cosmic-ray showers obtained with an arrangement of counters and cloud chamber (Fig. 1) particularly selective to electron produced groups. A detailed description of the apparatus will appear in a separate publication. Here we summarize the results of a more extended study of the showers and related effects.

TYPES OF SHOWERS

The average coincidence counting rate with the arrangement of Fig. 1 was 0.162 count per min. making the average wait for a photograph about six minutes. 174 successful photographs were taken. In 94 of these the tripping of the lower counting units could be attributed to shower electrons from the lead. The remaining 80 (46 percent of the total) showed no electron showers below the lead. In 49 (27 percent) of the photographs not more than one straight electron track per picture was visible in the lower

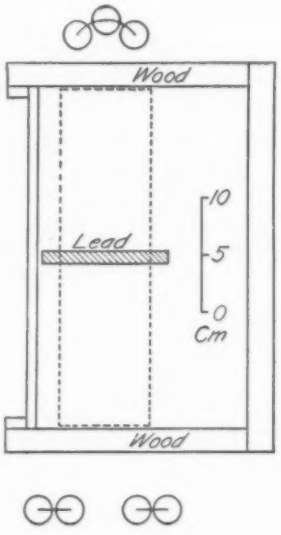

FIG. 1. Geometrical arrangement of counting tubes, cloud chamber and lead scattering block. The lead sheet is 34 cm long and 1.3 cm thick. The counters have a sensitive length of about 19 cm. Above the chamber are three tubes connected in parallel to form one unit, and below are two units, each with two tubes in parallel. A triple coincidence of the three units sets off the expansion.

[1] Stevenson and Street, Phys. Rev. **48**, 464 (1935).

FIG. 2. A shower of 22 rays produced by an electron. The slight displacement of the ray above the lead is due to an irregularity in the expansion, a fact which has been verified by stereoscopic photographs of straight rays.

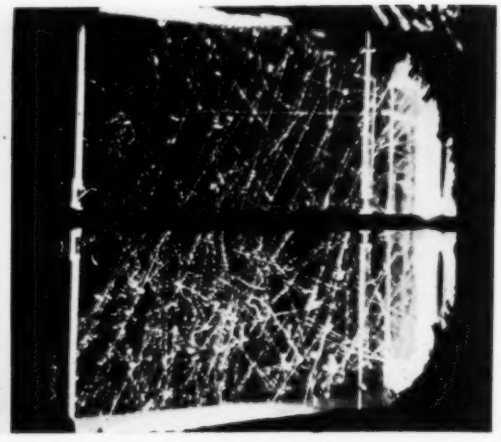

FIG. 3. The most complex shower phenomenon photographed. Several shower centers in the lead are evident.

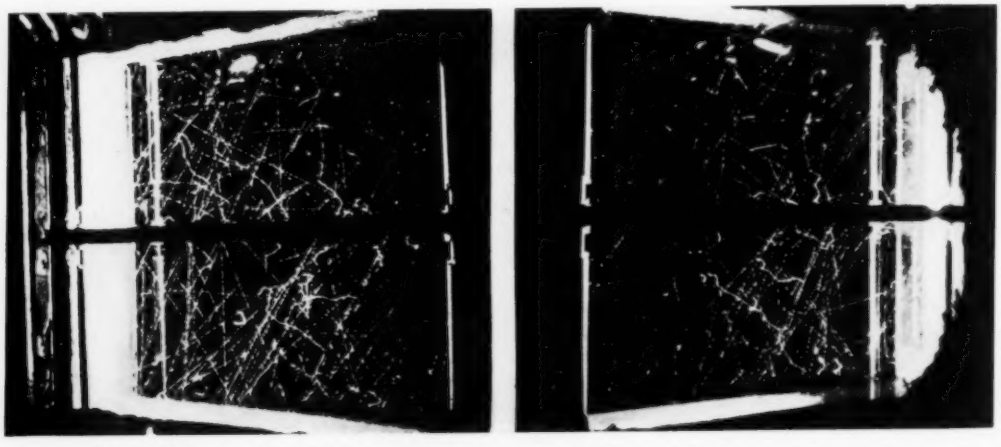

FIG. 4. A stereoscopic pair (each at 30° with the normal) showing another case of many associated rays incident from above.

section of the chamber. The tripping of the lower counters in such cases is probably due to electrons ejected from the walls of the counters by photon showers. In 14 of these cases an electron incident on the lead from above was either stopped or sharply deflected with the possible production of photons.

Of the 94 photographs showing electron sprays from the lead there were 71 with single shower centers, 17 with 2, and 3 with 3 centers. The 3 remaining photographs were of large bursts with many rays entering the chamber from above and an undetermined number of "secondary" showers produced in the lead. Figs. 2, 3, and 4 illustrate certain interesting types. (See earlier letter for other illustrations.) The 71 single showers may be further classified into three groups; 48 produced by electrons, 17 by some nonionizing raidation which is assumed to be of photon character throughout this paper, and 6 whose centers fall outside the lighted area of the lead. The 17 double-center showers consist of 6 due to 2 electrons, 1 due to 2 photons, 7 due to 1 electron and 1 photon, and 3 with one of the

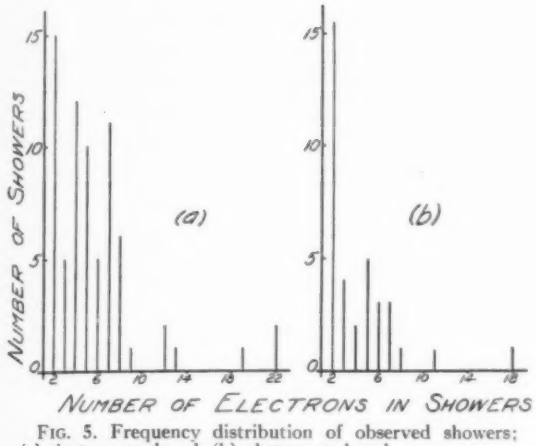

FIG. 5. Frequency distribution of observed showers; (a) electron produced, (b) photon produced.

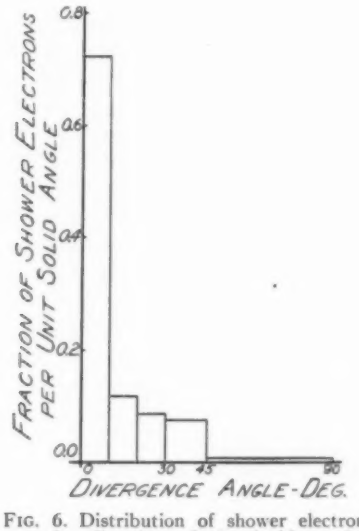

FIG. 6. Distribution of shower electrons about the direction of the incident electron.

centers out of view. The three triple-shower groups are particularly interesting, for in each case two electrons enter on almost parallel paths and each produces a shower in the lead. All show an additional photon produced shower. A photograph of such a triple group was reproduced in the earlier letter.[1]

The mechanism of discharge of the upper counter in those cases where no electron entered the top of the cloud chamber is not evident from our data. There were 22 such cases. Possibly soft secondaries were produced by photons in the walls of the top counter. The latter may have been incident from above or due to back scattering from the lead. The assumption of a soft electron with too low energy to penetrate the top of the chamber is an alternative explanation. Back scattering of electrons was not an appreciable factor, although five pairs were observed traveling up from the lead. Three of these occurred in one photograph (Fig. 2).

CHANCE OF THE PRODUCTION OF A SHOWER BY AN ELECTRON

A consideration of the multiple showers leads to an estimate of the probability of production of a shower by an electron. On the photographs showing one or more showers we find 72 electron tracks, in addition to one shower producing element per picture, which either traverse or terminate in the lead within the field of view. If the average chance of production of a shower by one of these electrons is P the number of additional showers expected from them would be $72P$. Actually 17 of the 72 electrons in question gave rise to showers. Thus $P \sim 0.24$. In this rough calculation no account has been taken of the enhanced probability of recording a multiple shower. This correction should not reduce P to a value less than 0.08 since in at least one-third of the multiple shower cases any one of the individual showers would have been recorded. Anderson *et al.*,[2] however, found that the total shower phenomena from a thousand single electrons passing through a cm of lead consisted of but two pairs. Thus the electrons we observe which are associated with a shower-producing radiation must have a much greater chance of producing showers than electrons taken at random in the cosmic radiation.

THE SHOWER ELECTRONS

The size distribution plots of the observed showers are given in Fig. 5. The true distribution can be obtained by correcting for the differential selectivity of the counter arrangement for various

[2] Anderson, Millikan, Neddermeyer and Pickering, Phys. Rev. **45**, 352 (1934).

sized showers. This calculation for the present arrangement is extremely difficult and we have found no satisfactory way to obtain it.

The angular distribution of the shower electrons about the directions of the incident particles for the electron produced showers has been determined and is given in Table I. When the data are transformed to express the relative numbers of secondaries per unit solid angle, the plot of Fig. 6 results. A comparison of the angular distributions for large and small showers was made by dividing the showers into two groups, those of more than and those of less than seven particles. This choice placed approximately the same number of shower electrons in each group. Within the expected statistical fluctuations the distributions were the same.

TABLE I. *Number of shower electrons in the angular range.*

0–10°	10–20	20–30	30–45	45–90	> 90
113	56	65	123	64	1

SOME FURTHER CONSIDERATION OF THE PROCESSES INVOLVED IN SHOWER PHENOMENA

The above data show clearly the important role played by photon sprays in the shower phenomena. In more than half of the photographs the explanation of the tripping of one or more of the counters required the assumption of such photon sprays. Since a gamma-ray photon traversing a counter has a chance of about 0.01 of exciting it, large numbers of photons must be involved. This is in agreement with the conclusions of Geiger[3] and his co-workers from counter observations. However, since a considerable fraction of the coincidences observed with the arrangement of Fig. 1 could be explained on the basis of the direct action of electrons alone, the influence of this mechanism should not be overlooked in interpreting counter studies of showers.

From our data nothing can be said concerning the mechanism by which an electron gives rise to shower electrons. The incident electron may actually produce one or more photons which in turn eject the shower particles.

[3] Geiger and Zeiler, Zeits. f. Physik **97**, 300 (1935); Geiger, Erg. exakt. Naturwiss. **14**, 42 (1935).

MARCH 15, 1936 PHYSICAL REVIEW VOLUME 49

Contact Potential Measurements on Tungsten Filaments

DAVID B. LANGMUIR,* *George Eastman Research Laboratory of Physics, Massachusetts Institute of Technology*

(Received January 29, 1936)

Changes in contact potential of the surface of a tungsten filament have been measured by using a tube containing two filaments. Changes were produced by varying the amount of thorium on the surface, and by varying the temperature. (a) *Changes produced by activation.* When electron emission (i) with very low accelerating fields is compared with the contact potential (V) measured on the same surface and at the same temperature, the theoretical law $d\ln i/dV=e/KT$ is obeyed. If emission under influence of higher fields, or contact potential at temperatures different from that of emission are used for comparison agreement does not exist. (b) *Changes produced by temperature variations.* Both activated and deactivated thoriated tungsten surfaces showed an increasingly negative contact potential (increasing work function) with rising temperature, the activated surface having the larger rate of change. The difference between the temperature coefficients of the activated and deactivated surfaces observed was 3.3×10^{-4} volt/deg. A relatively large anomalous effect observed at temperatures below the emission range is ascribed to a reversible gas reaction. Pure tungsten seems to show a temperature coefficient of opposite sign, indicating a decreasing work function with rising temperature.

* Now employed by RCA Manufacturing Company, Research and Development Laboratory, Radiotron Division, Harrison, New Jersey.

Introduction

RICHARDSON'S equation[1] for the emission of electrons from metal surfaces has been discussed by many workers. A modified form of this equation which takes into account certain factors which are neglected in the simpler law may be written

$$i = 120(1+S)\bar{D}(T)T^2\epsilon^{-b(T)/T}. \quad (1)$$

Here i is the current per sq. cm of apparent area; 120 amp./cm^2 deg.^{2} is Dushman's universal emission constant;[2] S is a function of the surface geometry,[3] the crystal orientation, the surface contamination[4] and the electric field and may be positive or negative. $\bar{D}(T)$ is the average transmission coefficient of electrons within the metal at the surface,[5] and T the absolute temperature. $b(T)$ is proportional to the true work function of the surface, and according to the Fermi-Dirac statistics, $b=(W_a-W_i)/k$ where W_a represents the height of the potential barrier at the metal surface and W_i a "normalization" constant depending on the number of electrons per unit volume in the metal. Both of these quantities may be functions of the temperature.[6, 7] At very low accelerating fields the effect of irregularities in the surface becomes less important, however, and at zero field the value of S should approach zero. The transmission coefficient $\bar{D}(T)$ has been discussed by Nottingham,[5] who finds that for simple thoriated tungsten surfaces its value is independent of the state of activation of the surface.

If i_1 and i_2 equal the zero-field emission from a tungsten surface containing different amounts of thorium at a temperature T, then taking these considerations into account

$$\ln i_1 - \ln i_2 = -(W_a-W_i)_1/KT+(W_a-W_i)_2/KT. \quad (2)$$

Since the interior of the metal is the same for both surfaces, $(W_i)_1=(W_i)_2$ and

$$\ln i_1 - \ln i_2 = ((W_a)_2-(W_a)_1)/KT.$$

But $(W_a)_2-(W_a)_1=eV_{12}$ where V_{12} is the contact potential difference between the two surfaces, so the theory predicts that as the surface of a given metal varies, the logarithm of the electron emission should be a linear function of the contact potential difference between the states of the surface.

The contact potential of thoriated tungsten has been investigated by Kingdon and I. Langmuir,[8] and by Patai.[9] The former workers compared their results with the published emission constants for thoriated and pure tungsten, but found a discrepancy considerably larger than the experimental error.

From the manner in which both contact potential and emission measurements were made it could hardly be expected that an agreement between them would exist. The contact potentials were measured on a different filament, at a different time, and in a different tube from the emission experiments, so differences in activation may have existed. The contact potentials were measured at room temperature. The emission constants were evaluated by extrapolating relatively high field emission data. The deactivated state of the filament is probably appreciably different from pure tungsten.[10]

The aim of this research was to repeat these experiments eliminating the sources of error mentioned, and to obtain as much information as possible about the dependence of contact potential on temperature.

Experimental Method

A diagram of the tube used for most of the measurements is shown in Fig. 1. This was constructed in the way developed by Taylor.[11] The inside diameter was 30 mm and the length of the central section 5 cm. One of the two filaments was tungsten thoriated "E" wire 0.0125 cm in

[1] O. W. Richardson, *Emission of Electricity from Hot Bodies*, second edition (Longmans, Green, 1921).
[2] S. Dushman, Phys. Rev. **21**, 623 (1923). The constant 60 amp. per sq. cm per degree must be doubled to include the effect of electron spin.
[3] L. Tonks, Phys. Rev. **38**, 1030 (1931).
[4] R. P. Johnson and W. Shockley, Phys. Rev. **49**, 436 (1936).
[5] W. B. Nottingham, Phys. Rev. **49**, 78 (1936).
[6] P. W. Bridgman, *Thermodynamics of Electrical Phenomena in Metals* (Macmillan, 1934).
[7] J. A. Becker and W. Brattain, Phys. Rev. **45**, 694 (1934).
[8] I. Langmuir and K. H. Kingdon, Phys. Rev. **34**, 129 (1929).
[9] E. Patai, Zeits. f. Physik **59**, 697 (1930).
[10] W. Brattain and J. A. Becker, Phys. Rev. **45**, 694 (1934).
[11] J. B. Taylor and I. Langmuir, Phys. Rev. **44**, 6 (1933).

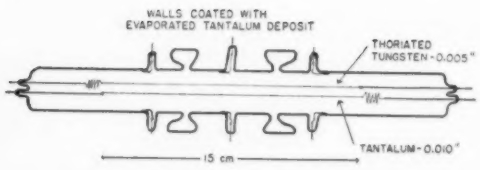

FIG. 1. Diagram of experimental tube.

diameter, 15 cm long. The other was tantalum 0.025 cm in diameter, also 15 cm long. A potential lead was attached to the end of the tungsten at which a spring[12] was mounted for keeping the filament taut.

Before putting the filaments into the final tube they were given a preliminary heat treatment. The tungsten was heated 80 minutes at temperatures gradually rising to 2200°, and then for several minutes at 2700°.

The tantalum was heated with gradually increasing currents up to 5 amperes[13] held for an hour at this temperature, and given short flashes up to 5.65 amp.

The glass jacket of the final tube into which these filaments were then sealed, contained no metal parts except the leads and 0.005-inch platinum wires sealed flush with the glass. No conducting coating was placed on the walls before evacuation.

The tube was sealed off after several hours of alternate baking (500°C) and flashing of filaments. The tantalum filament was then run at 5.2 amperes for $6\frac{1}{2}$ hours, at the end of which time a conducting coating had been deposited on the walls. This coating constituted the outer electrodes of the tube. Before making any thermionic measurements the tungsten was flashed at 2900° to remove the layer of tantalum which must have settled upon half of it.

The pressure in the tube could not be measured absolutely, but the positive ions produced were measured. Electrons flowed from one filament to the two end cylinders at +100 volts. The center cylinder and other filament were made −15 volts relative to the filament and collected a current of positive charges which was proportional to the electron current. The ratio of ion to electron current was 8×10^{-6}.

[12] K. B. Blodgett and I. Langmuir, Rev. Sci. Inst. **5**, 321 (1934).

[13] A. G. Worthing, Phys. Rev. **28**, 190 (1926). See correction **28**, 1331 (1926).

The thermionic characteristics of the tube showed great steadiness. From the first activation the thoriated emission was steady and reproducible. Over periods of several days the saturation emission stayed constant within 1 percent.

For studying the emission characteristics of the thoriated filament circuit *A*, Fig. 2 was used. In this way the tube was used as a conventional guard-ring type thermionic tube.

For studying the contact potential circuit *B* or *C* was used. The method involved measuring the electron current to the filament whose surface was to be studied as a function of the voltage on this filament. After obtaining such a characteristic curve the activation of the surface was changed and exactly the same procedure repeated. The results consist of a series of current-voltage curves identical except for a shift parallel to the voltage axis.

The errors most likely to be present in this system of measurement are those caused by a

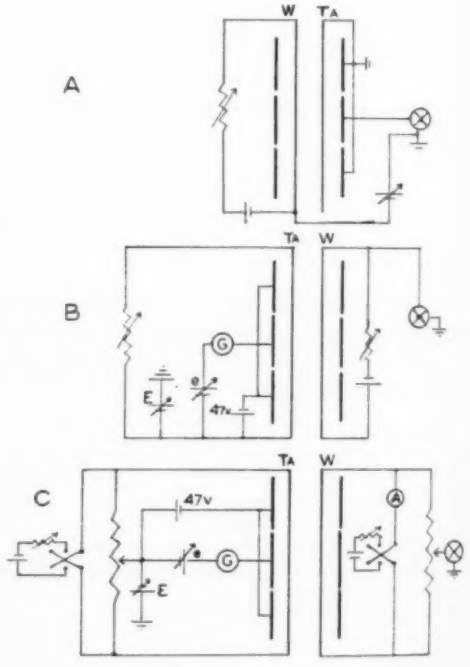

FIG. 2. Circuit diagrams. For studying the electron emission of the tungsten filament circuit *A* was used, while contact potential measurements were made with *B* or *C*.

changing geometrical arrangement due to shifts in the position of the filaments, and by changes in the contact potential of other surfaces than the one being studied. The first source of error was shown to be absent by observing the filaments at various temperatures in a cathetometer telescope. The exactness of parallelism of the curves was further evidence.

The second source of error can be eliminated by making the measurements in the proper manner. Fig. 3 shows a family of curves in which all potentials are held constant except that of the central cylinder surrounding the filaments. The ordinates represent the current collected by the tungsten filament, and it is seen that one or more maxima exist. At these points the current to the filament is independent of the potential on the surrounding cylinder. When measuring contact potentials the current was always adjusted to this maximum value, by varying the cylinder potential, before reading. Changing surface conditions on the end cylinders could still introduce errors, but experiment showed that a change in contact potential on these cylinders of 0.04 volt was necessary to cause an error in the measurement of 0.01 volt. The contact potential of the center cylinder never changed by so great an amount as this during one series of measurements, however, so it seems a safe assumption that variations on the end cylinders are not an appreciable source of error.

The contact potential of the emitting filament also had to remain constant if an accurate result was to be obtained. This condition was checked by observing the total emission from the cathode filament before each contact-potential run. This emission remained constant within 1 percent over periods of weeks if the thoriated tungsten filament was kept below a temperature at which evaporation of thorium took place. If the thoriated filament was flashed so as to deactivate it an increase of emission from the other filament of a few percent was observed. In this event the emission could be restored to its former value by flashing this filament at a suitable temperature.

It might be mentioned that a prolonged flashing of a thoriated filament near a tantalum filament can increase the tantalum emission 1000-fold.

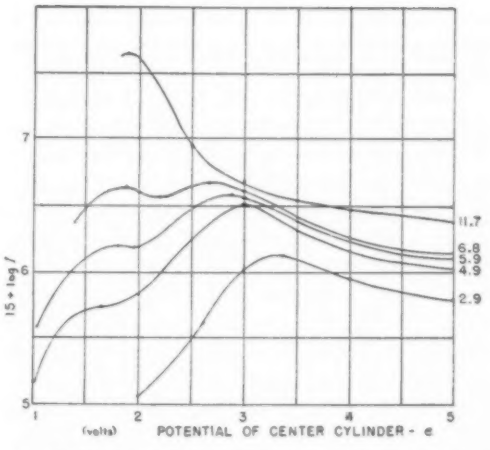

FIG. 3. Curves showing current to the tungsten filament as a function of the potential of the surrounding cylinder, for various values of the applied potential difference (E) between the two filaments. The end cylinders were held at -47 volts to the tantalum cathode. (Circuit B, Fig. 1.)

RESULTS

Fig. 4 shows some typical curves of emission from the thoriated filament as a function of voltage, measured with circuit A. The zero field emission was estimated from the knees of the curves.

A typical family of curves from which contact potential differences were measured is shown in Fig. 5. Through one of the sets of points a curve was drawn as accurately as possible The displacement of the other points from this curve along a direction parallel to the voltage axis was then measured with a scale. The displacements rarely deviated by more than 0.01 volt between top and bottom of the curves.

The steepness of the curves is essential to accurate measurements. The field distribution in the tube was such as to give a much more rapid variation of current with voltage than is present in most vacuum tubes. Currents below the space-charge-limited range were used.

The relation between emission and contact potential is shown in Fig. 6. The deactivated state is chosen as a point of reference, and its contact potential arbitrarily set at zero. The abscissae show the differences in contact potential from this state observed for surfaces activated to varying degrees. The ordinates represent the logarithm of the emission at zero

field. Four different temperatures were used, and the contact potential and emission measurements were made at the same temperatures.

The lines are drawn with slopes $11{,}600/2.3T$, where T is the temperature of measurement.

The importance of measuring the emission at zero field and the contact potential difference at emission temperature is shown in Fig. 7. Here the circles show another set of measurements similar to those of Fig. 6, and the solid line is drawn with the slope corresponding to the temperature of measurement of both quantities. The squares show the curve obtained by comparing contact potential at emission temperature with emission under a 140-volt applied field. The crosses show zero field emission as a function of contact potential difference at room temperature.

Dependence of Contact Potential on Temperature

The variation of contact P.D. with temperature presents a more difficult problem experimentally than the measurement of contact potential differences at constant temperature. It is difficult to change the temperature of a filament without passing current through it, and the voltage drop produced is likely to be greater by a large factor than the expected change in contact P.D. The measurements presented here were made with a d.c. drop along the filament, and are subject to criticism on that account, but that they are fairly accurate at least in the low temperature range is indicated by the tube characteristics.

It would be expected, for example, that curves of the type shown in Fig. 5 taken with a drop along the filament would differ in form from one taken without the drop. No such difference was observable with moderate heating voltages. Reversing the direction of current through the thoriated filament caused no change in the form of the characteristic at such voltages. The evidence seemed to indicate that the current which reached the thoriated collecting filament reached it only along a small part of its length, or along a region in which the current-voltage variation was linear.

Circuit *C* was used for the measurements. The sliding contact on the drop wire across the filament was adjusted so that reversing the direction of the heating current caused no change in the thermionic current collected. This adjustment varied as the heating voltage changed and was tedious, and in most of the measurements the following procedure was adopted. A convenient

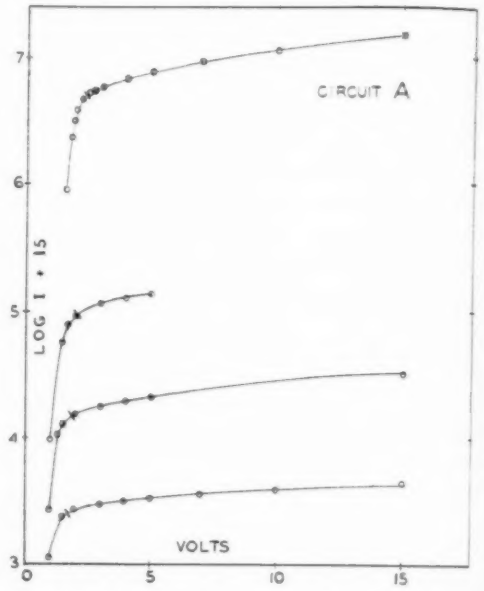

Fig. 4. Emission from the tungsten filament as a function of the voltage applied to the surrounding cylinders. (Circuit *A*, Fig. 1.)

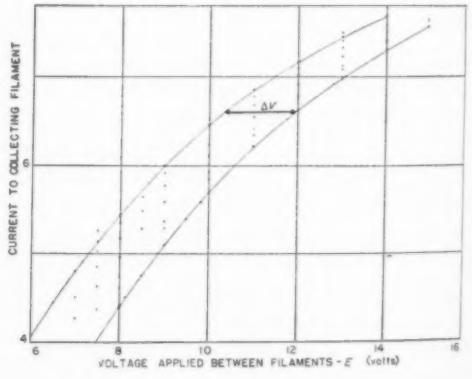

Fig. 5. Curves from which contact potential is measured showing current collected by the tungsten filament as a function of the voltage applied to this filament. The points show data for eight states of activation. Horizontal displacement represents contact P.D. (Circuit *B*.) The ordinates represent $\log_{10} I+15$.

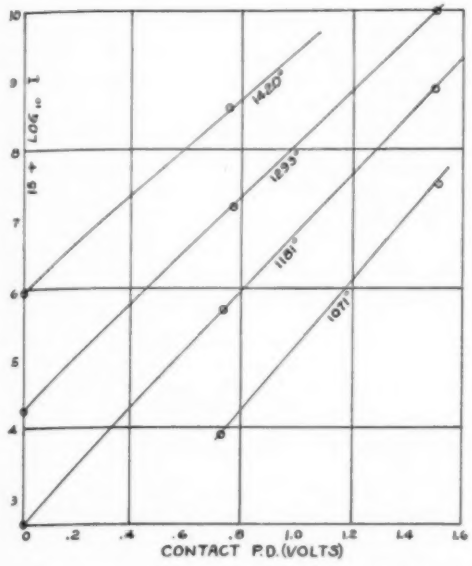

FIG. 6. Logarithm of electron emission plotted against contact P.D. The deactivated surface is arbitrarily chosen as zero point for the abscissa. Zero field electron emission is plotted, and the contact P.D. and emission were measured at the same temperature. The solid lines are drawn with slopes equal to $e/2.3kT$.

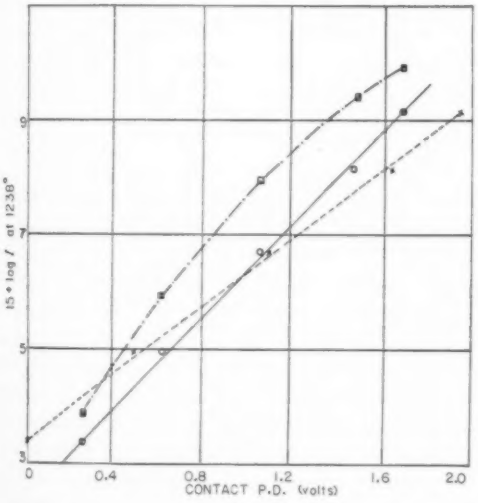

FIG. 7. Curves showing the importance of temperature and electric field in comparison of contact P.D. and emission. Circles show zero field emission at 1238°K plotted against contact P.D. at same temperature. Crosses show the same but with contact P.D. values obtained at room temperature. Squares show emission with 140-volt applied potential plotted against contact P.D. at 1238°. The solid line has the theoretical slope.

point on the curve of Fig. 5 was chosen, and the current i collected by the thoriated filament set to the chosen value i_0 by varying the potential E applied to this filament. The filament was then heated with the heating current A. E was readjusted to make $i=i_0$. Then A was reversed, and E adjusted again to make $i=i_0$. If E_0 is the original value of E (with the filament cold) and E_1 and E_2 the two values with the filament hot, the contact potential difference between the cold and hot surfaces was calculated by the formula

$$\Delta V=(E_1+E_2)/2-E_0.$$

At low temperatures where the voltage drop along the filament cannot cause any appreciable error the accuracy of the results is limited by uncertainties in the temperature scale of the filament. The resistivity and emissivity of tungsten at low temperatures has been determined,[14] but the application of these results to this problem is difficult. The nearness of the other hot filament, and the losses due to leads whose temperature is unknown cause uncertainties. The temperatures below 900° have been determined by extrapolation, with the low temperature data as a guide, but results in this range must be considered as of a qualitative nature.

Fig. 8 shows results obtained with a thoriated filament in various states of activation. To bring all the curves on the same graph each is shifted vertically by an amount corresponding to the contact P.D. at room temperature so that zero corresponds arbitrarily to the condition of each surface with zero heating current.

The curves in the high temperature range show behavior to be expected from measurements of emission,[6, 7] namely, a slow increase of work function with temperature, the magnitude being of the order of magnitude of 10^{-4} volt/degree. At lower temperatures a much more pronounced and unexpected change is evident. The work function of the deactivated state decreases abruptly by over 0.3 volt when the temperature rises from room temperature to approximately 700°. The activated state shows also a rapid variation, but in reversed direction. Intermediate states of activation show smaller variations, but with a more complex form.

[14] I. Langmuir and J. B. Taylor, J. O. S. A. **25**, 321 (1935).

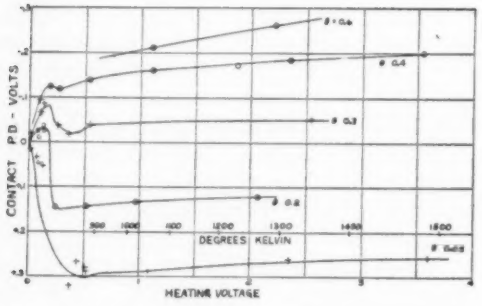

FIG. 8. Variation of contact P.D. with temperature of thoriated tungsten filament. Approximate values of surface coverage are shown. Contact P.D. at room temperature is taken as zero point for each curve.

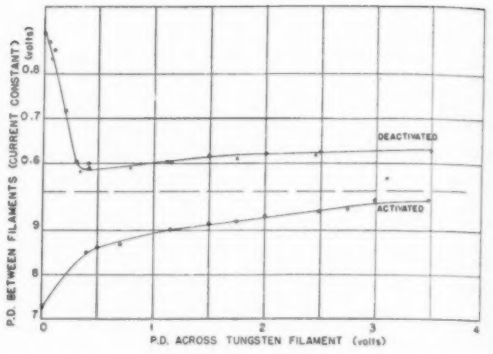

FIG. 9. More accurate curves of contact P.D. against heating voltage.

That this low temperature effect is due to a gas reaction seems probable. The surface of the filament seems to be in equilibrium with some gas or vapor which increases the work function of deactivated tungsten and decreases that of activated tungsten. This is analogous to the behavior of oxygen,[15, 16] although it does not seem that the gas can be oxygen in this case, since it leaves the filament at such a low temperature.

When the filament was allowed to cool from over 1000°K, the reaction proved to be reversible. The contact potential always returned to within 0.02 volt of its original zero value. The deactivated condition returned to this value in a few seconds, as fast as the filament could cool, but the activated state showed a decided time lag, requiring about half an hour to return to zero.

An interesting aspect of the phenomenon is the fact that it is unobservable by electron emission measurements. The emission was steady and reproducible throughout. The fact that the normal behavior of a thoriated surface was observed makes it of interest to observe the contact potential variations of the surface in the higher temperature range. Fig. 9 shows curves on the activated and deactivated states plotted as contact potential difference *versus* heating voltage. Fig. 10 shows the same data with temperature as abscissa. The deactivated state shows a coefficient of 1.6×10^{-4} volt/degree, the work function increasing with temperature. The activated state has a coefficient of 5.2×10^{-4} volt/degree. The difference between these values should be more significant than the values themselves, as errors due to voltage drop along the filament should be the same for the two states and should subtract out. This difference is 3.6×10^{-4} volt/degree. This agrees well with Nottingham's results.[5]

The surface of a deactivated filament[17] probably contains an appreciable amount of thorium and will not show characteristics identical with those of pure tungsten. For this reason a tube was built containing a pure tungsten (218 wire) filament. The other filament was thoriated *E* wire. Both were 0.0125 cm in diameter and about 15 cm long. The cylinders were of sheet tantalum 2 cm in diameter.

The tube was treated on the pumps for several days, baking at 400°C, heating the metal cylinders to red heat by high frequency, and flashing the filaments. Before sealing off two getter tablets were flashed, and after seal-off three auxiliary tungsten (thoriated) filaments were glowed at high enough temperature to cause evaporation. In spite of these precautions the emission of the thoriated filament when activated showed a tendency to drift, and it was necessary to immerse the tube in liquid air during measurements. When this was done thermionic effects were stable enough to make measurements feasible.

To avoid possibility of error due to surface contaminations a contact potential reading ob-

[15] K. H. Kingdon, Phys. Rev. **24**, 510 (1924).
[16] A. L. Reimann, Phil. Mag. **20**, 134 (1935).
[17] A. L. Reimann, *Thermionic Emission* (Wiley & Sons, 1934).

tained with the filament hot was compared immediately with one measured with zero heating current. The filament was then flashed for a few seconds at 1800° and the zero heating current reading checked. Then a new value of heating current was chosen and the cycle repeated. In this way the arbitrary zero point from which thermal changes of contact potential were measured was checked constantly throughout the experiment. This zero value of contact potential showed no measurable drift during the interval (at most a few minutes) required for a measurement at one temperature. Leaving the filament cold for longer times caused it to become about 0.3 volt more negative. Flashing restored it immediately to the more positive value.

The temperature scale in this experiment is even more indefinite than in the previous one. The liquid air must have caused a pronounced temperature gradient along the filament even with no heating current, and the lead losses were more important and more indeterminate than before.

The results obtained are shown in Fig. 11. The sign of the temperature coefficient observed is opposite to that found with the thoriated filaments, and indicates a decreasing work function with rising temperature. The magnitude of the change observed agrees within the rather large experimental error with that predicted by Nottingham from studies of emission.[5]

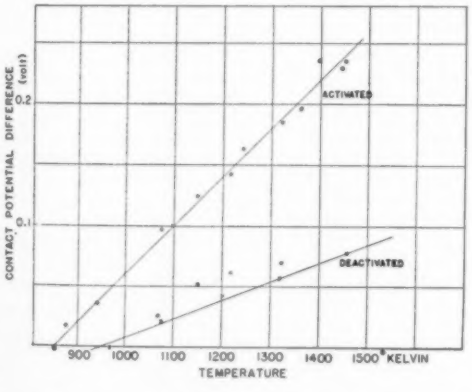

FIG. 10. The curves of Fig. 9 plotted with temperature as abscissa.

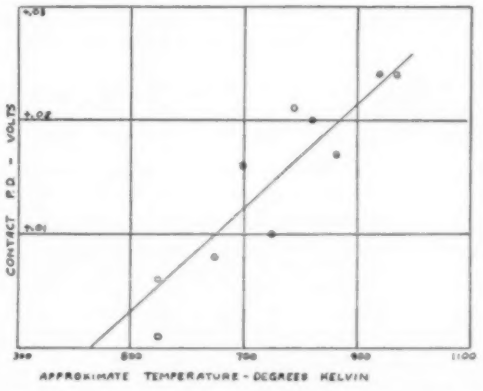

FIG. 11. Variation of contact P.D. of pure tungsten with temperature. The line is drawn with slope 4.3×10^{-5} volt/degree. This is the value assigned by Nottingham,[5] and is used here as it appears to be the only published value of this temperature coefficient.

As a check on the unexpected direction of this shift an attempt was made to evaporate thorium from the other filament in the tube onto the tungsten surface, to see whether the thoriated surface so produced showed an opposite effect as should be expected. This seemed to show a decrease in the negative slope of the line. The amount of thorium deposited represented only a small percent coverage, however, and the experiments were discontinued before a more thorough test could be made.

The author does not consider the temperature coefficients presented here conclusive. It would be highly desirable to study the problem more thoroughly, eliminating any doubts caused by voltage drop along the filament, and with unimpeachable vacuum conditions. This is part of the research program at the Massachusetts Institute of Technology.

The author acknowledges gratefully the constant guidance of Professor W. B. Nottingham. He also is indebted to the Research Laboratory of the General Electric Company for building one of the tubes, to Mr. J. E. Ryan for assistance in glass-blowing, and to Mr. Ralph Johnson for his help on many occasions.

An Electron Microscope for Filaments: Emission and Adsorption by Tungsten Single Crystals[1]

R. P. JOHNSON AND W. SHOCKLEY, *George Eastman Research Laboratories, Massachusetts Institute of Technology*

(Received January 6, 1936)

A new and simple electron microscope has been designed for small cylindrical filaments. Die marks are found to be prominent in the electron images of all drawn wires. The activation of thoriated tungsten has been studied. Electron emission from single crystals grown in drawn pure tungsten filaments varies around the wire circumference and depends systematically on crystallographic direction. This variation of emission with crystallographic direction is more pronounced and complex when the filament is allowed to self-activate in cesium or potassium vapor.

THE MICROSCOPE

THE usual methods of electron optics[2] cannot be applied directly to study the emission from small round filaments, because of the conflicting symmetries of lens system and object. If only peripheral magnification is required, no electron lens is needed. The wire is mounted in the axis of a glass tube (Fig. 1) with fluorescent material on its inside wall,[3] and the emitted electrons are drawn over to the wall so rapidly that their initial nonradial velocity components have not time to take them far from a strictly radial path. On the wall is formed an electron image of the wire, magnified in circumference by the ratio b/a of tube radius to wire radius, not magnified in length. We estimate the resolving power by considering two electrons, one leaving the filament along a certain radius, the other with an initial velocity component $(2kT/m)^{\frac{1}{2}}$ normal to this radius and to the wire axis. The angular separation between the end-points of the paths is

$$\theta = 2\left(\frac{300kT}{\epsilon V}\right)^{\frac{1}{2}}\left(\ln\frac{b}{a}\right)^{\frac{1}{2}}\int_0^{(\ln b/a)^{\frac{1}{2}}} e^{-u^2}du;$$

for operating conditions, a 5-mil wire at 2000°K in a 2-in. tube, with 10,000 volts on the screen, this is about 1°. A similar computation for the initial velocity along the axis shows that points about 0.2 mm apart on the wire length can be separated. These estimates assume that the tube wall is an equipotential. The voltage V is applied to a helix of nickel wire wound to fit the inside wall snugly. Slow secondary electrons are emitted by the screen between helix turns and drift to the turns under a weak field, keeping the fluorescent

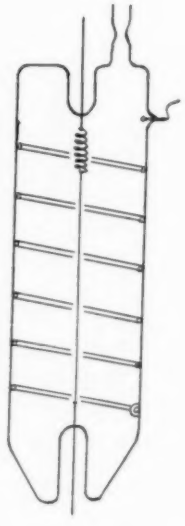

FIG. 1. Sketch of a typical tube.

[1] A report of this work was given at a meeting of the New England Section of the American Physical Society; abstracts in Phys. Rev. **48**, 973 (1935).

[2] Brüche and Scherzer, *Geometrische Elektronenoptik* (Berlin, 1934).

[3] After cleaning, the inside of the tube is coated with a ten percent solution of potassium silicate and the excess liquid is shaken off. This coat is allowed to dry for about two minutes, and willemite powder is blown on with a simple compressed-air dust gun, made of a glass bottle reservoir and a two-holed rubber stopper. Another method, which avoids the silicate binder, is to grind the inside with 120-mesh alundum, using a brass disk with about $\frac{1}{4}''$ clearance soldered on a long spindle which is turned in a lathe, and rub the willemite in dry. This gives a more uniform screen, but the difficulty of background radiation from the filament is more serious.

surfaces from charging up. Tests show that distortion of the image by potential gradients in the screen is negligible.

Observation is possible over the temperature range where enough electrons are emitted to excite the screen and not enough to damage it, from ~1700°K to ~2400°K for clean pure tungsten.

Cold Emission and Surface Contaminations

If, after evacuation and before any heat treatment of the filament, the anode potential is applied while the filament is at room temperature, the screen is covered with bright splotches (Fig. 2). On raising the filament temperature these squirm about, disappear and reappear, and usually vanish permanently when the filament is dull red. We attribute these splotches to field emission from rough regions on the wire which are covered with alkali impurities during drawing and handling. It has been suggested that these places of high electron emission from cold wires with small fields may be significant in Geiger-Müller counter operation: some tests are in progress. At about dull red, narrow bright rings often appear around the tube and persist to higher temperatures. A flash above 2500°K is always sufficient to remove them permanently from pure tungsten. Two platinum samples were raised to the melting point without cleaning off these rings. It seems certain that severe heat treatment is necessary before field currents or thermionic currents characteristic of a metal can be obtained.

Fig. 2. Cold emission from a raw tungsten wire.

Stripes and Die Marks

The emission pattern of a clean drawn tungsten wire (Fig. 3) changes only in intensity over the observation range. The light and dark stripes, regularly spaced around the tube and continuous down its length, have appeared on the pattern of every drawn tungsten wire we have examined—more than a dozen samples, differing in size, manufacture, and purity. The stripes can be correlated with grooves, presumably die marks, on the wire, visible under an optical microscope. Neither grooves nor stripes are removed by hours

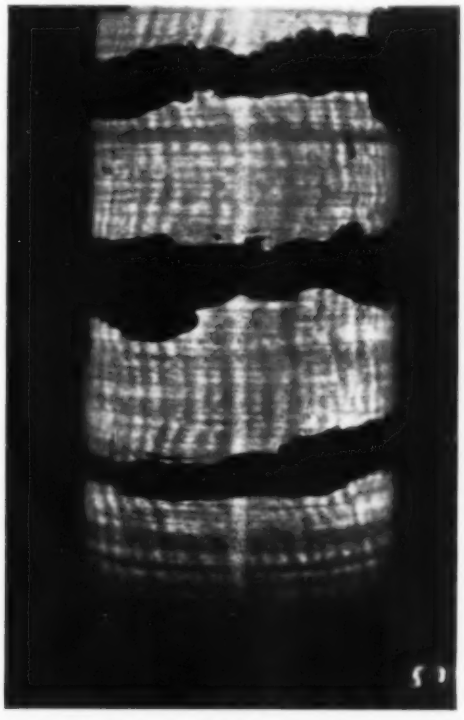

Fig. 3. Emission pattern of a drawn tungsten wire. In this tube the nickel helix was replaced by one of platinum paint.

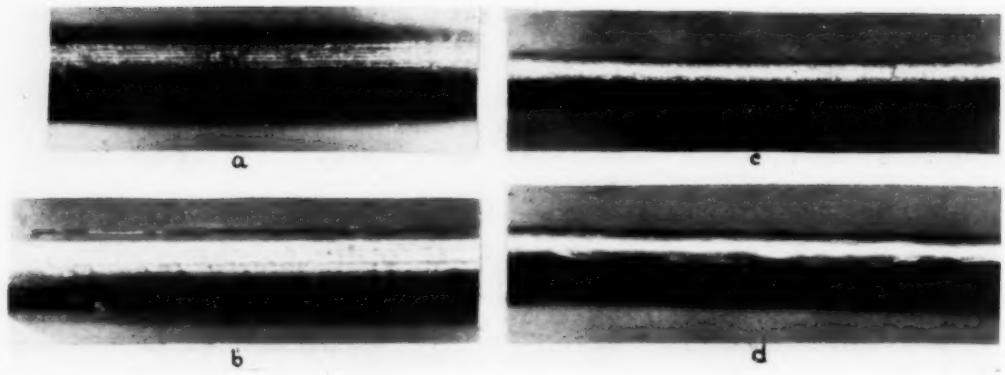

FIG. 4. Microphotographs of tungsten filament surfaces. (a) Raw wire from spool; (b) piece of same wire after about one hour at 2800°K; (c) wire smoothed by electrolysis; (d) piece of same wire after about one hour at 2800°K.

of heating above 2800°K (Fig. 4). Wires smoothed free of grooves by electrolysis or abrasion[4] give an electron image free of stripes. The pattern and optical appearance of tantalum are similar to those of tungsten; platinum and nickel (oxide-coated) show less prominent stripes and grooves.

THORIATED TUNGSTEN[5]

Immediately after a flash to 2800°K the pattern of a thoriated tungsten filament at 1200°K consists of intensely bright spots (Fig. 5). Many of these reappear in the same places after a subsequent flash to 2800°K, no matter what the intervening thermal history of the wire. During activation at 1850°K the thorium appears to migrate from these spot-sources and eventually to cover the surface almost completely. At 1200°K the activated filament shows very brilliantly the same pattern, with stripes due to grooves, as at 2000°K without a thorium coat.

CESIUM ON TUNGSTEN SINGLE CRYSTALS

When the tube contains cesium vapor in equilibrium with cesium metal at about room temperature, there is a lower observation range (~700°K to ~900°K) where the work function is greatly decreased by adsorbed cesium.[6] Above 900°K, where the equilibrium coverage of cesium is very small, the screen is dark until we reach the usual clean-tungsten range, 1700°K to 2400°K. Using smoothed drawn wires of pure tungsten (G. E. 218) containing large single crystals which in growth have followed the fiber grains in having a 110 axis parallel to the wire axis,[7] we find that the emission pattern on the tube, around

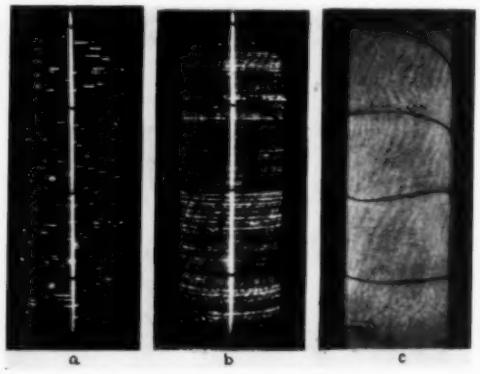

FIG. 5. Typical patterns of thoriated tungsten (1200°K). (a) immediately after flash to 2800°K; (b) after first 4 minutes of activation at 1850°K; (c) after 40 minutes of activation at 1800°K.

[4] Rapid electrolysis in NaOH or KCN will give a smooth, glassy surface, but the rate requires careful control, and it is impossible to keep the diameter uniform. A grinding engine has been constructed and is now in use, which polishes wires up to 40 cm long, leaving them uniform in cross section, round, and microscopically smooth.

[5] For a review of this subject, see I. Langmuir, J. Frank. Inst. **217**, 543 (1934).

[6] J. B. Taylor and I. Langmuir, Phys. Rev. **44**, 423 (1933).

[7] M. Ettisch, M. Polanyi and K. Weissenberg, Zeits. f. physik. Chemie **99**, 332 (1921).

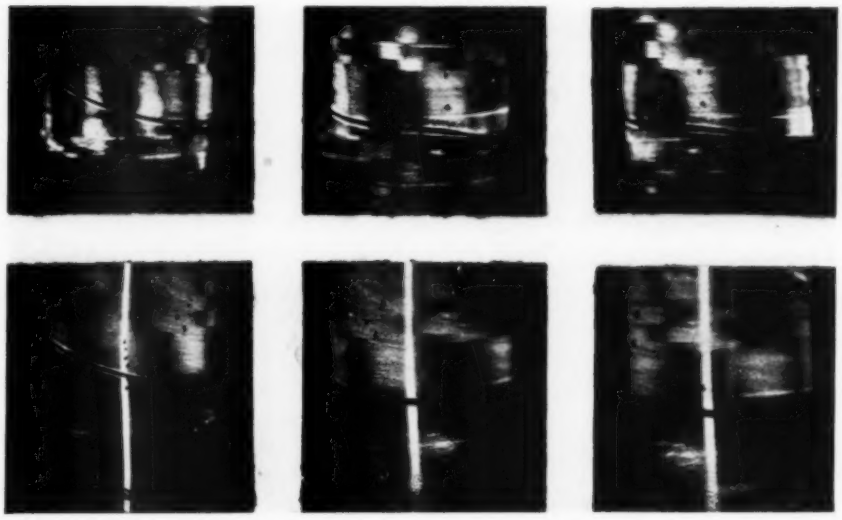

FIG. 6. Emission patterns of a smoothed tungsten wire containing several large single crystals, in equilibrium with saturated cesium vapor at room temperature. Upper row at ~825°K (intermediate between *C* and *D*, Fig. 7), lower row at 2000°K. Left column, looking along 100 axis of large crystal; right column, looking nearly along 110 axis of large crystal; center column, intermediate direction. Black dots are ink spots on the tube for reference.

each single crystal and over both observation ranges, is divided into four quadrants, the pattern in any quadrant being a mirror image of the patterns in the adjacent quadrants (Figs. 6, 7). This is just the symmetry of the tungsten lattice about the 110 axis, with the quadrants lying between another 110 and a 100 axis, both perpendicular to the wire axis. X-ray Laue pictures allowed us to identify the axes marked on the diagrams. As the temperature is lowered from the hot tungsten range, the first regions to become bright (due to adsorbed cesium) are those which were darkest on the hot tungsten pattern. At still lower temperatures the patterns become more complicated, and "fine structure" develops, but in general regions of high emission from hot tungsten are regions of low emission, indicating low cesium coverage, from the Cs–W surface, and *vice versa*.

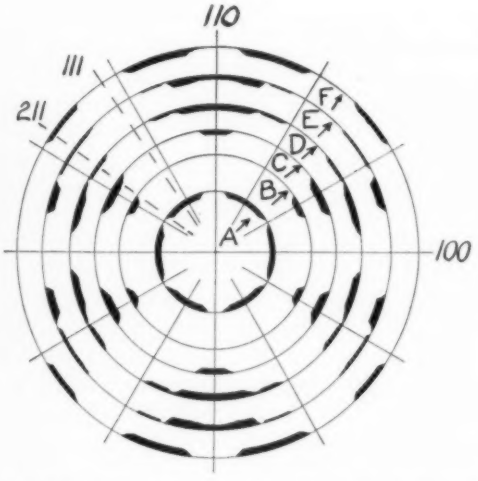

FIG. 7. Diagrams of patterns for wire of Fig. 6: dependence of brightness on direction, for a given filament temperature, is shown by thickness of line. Brightness of brightest parts of Cs-W patterns increases toward higher temperature. Wire axis, 110, is perpendicular to plane of diagram; prominent lattice directions in the plane are indicated. *A*~2000°K; *B*~900°K; *C*~850°K; *D*~800°K; *E*~750°K; *F*~700°K.

POTASSIUM ON TUNGSTEN

With the single-crystal filament in a potassium atmosphere symmetrical low temperature patterns were again found, but much fainter than with cesium. If the cold filament, surrounded by potassium vapor, is given a "bombing" treatment[8] for one minute, and then is raised for one

[8] Alkali vapor in a tube attacks the screen and diminishes the fluorescent yield. After this decomposition has begun, setting the anode voltage above 6000 v produces rapidly changing splotches and rings on the tube wall accompanied

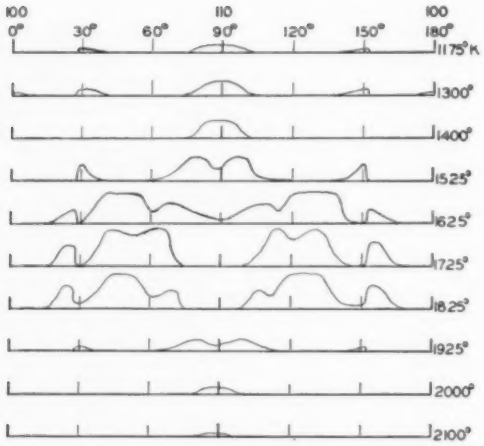

FIG. 8. Influence of preparation temperature on single-crystal patterns at ~775°K. Filament in equilibrium with saturated potassium vapor at 220°C; preparation temperatures at right. The curves, sketched during observation, show dependence of emission on angle around a semicircumference of the tube with the 100 axis as diameter.

minute to a "preparation temperature" between 1200°K and 2100°K, the low temperature equilibrium patterns depend markedly in intensity, structure, and persistence on the preparation temperature (Fig. 8). The following hypothesis explains qualitatively all the observations: bombing coats the filament with a thick layer of oxygen,[9] which at a preparation temperature evaporates from the filament nonuniformly, the rate depending on crystallographic direction. When the partially oxygenated filament is then allowed to coat with potassium, the potassium coverage depends on lattice direction and oxygen coverage, and the electron emission depends on all three.

RECRYSTALLIZATION

We have used this electron microscope, with cesium, to observe grain growth in a smoothed pure tungsten wire (G. E. 218). The Cs–W pattern of the raw wire was uniform, indicating a microcrystalline surface structure below the resolving power of the instrument. A flash to 3100°K produced several single crystals long compared with the wire diameter, and the growth of these during subsequent flashes could be readily followed on the Cs–W patterns at ~800°K, well below the recrystallization temperature (Fig. 9).

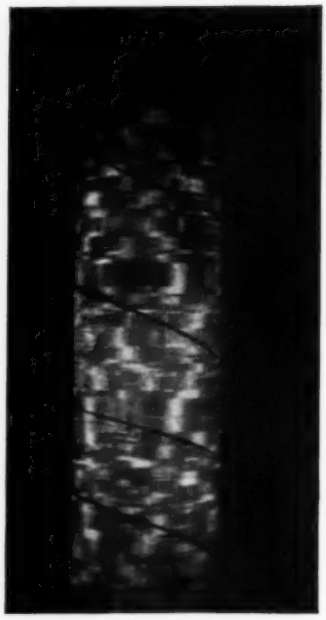

FIG. 9. Cs-W pattern at ~800°K, showing the degree of recrystallization produced by several flashes to 3100°K. (G. E. 218 wire, smoothed by abrasion.)

In recrystallized drawn tungsten wires long crystals are unusual, and the orientation is presumably influenced by the drawing. Preliminary investigations with single-crystal Pintsch filaments,[10] where the crystal orientation is random with respect to the wire axis, encourage the hope of obtaining an emission and adsorption map for all the lattice directions in tungsten.

We are greatly indebted to Professors W. B. Nottingham and B. E. Warren, to Dr. Irving Langmuir, and to Mr. W. E. Hazen for assistance and advice.

by red sparkles at the wire, as if the wire were being struck by particles liberated from the wall through electron impact. (Stable patterns can be maintained for anode voltages below 4000 v.) After this bombing treatment the pattern below 1000°K consists of irregular bright splotches and rings, like that of a raw wire.

[9] Oxygen is assumed, since the preparation temperature range resulting in high emission is almost the same as that observed by K. H. Kingdon (Phys. Rev. **24**, 510 (1924)) to result in high emission from a Cs-O-W surface.

[10] C. J. Smithells, *Tungsten: Metallurgy, Properties and Applications* (New York, 1927), in particular, p. 68.

Photoelectric Effect of Aluminum Films Evaporated in Vacuum

E. GAVIOLA[1] AND JOHN STRONG, *California Institute of Technology*

(Received December 21, 1935)

Sensitivity curves of aluminum films deposited by evaporation in vacuum have been determined. A new threshold value of 2830A and a selective maximum around 2700A have been found. The cell has the form of a horn, absorbing all the incident light. Charcoal was used for producing high vacuum and for giving off gases that influence the position and inclination of the sensitivity curves.

THE photoelectric effect of aluminum surfaces has been repeatedly studied. For the threshold of the sensitivity, values lying between 5000A[2] and 3342A[3] have been observed. The general trend in successive investigations, as the technique for obtaining good vacua and outgassed surfaces improved, has been to displace the threshold to the violet. The work reported in this paper follows that general trend. We find a long wave-length limit for aluminum films distilled in vacuum at 2830A, 500A below the smallest value previously found.

APPARATUS

The cell used is illustrated schematically in Fig. 1. It consists of a Pyrex tube of 25 mm diameter in the form of a horn. At one end it is closed by a quartz plate P sealed with Apiezon wax, in the other it contains a 6-turn coil of 40-mil tungsten wire, supported by two insulated tungsten leads. The electrode K provides contact with the internal surface of the horn and the well-insulated and appropriately bent tungsten wire A is used as anode. The cell is open to a side tube C, which contains charcoal. It is connected to the pumping system through the stopcock B and the liquid-air trap D. For the stopcock B Apiezon wax was used instead of grease.

The cell was prepared in the following way. First the tungsten coil, with its glass seal, but detached from the cell, was loaded with small pieces of aluminum wire and attached to contacts inside a vacuum bell jar, in order to melt the aluminum, outgas it partially and clean it from its thick coat of oxide. Then well-washed and vacuum-cleaned charcoal was placed in the side tube C, the window P put in position and the coil E attached to the cell. The system was then connected to a Hypervac mechanical oil pump through the liquid-air trap D. A small cylindrical furnace kept the charcoal at red heat during evacuation. After pumping thus for 48 hours the stopcock B was closed, the cell separated from the trap D, and the charcoal allowed to cool down and subsequently immersed in liquid air, while a glow discharge was passed between the electrodes K and A in order to outgas partially their surfaces. A small potential difference was applied to the terminals of the coil E so as to keep it at dull red heat without producing evaporation of aluminum. The cell was covered with asbestos, leaving the window and the stopcock B unenclosed. After 2 hours of this treatment the asbestos insulation was removed, and the electrical connections were interrupted in order to let the glass cool down. Once this was done, a potential difference of 7 volts was applied to the tungsten filament for 16 seconds and a thin clean bright reflecting aluminum film was deposited on the glass walls of the cell. As the distilling aluminum travels in straight lines and condenses totally upon the first impact against the walls, if the vacuum is good, the quartz window and the electrode seal A remain free from metal. The amount of aluminum in the tungsten filament allows the deposition of successive layers when desired. The cell was then ready for use.

An atmospheric-pressure quartz-mercury arc served as light source. Its radiation was resolved by a Müller-Hilger double quartz monochromator. The horn-shape of the cell insured the

[1] Fellow of the John Simon Guggenheim Memorial Foundation.
[2] R. Pohl and Peter Pringsheim, Verh. d. D. Phys. Ges. **16**, 336 (1914).
[3] S. C. Roy, Proc. Roy. Soc. **A112**, 599 (1926).

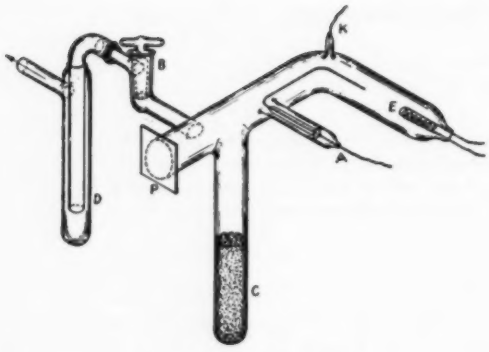

FIG. 1. Photoelectric cell.

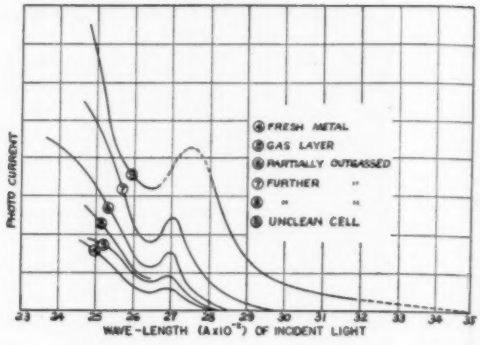

FIG. 2. Characteristic of cell containing evaporated aluminum film.

total absorption of the light that reached it through the window.

The photoelectric current was read on a string electrometer with a microscope. The intensity distribution of the light entering the cell was determined with a vacuum thermocouple connected to a galvanometer.

EXPERIMENTAL PROCEDURE AND RESULTS

The first measurements were made with a cell that had not been properly outgassed. Curve 9 of Fig. 2 represents the sensitivity function obtained in that case. The rest of the curves of Figs. 2 and 3 were determined with a better cleaned and outgassed cell. Curve 4 (Fig. 2) is characteristic of a freshly distilled aluminum film while the charcoal was in liquid air. The threshold lies at about 2830A and a zone of selectivity is noticeable at about 2700A.

The charcoal was then allowed to warm up to room temperature, to give off residual gas that would form layers on the aluminum surface. Curve 5 was then obtained. The cell was subsequently "outgassed" by placing the charcoal back in liquid air while 4 volts were applied to the tungsten coil for 2 minutes, heating the cell up to 100–200°C. Curve 6 gives the results then obtained. The repetition of the same brief treatment yielded curve 7, displaced further in the same direction as the previous ones had been. The application of 4 volts on the coil for 10 minutes produced a retrogression of the sensitivity to the values represented by curve 8.

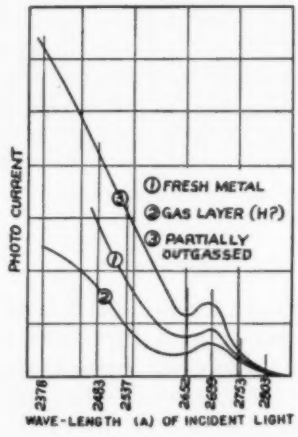

FIG. 3. Characteristic of cell containing evaporated aluminum film.

This effect may be due to further "outgassing" of the surface or to the slow distillation of fresh aluminum, forming a thin new layer on top of the old film.

If a new thick deposit was formed and the operation of warming up the charcoal and then "outgassing" in steps was repeated, the results obtained did in general not reproduce the previous ones, with the sole exception of the curve characteristic of the fresh film distilled in good vacuum. There were nevertheless two types of behavior to be noticed. In some cases the sensitivity curve would suffer displacements more or less parallel to itself, as in Fig. 2, while in others the threshold value would remain the same while the sensitivity in the further ultra-

violet would increase or decrease in amounts practically proportional to the distance from the long wave-length limit, as in Fig. 3. This irregular behavior suggests that the gases given off by the charcoal when allowed to warm up had different composition in different cases.[4]

The selective maximum at about 2700A was present in all the measured curves, indicating a certain independence of the nature and thickness of the gas layers.

Discussion

The metal used for loading the tungsten coil was commercial "pure" aluminum, containing, besides hydrogen and air, small amounts of Fe, Zn, Ga, Ni, Cu, Si, Mg and Sn, as determined by a qualitative spectroscopic analysis.[5] The iron is present in the evaporated film to the extent of 0.2 percent by weight. To these we have to add the minute quantities of tungsten evaporated together with the aluminum. The threshold value 2830A obtained for fresh aluminum films cannot be thus considered as characteristic of pure aluminum, without further evidence. But it suggests that all the values determined previously, and lying between 3342 and 5000A, were affected by the presence of small or large amounts of aluminum oxide on the surface.

[4] Compare Joh. Kluge, Ann. d. Physik **82**, 432 (1927); R. J. Cashman and W. S. Huxford, Phys. Rev. **48**, 734 (1935).

[5] E. Gaviola and John Strong, Phys. Rev. **48**, 136 (1935).

MARCH 15, 1936 PHYSICAL REVIEW VOLUME 49

An Abnormal Electrical Conductivity in Powdered Tellurium

C. Hawley Cartwright, *University of Michigan*

(Received December 16, 1935)

It was found that tellurium powder under a pressure of 1000 kg/cm² had about ten times greater specific electrical conductivity than that of a single crystal of tellurium under the same pressure. An investigation was made of the influence of the electrodes, particle size, condition of the surface of the powder and the medium surrounding the particles. This anomalous conductivity was most pronounced in the purest tellurium (specific conductivity of 2.5 ohm^{-1} cm^{-1}) and it gradually disappeared in tellurium powders containing impurities (the addition of which increases the conductivity of the massive metal). The abnormal conductivity probably existed in impure tellurium but was simply masked by the normal increase in conductivity with pressure observed for conducting particles. Momentarily passing an electric current through the powder under pressure caused its volume to diminish; but, also the electrical conductivity was greatly decreased and, in the case of pure tellurium, it became almost the same as that of the massive metal. Under a hydrostatic pressure of 20,000 kg/cm² massive tellurium increases its electrical conductivity more than a hundred times and the rate of increase rises rapidly with pressure. This suggests that the anomalous conductivity of tellurium powder might be due to local pressures between particles that are greatly in excess of the average pressure that was measured. However, this explanation does not account entirely for the observed magnitude of the anomalous conductivity. It seems necessary to assume that (1) the conductivity of tellurium increases even much more for a nonuniform pressure than for a hydrostatic pressure, or (2) very sharp points occur between particles which produce strong enough electric fields to liberate electrons.

Introduction

THE electrical properties of tellurium, which appear so anomalous compared to those of conducting metals, can be attributed to its small free electron density. While there is approximately one free electron per atom in conducting metals, there is probably only one free electron per million tellurium atoms. Phenomena of small absolute magnitude which would be masked in ordinary metals may be observed in tellurium, where the background of free electrons is small, and they present anomalies by comparison with conducting metals. On this basis is found an explanation for the abnormally high Wiedemann-Franz ratio of tellurium, for its anomalous

thermoelectric power, temperature resistance coefficient and the influence of foreign atoms on its electrical properties.[1, 2] The experiments to be described now show that under a moderate pressure the electrical conductivity of powdered tellurium is several times greater than that of a single crystal of tellurium. Also this anomalous effect is small in absolute magnitude and might be masked in ordinary powdered metals.

Experimental Procedure

The tellurium used was taken from specimens used in a previous investigation[2] and the electrical conductivities of the massive metals are given in Table I. The powder was prepared by grinding and separating the grain sizes by sieves. The designation $<50\mu$ means that the particles passed through a sieve having holes $50\mu \times 50\mu$, 50μ to 85μ particles means that they passed through a sieve with openings $85\mu \times 85\mu$ but not through $50\mu \times 50\mu$ holes, etc.

Table I. *Conductivity of Te (polycrystalline massive metal).*

No.	% Impurity	κ(ohm^{-1} cm^{-1})	No.	% Impurity	κ(ohm^{-1} cm^{-1})
2	0.01	2.7	23	0.60 Cu	30
3	0.01	2.3	16	1.50 Cu	100
13	0.05 Cu	7.1	25	0.44 Bi	343
8	0.20 Cu	16.7	33	0.81 Ag	36

The powder was contained in a capillary glass tube serving as a cylinder and was mechanically compressed between two steel pistons. The cross-sectional area of the compressed powder was always 0.0216 cm^2 and the length was about 5 mm. The length was determined by a scale attached to the movable piston and was read with an accuracy of about ± 0.1 mm. In order to lessen the influence of the friction between the powder and the inside of the cylinder, the cylinder was turned each time that the pressure was changed. It is to be remarked that in these experiments truly hydrostatic pressure was not used, the primary pressure being exerted at the two ends of a specimen; however, the pressure from the inside of the cylinder was almost equal to the primary pressure because of the flow of the powder—this was determined experimentally from the crushing strength of fused quartz cylinders. The resistances of the specimens were determined by a precision bridge; the two steel pistons served as electrodes.

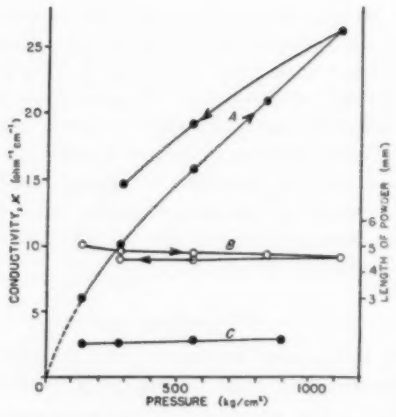

Fig. 1. *A*, conductivity of pure tellurium powder $<50\mu$; *B*, length of compressed powder; *C*, conductivity of a single crystal of pure tellurium.

Experimental Results

The anomalously high conductivity of pure tellurium powder can be seen from the data plotted in Fig. 1, which are tabulated in Table II. The electrical conductivity of the tellurium powder increases normally with pressure but the absolute conductivity of the powdered tellurium, even for these moderate pressures, is several times greater than that of a single crystal of tellurium under the same pressure. That the process was not reversible in the case of powder can be attributed to the pressure exerted by the cylinder and to a crushing and a packing of the particles.

To determine the origin of this anomalous conductivity-pressure phenomenon in tellurium powder, we made the following investigations:

Table II. *Conductivity of pure Te.*

Single Crystal of Pure Te			Te Powder $<50\mu$ Particles		
(kg/cm^2)	Length (mm)	κ(ohm^{-1} cm^{-1})	(kg/cm^2)	Length (mm)	κ(ohm^{-1} cm^{-1})
140	7.0	2.60	140	5.0	6.0
280	"	2.66	280	4.8	10.0
560	"	2.68	560	4.7	15.8
900	"	2.74	840	4.6	20.8
			1120	4.5	26.2
			560	"	19.1
			280	"	14.7

[1] C. H. Cartwright, Ann. d. Physik **18**, 656 (1933).
[2] C. H. Cartwright and M. Haberfeld-Schwartz, Proc. Roy. Soc. **A148**, 648 (1935).

Length of specimen

In Table III are given data for three different lengths of pure tellurium specimens composed of

TABLE III. *Conductivity of pure Te particles (<50μ) showing influence of length of specimen.*

kg/cm²	LENGTH (mm)	κ	LENGTH (mm)	κ	LENGTH (mm)	κ
140	8.7	4.9	3.2	8.0	1.1	9.5
280	8.2	7.2	2.9	11.0	1.0	14.5
560	7.6	13.0	2.8	17.8	1.0	22.5
840	7.4	15.1	2.8	23.8	0.9	25.4
1120	7.1	18.0	2.6	29.3	"	29.4
560	"	16.6	"	24.9	"	23.1
280	"	14.6	"	20.0	"	17.9

<50μ particles. Our principal result remains but it is observed that the shorter the specimen the greater the electrical conductivity. This is probably due to the friction against the cylinder playing a smaller role for the short specimens since the length of a specimen did not decrease uniformly with pressure. The fact that the length did not decrease more uniformly can be attributed partly to errors in its measurement but for our present purpose it seems better to record actual readings rather than smoothed values.

It is reasonable to assume that the electrons coming from the electrodes only furnished a negligible contribution to the observed conductivity since the mean free path is probably of the order of 10^{-6} cm. Although the length of a specimen only played a small role, we tried to minimize its effect by choosing a standard length of about 5 mm.

Particle size

In Table IV are given data for pure tellurium powder of 85μ to 92μ particles and for particles much less than 50μ. These last were prepared by regrinding powder that had passed through a 50μ×50μ sieve. The data for the two lengths of specimens of fine powder show probably better than the data in Table III that the length of a specimen plays a relatively unimportant role. It appears that the finer the powder the greater the conductivity; however, the influence of grain size does not appear large enough to be of great importance. It should be remarked that tellurium is so brittle that the data for grain size are uncertain since under pressure the 85μ to 92μ particles were broken so that many of them passed through a 50μ×50μ sieve.

TABLE IV. *Conductivity of pure Te powders.*

(kg/cm²)	85μ TO 92μ PARTICLES LENGTH (mm)	κ	≪50μ PARTICLES LENGTH (mm)	κ	≪50μ PARTICLES LENGTH (mm)	κ(ohm⁻¹ cm⁻¹)
140	4.8	5.2	5.0	7.6	2.6	7.4
280	4.5	8.6	4.8	12.0	2.4	12.5
560	4.3	12.5	4.5	17.8	2.3	18.1
840	4.1	16.4	4.4	21.2	2.3	20.3
1120	4.0	18.7	4.2	26.3	2.3	26.4
560	4.0	16.4	4.2	20.6	2.3	21.0
280	4.0	15.7	4.2	19.0	2.3	17.0

Surface effect

It might be thought that the abnormally high conductivity was due to a conductivity on the surface of the particles. The relatively small influence of the particle size is evidence against this hypothesis. If the conductivity were due to an adsorbed water film, to account for its absolute value the film would have to be several times more conducting than any known electrolyte. However, to control the influence of adsorbed water, tellurium was powdered and kept in benzene and found to have approximately the same conductivity as in air.

From our previous research[2] it was found that the presence of foreign atoms can greatly increase the conductivity of tellurium. To determine the influence of contact with air, some powder <50μ was investigated that had been prepared twelve months previously. The data are given in Table V. Washing this powder in water increased the conductivity about ten percent more than is shown in Table V. The data in Table V indicate that an oxide layer was slowly formed on tellurium powder but that it hindered rather than increased the electrical conductivity.

Surrounding medium

Tellurium powder was compressed under benzene, ethyl alcohol and water. In alcohol, the

TABLE V. *Conductivity of Te particles (<50μ) exposed to air 12 months.*

(kg/cm²)	LENGTH (mm)	κ(ohm⁻¹ cm⁻¹)
140	4.4	1.5
280	4.2	2.7
560	3.9	3.9
1120	3.6	8.9

powder had approximately the same conductivity as in air; in benzene possibly ten percent more; and in water about ten percent less. The effect seems too small to justify recording the actual data.

Impure tellurium

Tellurium alloyed with known quantities of copper, silver and bismuth, and thereby having a greater specific conductivity, were also investigated in the form of powder under pressure. Comparing the data in Tables VII and VIII with Table I shows that the conductivity of the powder does not increase proportionally to the specific conductivity of the massive metal. The purest tellurium powder under 1120 kg/cm² pressure had ten times greater conductivity than massive tellurium; powdered tellurium containing 0.60 percent copper was only slightly more conducting than pure tellurium powder and it had about the same conductivity as the massive alloy. Therefore the anomalous conductivity of powdered tellurium can best be observed in pure tellurium. It seems possible that the effect remains in the same absolute magnitude but is simply masked by the larger background of normal conductivity for powdered metals.

Welding

In a previous investigation it was observed that age and heat treatment often increased the electrical resistance of tellurium crystals. This was explained by the occurrence of internal cracks since the original conductivity could be regained by slightly compressing the specimen or momentarily passing an electric current through it. The present results on the conductivity of powders (where the idea of cracks has been carried to an extreme) seem contradictory. The press was not suited for attaining high enough pressures to form a compact mass of the tellurium powder and thereby to remove the artificial cracks but it was thought that the effect of a higher pressure could be obtained by momentarily passing an electric current through the powder when it was under pressure. Three experiments on pure tellurium powder are recorded in Table VI. The currents of 2, 3 and 15 amperes were allowed to flow for approximately one second. The specimens were considerably shortened because of the passage of the currents and their color was seen to change from a dull gray to a silver brilliance. Although the currents did not warm the specimens noticeably (the resistance was less than one ohm), they were compressed and welded into compact pieces that were mechanically rigid and could be removed from the cylinder. To determine whether the unexpectedly large decrease in conductivity was due to the presence of air during the welding process, we put alcohol and benzene on two specimens (data in Table VI) before welding. It was possible to see from the change in color of the powder that these liquids had penetrated by capillary action. The results showed no great difference between the powder welded in air and under a liquid.

In Table VII are recorded similar experiments for tellurium containing impurities. It is to be observed that in all cases except for tellurium containing bismuth that the welding process decreased the conductivity. In Table VIII are

TABLE VI. *Conductivity of powdered specimens placed under pressure and then sending electric currents through them, (1) in air, (2) in alcohol and (3) in benzene.*

<50μ PARTICLES (kg/cm²)	LENGTH (mm)	κ	<50μ PARTICLES (kg/cm²)	LENGTH (mm)	κ	50μ TO 85μ PARTICLES LENGTH (mm)	κ (ohm⁻¹ cm⁻¹)
140	5.5	6.7	140	5.7	6.5	4.5	8.2
280	5.3	10.7	280	5.4	10.3	4.3	9.7
560	5.0	15.6	560	5.0	15.8	4.0	16.1
900	4.8	19.2	900	4.9	20.6	3.8	22.9
280	4.8	17.0		*in alcohol*		*in benzene*	
1120	4.6	22.2	900	4.8	21.3	3.8	24.4
1120(2 amp.)	4.5	13.8	900(2 amp.)	4.6	16.2	3.7	15.1
1120(3 amp.)	4.2	4.5	900(3 amp.)	4.3	4.2	3.4	4.6
1120(15 amp.)	3.9	5.8	900(15 amp.)	4.0	5.2	3.2	5.8
280	3.9	5.3	280	4.0	4.8	3.2	5.4

TABLE VII. *Data similar to that of Table VI on Te containing impurities (<50μ particles).*

(kg/cm²)	LENGTH (mm)	κ	LENGTH (mm)	κ	LENGTH (mm)	κ (ohm⁻¹ cm⁻¹)
	Te+0.05% Cu		Te+0.20% Cu		Te+0.60% Cu	
140	4.8	7.6	5.0	8.4	4.9	10.1
280	4.5	12.5	4.5	13.3	4.6	13.9
560	4.3	18.3	4.4	20.8	4.4	22.7
840	4.1	22.9	4.2	25.6	4.2	28.8
1120	3.9	26.2	4.0	29.9	4.0	30.9
1120(5 amp.)	3.8	5.3	3.8	4.3	3.3	4.6
	Te+1.50% Cu		Te+0.81% Ag		Te+0.44% Bi	
140	5.0	10.0	5.4	9.8	4.8	30.0
280	4.8	14.8	5.1	14.0	4.5	47.0
560	4.5	21.8	4.9	22.0	4.4	54.0
840	4.4	25.8	4.6	28.3	4.2	87.0
1120	4.3	29.5	4.5	31.0	4.1	105.0
1120(2 amp.)	4.2	27.5	4.4	18.5	—	—
1120(3 amp.)	3.8	11.2	4.2	11.9	3.9	120.0
1120(8 amp.)	3.4	13.0	3.9	18.0	3.5	240.0
1120(15 amp.)	3.3	17.8	3.7	25.2	3.4	360.0

TABLE VIII. *Conductivity of single crystals containing impurities.*

(kg/cm²)	LENGTH (mm)	κ	LENGTH (mm)	κ	LENGTH (mm)	κ	LENGTH (mm)	κ(ohm⁻¹ cm⁻¹
	PURE Te		Te+0.60% Cu		Te+0.81%Ag		Te+0.44% Bi	
140	7.0	2.60	8.8	27.1	11.2	20.0	9.1	232
280	7.0	2.66	8.8	27.4	11.2	21.8	9.1	263
560	7.0	2.68	8.8	27.8	11.2	22.6	9.1	302
900	7.0	2.74	8.8	28.2	11.1	22.7	9.1	322
900(15 amp.)	7.0	2.80	8.8	32.0	10.6	36.0	9.1	418

given the electrical conductivities of tellurium single crystals under pressure (the pressure was exerted on the two ends of a specimen held in a glass cylinder).

Higher pressures

As a final experiment, it was decided to use higher pressures and the data for pure tellurium powder, $<50\mu$, are given in Table IX. The press

TABLE IX. *Conductivity of pure powdered ($<50\mu$) Te at higher pressures.*

(kg/cm²)	LENGTH (mm)	κ	(kg/cm²)	LENGTH (mm)	κ(ohm⁻¹ cm⁻¹)
470	4.0	9	3270	3.3	34
940	3.8	15	3740	3.3	37
1400	3.7	17	4200	3.2	40
1870	3.5	23	4700	3.1	42
2340	3.5	27	5130	3.0	43
2800	3.4	31	5600	2.9	44

broke for a compression of 9000 kg/cm² and the data beyond 5000 kg/cm² are therefore open to question. The friction between the powder and the cylinder (in this case, a glass capillary tube imbedded in steel) was so great that the cylinder was not turned; hence, the average pressures were probably less than are recorded.

Although it could not be conveniently arranged to measure the electrical conductivity of a powder specimen under higher pressure, some tellurium powder was pressed between steel plates at about 25,000 kg/cm². This formed a compact piece of tellurium which when removed from the press had only about the same conductivity as that of a piece formed from molten tellurium.

DISCUSSION

From these experiments we conclude that the length of the specimens, the size of the particles and a surface conductivity played but a small part in accounting for the anomalously high conductivity of tellurium powder.

TABLE X. *Bridgman's measurements on single Te crystals at high pressures.*

(1000 kg/cm²)	κ/κ_0	(1000 kg/cm²)	κ/κ_0	(1000 kg/cm²)	κ/κ_0
0	1.00	7	9.1	14	46.5
1	1.40	8	12.0	15	56.5
2	1.95	9	15.5	16	67.6
3	2.70	10	19.7	17	80.0
4	3.73	11	24.8	18	94.3
5	5.08	12	30.9	19	104.0
6	6.85	13	38.0	20	127.0

An explanation that immediately suggests itself is that there is a strongly preferred direction for electrical conductivity in tellurium crystals. From previous work on single crystals, this is not found to be the case and polycrystalline tellurium has approximately the same resistance as a single crystal. The experiments on welding also deny this hypothesis.

Tellurium is extremely brittle and when it is broken, very sharp edges and points are produced. The high conductivity of tellurium powder might be due to conduction electrons being liberated at the sharp points because of the existence of very high electric fields. Dr. B. Bloch pointed out to me that the experiments on changing the dielectric constant of the medium surrounding the particles should not influence the observed electrical conductivity; a high dielectric constant decreases the electric field strength but it is counterbalanced by an increase in the number of surface charges. Whether or not the anomalous conductivity of powder tellurium is due to the liberation of electrons at sharp points was therefore not determined from these experiments; but, evidence against this hypothesis is the fact that the size of the particles did not play a greater role.

Bridgman[3] has measured the electrical conductivity of single crystals of tellurium up to a hydrostatic pressure of 20,000 kg/cm² and Table X has been calculated from his data.

The approach of tellurium to metallic conduction under high pressures at first seems to explain the anomalously high conductivity of tellurium powder; namely, that local pressures exist between particles that are greatly in excess of the

[3] P. W. Bridgman, Proc. Am. Acad. **70**, 71 (1935). Bridgman has also studied black phosphorus and its data are nearly the same as those given for tellurium in Table X. The specific resistance of black phosphorus is about the same as that of pure tellurium.

average pressure measured. This appears to offer an explanation for the fact that the conductivity of pure tellurium powder under pressure decreases by the welding process if one assumes that local high pressures are thereby relieved. However, any local pressure would be limited by the crushing strength of tellurium to about 20,000 kg/cm². With an average pressure of 1000 kg/cm², if a local pressure of 20,000 kg/cm² occurred, the local conductivity would be increased a hundred times (taking Bridgman's value for hydrostatic pressure) but only five percent of the area would be effective so that the average conductivity could only increase five times. This computation for the local pressure and conductivity at the point of contact between particles neglects the much smaller pressures within the particles which would greatly diminish the observed conductivity. For high local pressures to account for our results, it seems necessary to assume that the increase in conductivity is even very much greater for nonuniform pressure than for hydrostatic pressure.

The question arises as to why the electrical conductivity of massive tellurium should increase so greatly with pressure. Let us recall that usually for good conducting metals the conductivity increases one to two percent for a pressure of 12,000 kg/cm². Bismuth, antimony, arsenic and strontium on the other hand decrease in specific conductivity at high pressures. Electrical conductivity can be considered as proportional (1) to the density of free (conduction) electrons and (2) to their mean free path. As high pressure can influence both of these factors it can cause either an increase or decrease in conductivity. In the case of tellurium where the conductivity increases a hundred-fold for a pressure of 20,000 kg/cm², it is more reasonable to assume that the number of free electrons increases rather than that their mean free path increases a hundred times. Assuming the mean free path to be the same as in ordinary metals, this would mean that the number of free electrons need only increase from about one per million atoms to one per ten thousand atoms of tellurium.

An increase in conductivity with pressure seems to signify that a change in the structure and intermolecular forces in tellurium can produce free electrons: It was also found that the conductivity of tellurium can be increased by the presence of foreign atoms; in fact, about 0.1 percent of bismuth or antimony suffices to increase the conductivity a hundred times. Since both pressure and the presence of foreign atoms increase the number of free electrons, it may be that the process of their production is similar for the two cases, i.e., by a change in the structure and the intermolecular forces. Evidence that the structure and intermolecular forces greatly influence the number of free electrons is also shown by the data given in Table XI, which are taken from the work of Kraus and Johnson[4] for pure tellurium. The negative temperature coefficient and the sudden increase to almost metallic conduction on melting both are to be explained by an increase in the free electron density for the mean free path should decrease. On melting, tellurium expands about five percent; therefore, although high pressure seems to furnish free electrons as well as melting the tellurium, the structures and intermolecular forces must be different in the two cases.

TABLE XI. *Conductivity of pure Te as a function of temperature (Kraus and Johnson).*

TEMP.	κ(ohm^{-1} cm^{-1})		TEMP.	κ(ohm^{-1} cm^{-1})	
(22)	(2.5)		431.8	1508	
363.0	67.6	Solid	449.1	1728	Liquid
380.5	75.2		457.2	1810	
404.7	85.5		480.5	2050	

We may recall that in these experiments the absolute magnitude of the anomalous conductivity of tellurium powder is very small and the effects would probably be completely masked in good conducting powdered metals where the normal conductivity is about a million times greater than in tellurium.

For the opportunity of making these investigations, I am grateful to Professor Jacques Errera of the University of Brussels, le Fonds National Belge de la Recherche Scientifique, and the C. R. B. Educational Foundation. I wish to thank Professor Dennison for his helpful suggestions.

[4] C. A. Kraus and E. W. Johnson, J. Phys. Chem. **32**, 1281 (1928).

The Nebular Redshift

ROY J. KENNEDY AND WALTER BARKAS, *University of Washington*

(Received January 31, 1936)

The possibility of an effect of the free electrons in a highly ionized gas on the frequency of light traversing it has been investigated. Electrons to a density of about 5×10^{12} per cc were produced in a series of low voltage arcs. Light of wave-length 5461A was passed through the arcs and a frequency shift sought by means of an interferometer in vacuum. A shift of approximately two parts in 10^{10} could have been detected. A very satisfactory null result was obtained. This is interpreted with special reference to the possibility of explaining the nebular redshift by such a mechanism. It is concluded that the shift is not attributable to interstellar electrons.

INTRODUCTION

THE discovery by Hubble and Humason[1] that statistically the wave-lengths of spectral lines of distant nebulae experience a fractional shift toward the red proportional to the distances of the nebulae seems at present best explained in terms of an expanding universe. The form of the observed relationship, however, suggests the possibility that it may depend in some way on intergalactic matter; almost any mechanism of interaction would yield proportionality between the redshift and distance, at least to a first approximation.

A theory of Zwicky,[2] according to which the gravitational interaction occurring between the photon and intergalactic matter gives rise to a loss of momentum and therefore of frequency by the photon, has been shown untenable on the basis of the relativity theory of gravitation by Tolman, Ehrenfest and Podolsky.[3] The hypothesis of the present writers, a test of which is the main subject of this paper, was suggested by the well-established fact that the gas in intergalactic space is practically completely ionized. It merely postulates a frequency shift in the photon in its interaction with a free electron, the mechanism of the interaction and the magnitude of the individual shifts not being assumed in advance. When the test had been about completed an essentially equivalent theory of Abraham[4] appeared. He, however, employed the classical Thomson theory of scattering in combination with the quantum photoelectric equation and was thereby enabled to assign a definite numerical value to the frequency shifts due to individual encounters of photon and electron. Such a procedure must naturally be regarded sceptically, but it does suggest a shift of frequency in the observed direction. The writers have preferred to make no quantitative predictions of an effect. Nevertheless only a slight and plausible modification of the theory of the Compton effect, to permit a slight radiation of energy by the electron during its reaction with the photon, would be required to yield an effect of the kind observed.

[1] Hubble and Humason, Astrophys. J. **74**, 43 (1931).
[2] Zwicky, Proc. Nat. Acad. Sci. **15**, 773 (1929).
[3] Tolman, Ehrenfest and Podolsky, Phys. Rev. **37**, 602 (1931).
[4] Abraham, Comptes rendus **15**, April 8 (1935).

THEORY AND PROCEDURE

As basis of the present theory we assume merely that a photon loses energy to electrons in proportion to its frequency and either continuously or discretely, the rate in the latter case depending on the probability of encounters. In either case the mean loss per unit length of its path is evidently proportional to the density of free electrons, and we may therefore write $d\nu=-k\rho\nu dx$, where k is the unknown constant of proportionality, ν is the frequency, ρ the density and dx the length of the element of path. Assuming ρ to be roughly constant, this expression can be integrated to give $\nu=\nu_0\epsilon^{-k\rho l}$, where l is distance between source and observer. As a first approximation, then

$$\delta\nu/\nu_0=(\nu_0-\nu)/\nu_0=k\rho l. \qquad (1)$$

This expression is of the same form as the Hubble-Humason law.

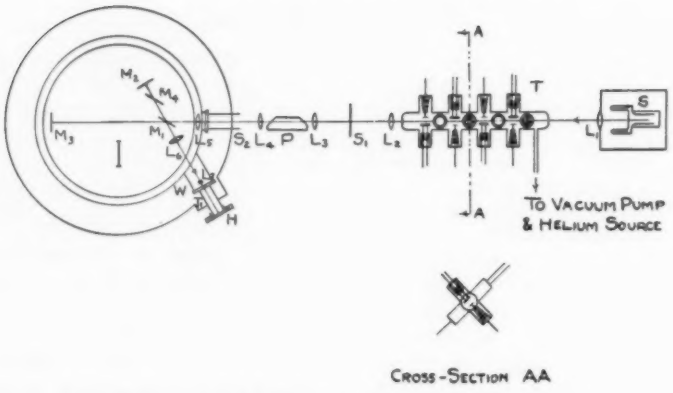

FIG. 1. Schematic diagram of apparatus showing light path.

Now although the value of l for the nebulae is enormous, nevertheless since ρ can be shown to be very small, even with complete ionization of the gas in intergalactic space, it turns out to be feasible to test our hypothesis experimentally. This is so because a very large value of ρ can be produced in the low voltage arc and an extremely small value of the ratio $\delta\nu/\nu_0$ can be detected. The experiment consists of comparing the frequency of a spectral line in a beam passed through a series of arcs, with the frequency of the same line when the path contains no ions.

The experimental arrangement is shown in Fig. 1. Light from the mercury-vapor arc S is collimated by the lens L_1 and passed through a series of helium arcs in the discharge tube T to the lens-and-prism system L_3PL_4 which separates out the green line λ5461. The interferometer I forms an interference pattern focused on a photographic plate in the holder H which automatically shifts the plate between exposures which are made with the helium arcs alternately on and off.

The source is a low voltage discharge in mercury vapor, between a cylindrical anode and an oxide-coated helical hot cathode. The discharge tube is illustrated in Fig. 2 which is self-explanatory. The luminous part of an arc is mainly confined to the jacketed part of the central tube and the light passes out through a window set close to it in order to minimize the amount of reversal of any of the numerous components of the green line which was used. The interference pattern had been found to be sharpest when the arc was kept at a temperature within a very few degrees of 35°C, hence it was jacketed with ether maintained at the boiling point by heat from the arc and condensed in a water-jacketed condenser. With the current in filament and arc kept constant by an automatic regulator, the brightness of this source exhibited no measurable variations as the helium arcs

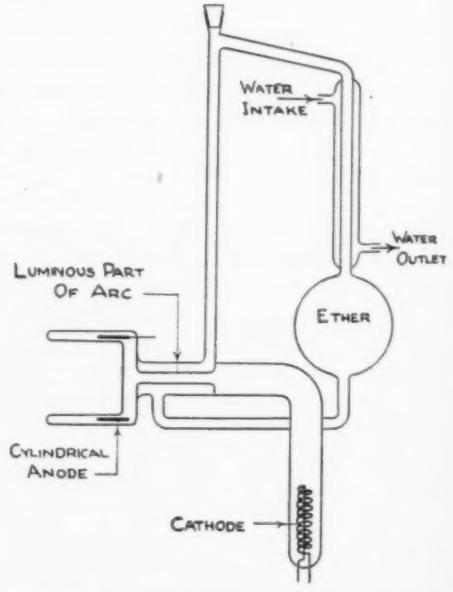

FIG. 2. Low voltage discharge in mercury vapor used as a light source.

(which employ the same source of direct current) were turned on and off; this steadiness was essential because otherwise there might have occurred a spurious shift of the interference pattern correlated with the discharge in the helium tube. This sort of spurious effect is discussed in a paper referred to below.[5]

The interferometer is of the Michelson type, built almost entirely of fused quartz and contained in a vacuum chamber kept at a temperature constant to within about 10^{-3} degrees C. The vacuum is necessary in order to keep the optical path-difference constant. The interferometer is compensated accurately for temperature. The fixed path difference is slightly more than 600,000 wave-lengths of the line λ5461. Sections of the interference pattern (a system of concentric rings) were automatically photographed in such a way that exposures taken with the helium arc on were interleaved with those taken with the arc off. By this procedure errors due to differences among individual photographic plates were minimized.

The measurements of the plates were made with a comparator in which the interference rings were compared directly with those on a nearly identical reference plate which was taken as a standard. With this device each exposure could be measured with a probable error corresponding to a variation in path-difference of about 10^{-3} wave-length. That is, the probable error for each exposure corresponds to a variation in frequency of one part in $1000\times600{,}000=6\times10^{8}$.

The interferometer and comparator are discussed in more detail elsewhere.[5]

The ionized gas was contained in a tube 40 cm long provided with plane-parallel windows at the ends. Equally spaced along the tube were eight units, each consisting of an oxide-coated cathode set 1 cm away from a flat nickel anode. The cathode was made of heavy tungsten ribbon folded in zigzag fashion with the edge lying in a plane parallel to that of the anode; the area was sufficient to provide a current of over 1 ampere per unit without saturation. In order to provide uniform ionization on the average over the whole area of the light beam, which traversed a path 1 cm square along the axis of the tube, successive units were rotated 90° with respect to each other about the axis. Each cathode was heated by a separate secondary coil of a transformer, and each unit had its own ballast resistances, so the several units could be operated very stably in parallel.

The ionized gas was helium at the pressure (1.5 mm of mercury) which had been found to give maximum ionization. The pressure was measured with a butyl phthallate gauge; a mercury gauge would, of course, have contamined the helium and given rise to objectionable mercury lines in the ionization tube. Helium was used because it has no spectral lines near the mercury green line, and so permitted the use of a low resolving power monochromator and consequently a maximum intensity of light.

Results and Interpretation

One hundred and ninety-six (196) exposures were made with the helium alternately ionized and unionized. The average difference was $(1.4\pm0.9)\times10^{-4}$ fringe; this is clearly a null result. It corresponds to a frequency shift of one part in $600{,}000/(1.4\times10^{-4})=4\times10^{9}$.

By using this result in formulae (1) we can show that the nebular redshift is not to be attributed to interstellar electrons in a static universe. The value of ρ in similar circumstances has been determined by the Langmuir probe method by Kenty,[6] and Compton and Eckart[7] and Druyvesteyn,[8] and from line absorption measurements by de Groot.[9] Their results enable us to set $\rho=5\times10^{12}$. The length of the ionized path, l, is 40 cm. Therefore from Eq. (1)

$$k=\frac{\delta\nu/\nu_0}{\rho l}=\frac{1.4\times10^{-4}}{6\times10^{5}\times5\times10^{12}\times40}=1.2\times10^{-24}.$$

This is to be regarded as an approximate upper limit to the possible magnitude of the mean fractional shift per electron.

Now Hubble's value of $(1/l)(\delta\nu/\nu_0)$ is 6.0×10^{-28} per cm, from which and the above value

[5] Kennedy and Thorndike, Phys. Rev. **42**, 400 (1932).

[6] Kenty, Phys. Rev. **32**, 625 (1928).
[7] Eckart, Phys. Rev. **25**, 139 (1925).
[8] Druyvesteyn, Zeits. f. Physik **64**, 781 (1930).
[9] De Groot, Zeits. f. Physik **60**, 617 (1930).

of k we find by Eq. (1) the value of the density of intergalactic electrons

$$\rho \geq 5.0 \times 10^{-4} \text{ per cc.}$$

Making the least favorable assumption for the present purpose, i.e., that intergalactic matter consists entirely of doubly-ionized calcium, the number of atoms per cc is one-half of ρ, or 2.5×10^{-4}, and since the mass of the calcium atom is 6.7×10^{-23}, the corresponding density of matter is $\rho_0 = 1.7 \times 10^{-26}$.

It has been shown[10] that there are but three possible types of static universe, i.e., those characterized by the line elements of Einstein, of de Sitter and of the restricted theory of relativity. Of these only the first allows an appreciable density of matter, and for it we have the relation[11] $1/R^2 = 4\pi(\rho_0 + p)$, where R is the radius of curvature of a spatial section of the universe and p the mean pressure exerted by the matter of the universe; both ρ_0 and p are expressed in relativistic units in which the velocity of light and the gravitational constant are made equal to unity. Since p is presumably not negative, evidently $R \leq (1/4\pi\rho_0)^{\frac{1}{2}}$. Translating this expression into c.g.s. units and substituting our computed value of ρ_0 we find $R \leq 7.1 \times 10^{25}$ cm $= 7.6 \times 10^{7}$ light-years. But this is only about a sixth of the distance to which the 100-inch telescope has penetrated, and so can scarcely be a plausible value for the radius of the universe. Hence we conclude that our hypothetical mechanism of the nebular redshift is not tenable. Abraham's theory, according to which k turns out to be about one-half our computed value, is likewise contradicted by this conclusion.

Another fairly obvious test of a theory of the kind here proposed is suggested by the existence of the interstellar calcium cloud in our own galaxy. Here as in intergalactic space the calcium is almost entirely doubly ionized, so one might expect the lines of the remoter stars to exhibit a shift proportional to distance. At the time when the experimental test was undertaken, however, the best figures on the electron density in the cloud (those of Gerasimovič and Struve[12]) were too low to provide as sharp a test as the experimental one. But since then Eddington[13] has demonstrated very plausibly that the density is at least 200 times as great as had been computed by the previous writers. Since a value of $\delta\nu/\nu_0$ of a very few parts in a million could probably be detected on averaging out Doppler effects, and Eddington's value of ρ is around 10^{-2} per cc, we should find for $l = 10{,}000$ light-years $\simeq 10^{22}$ cm a value of k from Eq. (1)

$$k \simeq 10^{-6}/(10^{-2} \times 10^{22}) = 10^{-26};$$

this is too small to yield the *intergalactic* shift. This result provides good confirmation of our conclusion against the general effect, and in addition rules out Abraham's value for k, which is too small to be tested by the experiment.

Finally our hypothesis and Abraham's appear to require an asymmetrical broadening toward the red in the Fraunhofer lines. The electron densities and optical depths of the stellar chromosphere and photosphere are still controversial but apparently are sufficient to yield (on this theory) shifts which could not well have escaped observation.

[10] See for example Tolman, *Relativity, Thermodynamics and Cosmology* (Oxford, 1934), p. 333, et seq.
[11] Tolman, reference 10, p. 340.
[12] Gerasimovič and Struve, Astrophys. J. **69**, 7 (1929).
[13] Eddington, M. N. of Roy. Astronom. Soc. **95**, 2 (1934).

The Absorption of Neutrons Detected by Boron and Lithium

DANA P. MITCHELL, *Pupin Physics Laboratories, Columbia University*

(Received January 20, 1936)

The neutron-nucleus collision cross sections of various elements have been investigated for neutrons that are detectable by means of (1) the boron and (2) lithium neutron capture reaction and that are strongly absorbed by cadmium. The collision cross section for such slow neutrons detected by boron is for hydrogen about 75 percent of that for neutrons detected by lithium, for HgO about 72 percent, for Sm about 180 percent, and for Al, B, C, Fe, and Li is the same within 10 percent for either boron or lithium detection. With either detector the absorption of cadmium and boron each approximates a single exponential, the absorption coefficient in each case not decreasing more than 25 percent for intensity reduction of 90 percent. The absorption coefficient of lithium for neutrons detected by boron decreases 40 percent, and for neutrons detected by lithium decreases about 30 percent at thicknesses that reduce the intensity 85 percent. Measurements were made with slow neutrons passed through an 8-mm paraffin layer. With lithium detection less than 10 percent increase in the absorption of Ag, HgO, boron glass (Pyrex), and Rh was observed when the temperature of the paraffin layer was changed from 293 to 90°K. The velocity distribution of the neutrons strongly absorbed by cadmium was approximately the Maxwellian for thermal equilibrium at room temperature; but when the paraffin was at the temperature of liquid air the neutron velocity distribution was too broad and flat to be described as Maxwellian for any particular temperature, although the distribution was shifted toward that for the lower temperature. The lithium reaction was found to be a sensitive detector of neutrons whose velocity is much higher than the mean thermal velocity at room temperature and well above the strong absorption range of cadmium. The collision cross section for neutrons, from paraffin at room temperature, that were filtered through 1 gram per cm² of cadmium was found to be larger in Rh, HgO, Au, and B than in cadmium. After filtering through 11.5 g per cm² of cadmium, the cadmium absorption was reduced to about a normal value for very high speed neutrons, collision cross section about 5×10^{-24} cm².

INTRODUCTION

THAT the probability of capture of neutrons is a function of the neutron velocity was shown by the well-known experiment of Fermi and his associates,[1] wherein they discovered that induced radioactivity can be greatly enhanced by surrounding the ordinary Rn–Be neutron source with paraffin or water. It was pointed out by Fermi that the increase in cross sections thus indicated was attributable to the reduction of the velocity of the neutrons by collision with hydrogen nuclei as they passed through the paraffin.

With the exception of the work in this laboratory, most of the investigation of these slow neutrons has been made with radioactive detectors. The purpose of the investigation here reported was twofold: (1) To obtain information concerning variations of neutron-nucleus collision cross sections of various elements for neutrons detected by means of the boron and lithium neutron capture reactions; (2) To investigate the neutron-nucleus interaction in some representative elements for neutrons not strongly absorbed by cadmium.

Disintegration by slow neutrons

When a neutron is captured by B^{10} or Li^6 the capturing nucleus is disintegrated[1,2] in accord with the following reactions:[3]

$$_5B^{10}+{}_0N^1={}_3Li^7+{}_2He^4,$$
$$_3Li^6+{}_0N^1={}_2He^4+{}_1H^3.$$

These two reactions are almost unique, as nitrogen is the only other element known[4] to be disintegrated directly by slow neutrons. The energy of the heavy particles emitted is such that they produce sufficient ionization in air to be easily detected.

Apparatus

The detecting apparatus consists of an ionization chamber, linear amplifier, and thyratron actuated counter previously described.[5] The

[1] Amaldi, d'Agostino, Fermi, Pontecorvo, Rasetti and Segrè, Ricerca Scient. **2**, 282, 380 (1934); Proc. Roy. Soc. **A149**, 522 (1935).

[2] Chadwick and Goldhaber, Nature **135**, 65 (1935).

[3] Taylor and Goldhaber, Nature **135**, 341 (1935).

[4] Chadwick and Goldhaber, Proc. Camb. Phil. Soc. **31**, 612 (1935).

[5] J. R. Dunning, G. B. Pegram, G. A. Fink and D. P. Mitchell, Phys. Rev. **48**, 265 (1935).

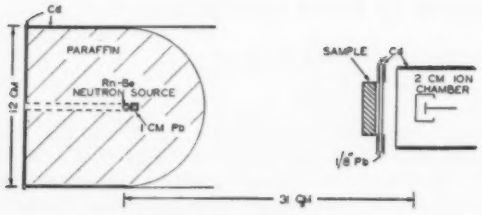

FIG. 1. Experimental arrangement for slow neutron absorption measurements.

chamber is lined with rolled lithium foil or coated with powdered boron with a little aquadag[6] as binder. The general arrangement of the source, absorber, and chamber is illustrated in Fig. 1.

Slow and Cd residual neutrons

Although most of the neutrons detected by these chambers are stopped by as little as 0.5 mm thickness of cadmium, many of the neutrons not so stopped—and in fact, those which pass through as much as 1.0 cm of cadmium—are detected. With the same chamber, the relative number of these residual (cadmium-penetrating) neutrons depends upon the amount of paraffin surrounding the source.[7] The size of the paraffin sphere shown in Fig. 1 is somewhat less than the optimum size to give a maximum number of slow neutrons that are within the strong absorption region of cadmium. With this arrangement, the residual neutrons represented about 19 percent of all neutrons detected with the boron chamber, and about 15 percent with a representative lithium chamber. Usually the collision cross section for these residual neutrons is much less than that of those neutrons which are stopped by cadmium. For this reason it has been our[8] custom to deduct this *residual neutron* count in all the determinations of *slow* neutron cross sections made in these laboratories.

Although it is probable that most of the neutrons referred to in the literature as "slow" do have energies approximating the thermal energy of the hydrogen in the material in which they were slowed down, the term has in general been applied to all neutrons having insufficient energy to produce measurable ionization by the projection of protons. Since an appreciable fraction of the residual neutrons detected by these chambers are sufficiently fast to project hydrogen nuclei, the word "slow" will be printed in italics when it is restricted to those neutrons which lie within the strong absorption region of cadmium.

Experiments with a chamber in which only the front was coated with a layer of lithium metal, 0.09 mm thick, also gave a residual of 15 percent. The effect of moisture in this lithium-lined chamber was demonstrated by breaking the seal, thereby permitting diffusion of air from the room into the chamber. Under these conditions, the residual ratio was more than doubled in two days.

This was probably due to a decrease in the efficiency of detection of *slow* neutrons due to the increased absorption of disintegration particles, from within the lithium, by the hydroxide on the surface, and an increase in the efficiency of detection of higher energy neutrons by the projection of hydrogen nuclei.

BORON *vs.* LITHIUM DETECTION

Slow neutrons are usually obtained from a source of high speed neutrons by multiple collision with hydrogen nuclei, so it is interesting to note first that the hydrogen collision cross section for *slow* neutrons detected by boron is somewhat less than for those detected by lithium. The value here obtained is 26 ($\times 10^{-24}$ cm^{-2}). For *slow* neutrons detected by lithium,[5] this value is about 35. Table I gives other collision cross sections as measured by boron and lithium detection.

TABLE I. *Nuclear collision cross section for neutrons stopped by 1 g/cm² of cadmium.*

MATERIAL	BORON DETECTION Transmission (Approximate)	BORON DETECTION Cross section ($\times 10^{24}$ cm²)	LITHIUM DETECTION Transmission (Approximate)	LITHIUM DETECTION Cross section ($\times 10^{24}$ cm²)
Al	0.7	2.0±0.3	0.75	1.5±0.2
C	.5	4.8± .4	.5	4.1± .4
Fe	.6	11.8± .6	.5	12± .5
HgO	.7	260±25	.6	360±40
Sm	.3	9000±25%	.5	5000±25%

Cadmium absorption

Although other elements such as gadolinium and samarium have been found[5] to have a larger absorption cross section for *slow* neutrons, cad-

[6] Acheson's Colloidal Graphite, National Carbon Co.
[7] J. R. Dunning and G. B. Pegram, Phys. Rev. **47**, 640 (1935).
[8] J. R. Dunning, G. B. Pegram, G. A. Fink and D. P. Mitchell, Phys. Rev. **47**, 416 (1935).

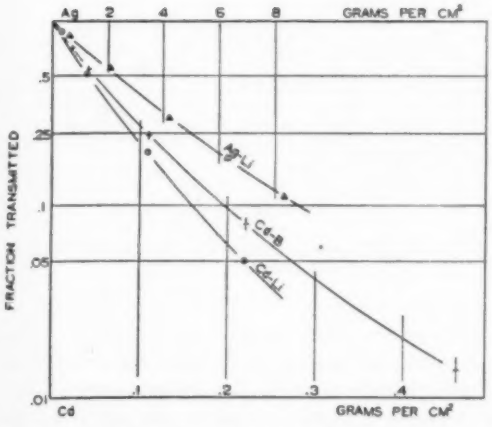

FIG. 2. Absorption of Ag by Li detection, of Cd by Li detection, and of Cd by B detection.

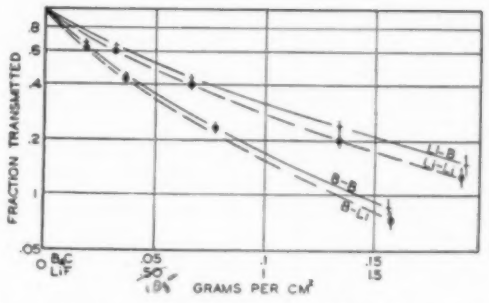

FIG. 3. Absorption of slow neutrons in Li and B measured with B and Li detectors.

mium is particularly important because it is the most available for use in large quantities and is easily rolled into sheets of any desired thickness.

Fig. 2 shows that the absorption by cadmium of *slow* neutrons detected by boron is approximately exponential (the absorption coefficient changing not more than 20 percent for an intensity reduction of 90 percent), as was found[5] to be the case for *slow* neutrons detected by lithium.

Boron and lithium absorption

Investigators[9, 10] using radioactive detectors have found that in general the collision cross section for slow neutrons is largest for a given element when that element is used as a detector. Measurements of the absorption of a large range of thicknesses of both lithium and boron, when detected by their disintegration, indicate that the basic cross section of these elements is practically the same for *slow* neutrons detected by boron as for those detected by lithium. These data are shown in the accompanying plot, Fig. 3, of the logarithm of slow neutrons transmitted against the mass per square centimeter of the absorbing sample. In each case, the absorber was placed in front of the ionization chamber as in Fig. 1. The lithium was in lithium fluoride, and the boron in B_4C[11] mixed with talc. The *slow* neutron cross section of the fluorine is 2.5×10^{-24} cm^{-2}, and the carbon as in Table I. The mass per unit area is the effective mass, account having been taken of the obliquity of part of the beam and the variation in intensity from different zones of the paraffin sphere. Such correction is very small, amounting to a maximum of about 3 percent for transmission of less than 0.1. The correction for the absorption of the talc in which the B_4C was mixed is only 7 percent.

The curvatures in Figs. 2 and 3 are, though small, an indication that the quality of the neutron beam is being changed by the filtering in the absorber itself. The change in cross section of the neutrons filtered out by the first layers of the absorber is more readily noticed by inspection of Table II. Here the cross sections are given as computed from measurements on the thin and thick samples of these absorbing materials. This effect is even less in silver than in cadmium—or, in other words, the absorption curve of silver for

TABLE II. *Effect of filtering on collision cross section for neutrons stopped by 1 g/cm² of cadmium.*

Material	Boron Detection: Transmission	Boron Detection: Cross section ($\times10^{24}\times$cm²)	Boron Detection: Decrease (%)	Lithium Detection: Transmission	Lithium Detection: Cross section ($\times10^{24}\times$cm²)	Lithium Detection: Decrease (%)
Ag				0.55	51	
				.11	47	8
Cd	0.55	2600		.52	2900	
	.07	2200	15	.07	2300	20
	.01	1800	30			
B	.65	510		.6	580	
	.08	370	27	.08	440	24
Li	.6	70		.6	70	
	.15	40	43	.13	50	29

[9] P. B. Moon and J. R. Tillman, Nature **135**, 904 (1935).
[10] Amaldi and Fermi, Ricerca Scient. **2**, 11–12 (1935).
[11] R. R. Ridgway (Norton Co.), Trans. Elect-Chem. Soc. **66**, 293 (1934).

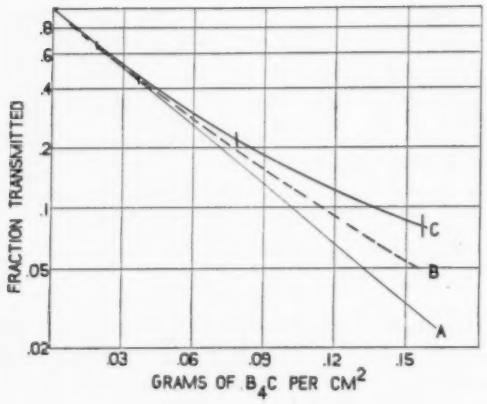

FIG. 4. *A*, the exponential form; *B*, the theoretical $1/V$ curve; *C*, absorption in boron observed with boron detector.

slow neutrons is more nearly exponential, as may be seen in Fig. 2.

Analysis[12] with a mechanical velocity selector has shown that the velocity distribution of slow neutrons that are highly absorbed by cadmium and detected by lithium, has a maximum closely coinciding with the maximum in a Maxwellian distribution; or, more specifically, the velocity distribution of these neutrons is approximately that to be expected if the neutrons are in thermal equilibrium in the paraffin from which they emerge. If the capture probability were, as currently[13] predicted, proportional simply to $1/V$, then the values of the integral

$$f(q) = \int_0^\infty e^{-q/V - V^2} V^3 dV$$

should represent a typical absorption curve for these slow neutrons.

As Mr. H. C. Torrey has computed the values of this integral, such a theoretical absorption curve has been plotted in Fig. 4 for comparison with one of the observed curves.

Cold neutrons

Another approach to the relation of the velocity of neutrons to the probability of capture has been made by several investigators, who observed the change in the efficiency of radioactive detectors when the temperature of the hydrogenic material in which the neutrons are slowed down is changed.

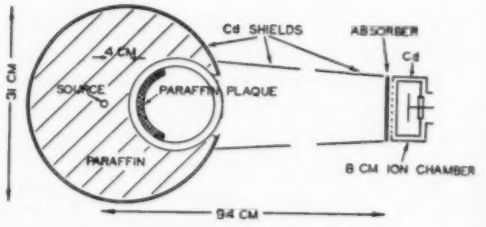

FIG. 5. Experimental arrangement for "cold" neutron absorption measurements.

Dunning, Pegram, Fink and Mitchell[14, 15] observed both a small increase in lithium detection efficiency and a small increase in the absorption of cadmium when the water through which the neutrons passed was lowered to the temperature of liquid air. Moon[9] and Tillman[16] observed a considerable increase in radioactivity induced in several substances when the paraffin used to slow down the neutrons was cooled from room temperature to 90°K.

Recently such experiments[17] have been made by Westcott and Miewodniczanski, who worked with temperatures of 77 and 20°K.

In the present experiment, the cold paraffin was in the form of a plaque 1 cm thick, so placed that neutrons already slowed down in paraffin at room temperature had to pass through this cold plaque before penetrating the absorber. The arrangement of the plaque in a soda glass Dewar partially surrounded by paraffin and Cd shields is shown in Fig. 5.

The cold paraffin was relatively thin, in order to avoid the high absorption of the very slow neutrons disclosed by the experimental work of Lukirsky and Zarewa.[18]

The results of the lithium detection measurements of the absorption in various materials of

[12] J. R. Dunning, G. B. Pegram, G. A. Fink, D. P. Mitchell and E. Segrè, Phys. Rev. **48**, 704 (1935).
[13] H. A. Bethe, Phys. Rev. **47**, 747 (1935).
[14] J. R. Dunning, G. B. Pegram, G. A. Fink and D. P. Mitchell, Phys. Rev. **47**, 796 (1935).
[15] J. R. Dunning, G. B. Pegram, G. A. Fink and D. P. Mitchell, Phys. Rev. **48**, 888 (1935).
[16] J. R. Tillman and P. B. Moon, Nature **136**, 66 (1935).
[17] Westcott and Miewodniczanski, Proc. Camb. Phil. Soc. **31**, 617 (1935).
[18] P. Lukirsky and T. Zarewa, Nature **136**, 681 (1935).

TABLE III. *Effect of cooling paraffin plaque in the path of slow neutrons. Lithium detection.*

MATERIAL	Ag	Cd	HgO	Pyrex	Rh
			FRACTION ABSORBED		
Neutrons stopped by 1 g/cm² of Cd					
293°K	0.47	1.0	0.50	0.54	0.44
90	.51	1.0	.53	.54	.47
Ratio	1.09	1.00	1.06	1.00	1.07
All neutrons detected					
293°K	0.38	0.78	0.39	0.41	0.38
90	.42	.79	.42	.44	.38+
Ratio	1.11	1.01	1.08	1.07	1.01

neutrons that have passed through the plaque in Fig. 5 are given in Table III. This table shows the fraction of *slow* neutrons absorbed when the plaque was at room temperature and when at liquid-air temperature, together with the increase in absorption in the latter case over the former, expressed as the ratio of the two absorption values. Investigators reporting similar experiments made with radioactive detectors have usually expressed such a ratio for all neutrons that affect the detector. For this reason, the second part of the table shows the absorption for all neutrons detected by lithium, instead of just those which are highly absorbed by cadmium.

The cadmium referred to in this table was that used to sort out the *slow* neutrons, and hence its absorption is 100 percent for those neutrons. Its absorption in the second part of the table indicates that the cadmium residual amounted to about 22 percent of all the neutrons detected. The precision of the "fraction absorbed," based upon the square root of the number of counts, is about ±2 percent. Differences such as those between the silver and mercury oxide are insignificant. Consistent with the earlier work[5] using lithium detection, the effect of cooling the neutron source under these conditions is notably less than that found with the radioactive detectors.

A velocity selector analysis, with lithium detection, of the velocity distribution of the *slow* neutrons from this "cold" source has shown[19] a much flatter distribution than the Maxwellian, for any particular temperature. This distribution appears consistent with the smallness of the ratios in Table III, but whether it is attributable to conditions at the source, to selective absorption in the intervening material, or to selectivity in the lithium reaction, is not yet clear.

Note added in proof: Recent experiments by Mr. Fink with the type of source described below in which the neutrons do not come through the walls of the Dewar and in which all the paraffin is cooled, have shown a much greater effect from cooling.

[19] G. A. Fink, J. R. Dunning, G. B. Pegram and D. P. Mitchell, Phys. Rev. **49**, 103 (1936).

RESIDUAL NEUTRONS

The effects of self-filtering mentioned previously, shown in Table II, are of sufficient interest to demand further investigation. When thicker samples are used, the measurements with lithium detection can no longer be confined to those neutrons which are stopped by 1 gram per square centimeter of cadmium. The residual neutrons—or, more specifically, those which pass through such a cadmium absorbing screen—become of principal importance. As the neutrons penetrating such thick absorbers are relatively few in number, the large ionization chamber shown in Fig. 5 was again used, together with a source that was recently developed in these laboratories by Mr. George Fink. This new source, and the general arrangement used in the following experiments with residual neutrons, is shown in Fig. 6. With this arrangement the slow neutron yield from this source is about six times that from a 12-cm diameter paraffin sphere in the same position. Measurements were made of the absorption of cadmium ranging from 29 milligrams to 11½ grams per square centimeter. The results are shown in Table IV.

TABLE IV. *Absorption by Cd of residual neutrons through Cd.*

FILTER (g/cm²) ABSORBER (g/cm²)	None	0.029	0.89	1.78
	collision cross section (×10²⁴ cm²)			
0.029	2300			
.42	1200			
.89	600	31		
1.78	310	26	22	
3.55	160	17	12	7.5
7.1	82	12	9	7.0
11.5	51	8	6	4.7

The effect of self-filtering is very evident, as the cross section determined from the individual samples ranges from over 2000 down to about 50 (each of the values here stated should be multi-

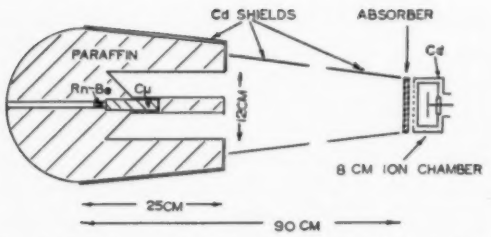

FIG. 6. Experimental arrangement for residual neutron absorption measurements.

plied by 10^{-24} cm^{-2}). The cross section in cadmium has really dropped to a much lower value for some of these neutrons. The additional columns in Table IV show the cross sections for neutrons that have filtered through cadmium screens of various thicknesses.

The continued decrease in cross sections with increased filtering probably indicates that the region of lithium detection includes neutrons which are well outside of the region of strong absorption in cadmium.

Other measurements of the absorption of cadmium, using those neutrons which pass through a boron carbide filter that contains 0.21 gram of boron per square centimeter, indicated a cadmium cross section of 60 when the cadmium absorbed 22 percent of the filtered neutrons, and of only 12 when enough cadmium was used to absorb 29 percent of these neutrons previously filtered through boron.

This indicates that the region of neutron energy most highly absorbed by cadmium is not the same as the energy band most highly absorbed by boron.

TABLE V. *Collision cross section for Cd residual and Cd absorbed neutrons.*

	Residual Neutrons			Cd Absorbed Neutrons	
Material	Absorber (g/cm^2)	Transmission	Cross section ($\times 10^{24}$ cm^2)	Cross section ($\times 10^{24}$ cm^2)	Reference
Ag	2.07	0.86	13	51	21
Au	2.53	.80	29	88	5
B	.22	.77	22	535	22
Cd	3.55	.84	12	3300	5
HgO	.57	.94	39	360	5
Rh	.72	.78	59	115	5

Residual neutron absorption data for other elements is shown in Table V. The experimental arrangement was as in Fig. 6, and the residual neutrons are those that passed through a cadmium filter of 1 gram per square centimeter. For comparison, the absorption cross section for the usual *slow* neutrons is given in the fifth column.

An item of particular interest is that the cross section in mercury oxide, rhodium, and possibly gold is for these residual neutrons larger than that of boron and even cadmium.

These results add to the evidence that neutron absorption is selective and characteristic of the absorbing nuclei. The differences among neutrons that lead to selective absorption are most simply, and adequately so far as required by these experiments, ascribed to differences in neutron velocity. A somewhat similar result was recently reported by Szilard,[20] who, with an indium detector, found the absorption of cadmium-filtered neutrons to be much smaller in cadmium than in indium.

As Amaldi[10] and Fermi have recently reported results on selective absorption, using radioactive detectors, the following experiments were performed.

With a lithium detector, silver and mercury oxide absorbers, each of which transmitted about 50 percent of the neutron beam, were measured together, likewise a combination of rhodium and mercury oxide absorbers was measured. In each case the transmission of the two absorbers together was found to be equal to the product of their individual transmissions within the statistical error.

The author wishes to express his obligation to Professor George B. Pegram, who suggested the general problem; to Professor J. R. Dunning, for his assistance and friendly encouragement during the progress of this work; to Professor E. Segrè and Mr. George Fink for assistance in the laboratory.

[20] Szilard, Nature **136**, 950 (1935).
[21] D. P. Mitchell, J. R. Dunning, G. B. Pegram, Phys. Rev. **49**, 199 (1936).
[22] D. P. Mitchell, J. R. Dunning, E. Segrè, G. B. Pegram, Phys. Rev. **48**, 774 (1935).

Note on Electron-Neutron Interaction

E. U. CONDON, *Palmer Physical Laboratory, Princeton University*

(Received February 3, 1936)

Assuming a possible short-range interaction between electrons and neutrons of the form $V=K\delta(\mathbf{r}_N-\mathbf{r}_e)$ where δ is the Dirac delta function and $\mathbf{r}_N$ and $\mathbf{r}_e$ are the vector positions of electron and neutron, respectively, it is shown that probably $|K|<30mc^2(e^2/mc^2)^3$ from consideration of the effect of the interaction on slow neutron scattering cross sections. If K is positive and a little less than this upper limit this interaction could be responsible for the observed isotope displacement of spectral energy levels.

IN most theoretical speculations of nuclear physics it is usual to omit consideration of terms in the Hamiltonian corresponding to short range forces between electrons and neutrons. In this note the situation is examined more closely.

Dee[1] showed that fast neutrons do not produce more than one ion pair in three meters of air path at normal conditions by interaction with the electrons. As there are 15 electrons in an air molecule and 2.7×10^{19} molecules/cm^3 this result says only that the cross section between electrons and neutrons (of about 5 MEV energy) is less than 8.3×10^{-24} cm^2. But this is not a very small upper limit being in fact larger than the cross section for scattering of fast neutrons by protons.

It is generally felt that the actual cross section must be very much smaller than this. If we suppose the interaction between the neutron and electron to be represented by a potential well (*or* wall) of depth (*or* height) V and radius of action a then the wave function of an electron's motion relative to the neutron is given by

$$\Delta\psi+(2m/\hbar^2)[W-V(r)]\psi=0$$

and the approximate solution due to Born for the scattering is

$$\psi=e^{ikz}-\frac{1}{4\pi}\frac{2m}{\hbar^2}\int\exp(i\Delta\mathbf{k}\cdot\mathbf{r})\,V(r)dv\cdot e^{ikr}/r$$

where $\hbar\Delta\mathbf{k}$ is the vectorial change in momentum of the electron in the scattering. The second term becomes $(\pm2ma^3V/3\hbar^2)e^{ikr}/r$ so in the usual way this gives for the total cross section

$$\sigma=4\pi(2ma^3V/3\hbar^2)^2$$

on the assumption that the electron wave-length associated with the change of momentum is large compared to the range of the interaction forces. A "reasonable" value for V is mc^2 and for a is (e^2/mc^2) so on this basis the expected "reasonable" cross section for scattering of electrons by neutrons is $\sigma=(16/9)\alpha^4\pi a^2$, where $\alpha=e^2/\hbar c$ or numerically, $\sigma=1.24\times10^{-32}$ cm^2. To get a cross section as large as Dee's upper limit one would need to have V equal to $2.6\times10^4mc^2$ if one keeps to the same range. This is "unreasonable" nor would it be "reasonable" to get the larger cross section by retaining mc^2 for V and increasing the range of action of the forces. Of course this calculation is really for a free electron rather than an electron bound in an atom but since for a 5 MEV neutron the energy of relative motion of electron and neutron (2500 volts) is large compared to the binding energy it is probable that the order of the result is not much different from the result of a calculation which does not neglect the binding.

Such considerations have been more or less generally known for some time. They make it desirable to have another approach which gives a smaller upper limit to the possible interaction. This is provided by consideration of the possible effect of electron-neutron interaction on the scattering of slow neutrons.

When the neutron energy is small, of the order of thermal energy, there is no possibility of excitation of the atom by the neutron impact so we are dealing with an elastic collision. The usual molecular considerations apply here to indicate that the slow moving neutron will

[1] Dee, Proc. Roy. Soc. **A136**, 727 (1932).

move in an effective potential field given by considering the normal electronic level of the "molecule" of atom+neutron. If we assume a force law of negligible range (alongside of atomic dimensions) we may write $V=K\delta(\mathbf{r}_N-\mathbf{r}_e)$ where K is the $4\pi Va^3/3$ of the square potential well, and the other is the Dirac δ function in three dimensions normalized so its volume integral is unity.

Then if $\rho(r_e)$ is the electron density in the atom and the neutron interaction is supposed weak enough not to affect it the potential energy of the system atom+neutron differs by $V(r)=K\rho(r)$ from the energy with the neutron absent. The scattering of slow neutrons by the atom will be governed by the wave equation

$$\Delta\psi+(2M/\hbar^2)[W-K\rho(r)]\psi=0,$$

in which M is the reduced mass of neutron and atom and W is the energy of the internal or relative motion.

The elastic scattering is given by an expression of the same form as before, with these differences, that now we are dealing with a long range force determined by the distribution in space of the bound electrons and the mass is here M instead of the electron mass m. The wave-length is now comparable with the range of the forces so the integral is a little more complicated. However it is the same function of electron density as the structure factor used in x-ray scattering work. Calling the coefficient of e^{ikr}/r in the scattered wave $f(\theta)$ we have

$$f(\theta)=-(4\pi)^{-1}\int \exp ik(\mathbf{n}_0-\mathbf{n})\cdot\mathbf{r}K\rho(r)(2M/\hbar^2)\,d\tau$$

$$=(2M/4\hbar^2)\int_0^\infty \frac{\sin \kappa r}{\kappa r}K\rho(r)r^2dr,$$

where $\kappa=(4\pi\sin\theta/2)/\lambda$ and λ is the de Broglie wave-length of the relative motion, $h/(2MW)^{\frac{1}{2}}$. By introducing the structure factor $F(\kappa)$ as defined on p. 140 of Compton and Allison, *X-Rays and Electrons*, this is

$$f(\theta)=-(2M/\hbar^2)K(4\pi)^{-1}ZF(\kappa)$$

so, as usual the differential cross section for scattering into $d\omega$ is

$$|f(\theta)|^2d\omega=(K^2M^2Z^2/4\pi^2\hbar^4)F^2(\kappa)d\omega.$$

The total cross section is then

$$\sigma=\sigma_0\frac{2}{\kappa^2}\int_0^\kappa F^2(\kappa)\kappa d\kappa$$

with $\kappa=4\pi/\lambda$ and $\sigma_0=4\pi(2MZK/\hbar^24\pi)^2$. Since $F^2(\kappa)\to1$ for $\kappa\to0$ it follows that σ_0 is the limiting value of the cross section.

The value of σ_0 in this case is larger than for the scattering of fast, free electrons by the factor $Z^2(M/m)^2$. Thus for scattering of slow neutrons by atomic hydrogen one need have K only 1/920 as great to get the same cross section as for the previous work.

We have next to consider the value of the integral over the form factor occurring in the cross section expression. For a first orientation the electron distribution is satisfactorily given by the Fermi-Thomas statistical method and for this distribution the form factor may be found in Compton and Allison, p. 148. From this the integral was calculated as a function of J where J is a complicated expression which reduces to $J=6.6V^{\frac{1}{2}}Z^{-\frac{1}{3}}$ where V is the value of the relative energy in electron volts. We find for $G(J)$ where $\sigma=\sigma_0G(J)$

J	$G(J)$	J	$G(J)$	J	$G(J)$	J	$G(J)$
0.0	1.00	0.6	0.18	0.3	0.38	0.9	0.11
.1	.74	.7	.15	.4	.30	1.0	.09
.2	.53	.8	.13	.5	.23	1.5	.05

The average relative energy Ve is equal to $\frac{1}{2}Mv^2$ where v is the average relative velocity of the neutron and the atom, if the atoms are at rest and the neutrons have room temperature thermal energy, $V\sim1/40$. For hydrogen then $J\sim1$ so the correction owing to the structure factor amounts to a factor of about 0.1. In addition there is another factor which undoubtedly plays a role here—the zero-point energy of oscillation of the atoms in a molecule.[2] For hydrogen this may amount to $V\sim\frac{1}{4}$ volt or ten times the thermal energy. This tends to cut down the cross section still more. In comparing hydrogen and deuterium the zero-point energy

[2] This idea that the zero-point oscillations of the hydrogen in a molecule may affect the slowing of neutrons by matter was suggested by Professor Rabi in a conversation last fall. See also Halban and Preiswerk, Nature **136**, 951 (1935) for experimental indications of such an effect.

will be less in the latter so this would tend to make the deuterium cross section greater. Also the difference in the reduced masses relative to the neutron introduces a factor of 16/9 in the ratio of the cross sections. Both work however to make the hydrogen cross section less than that for deuterium whereas Dunning[3] finds 35×10^{-24} cm^2 for hydrogen and 4×10^{-24} cm^2 for deuterium.

For heavier atoms the zero-point energy is negligible and owing to the appearance of Z^{-1} in J the form factor average $G(J)$ does not change by more than a factor of two. So the electron-neutron interaction would vary smoothly as Z^2. As there is no trace of such a "Moseley law" for the slow neutron cross sections we must conclude that this possible manifestation of the interaction contributes less than 10^{-24} cm^2 to the slow neutron scattering cross section of hydrogen.

If this be so one can set the limit

$$|K|<30mc^2(e^2/mc^2)^3,$$

which is much lower than the limit

$$|K|<2.6\times10^4mc^2(e^2/mc^2)^3,$$

which one sets from Dee's study of the upper limit of the ionization produced by fast neutrons.

Another way in which electron-neutron interaction would manifest itself is in the isotope displacement of spectral terms. If the interaction energy is of very short range type as we have been supposing then the energy difference between a heavier and a lighter isotope due to this interaction will be K times the total electron density at the origin for each neutron added to the nucleus. The particle density at the origin is zero except for s electrons, and the only contribution that will be observable in the shift of frequency of a spectrum line will be that from the particular s electron that is involved directly in the optical transition which produces the line.

Accordingly the energy is raised by $K\psi^2(0)$ for each neutron if the electron-neutron interaction is repulsive, where $\psi^2(0)$ is the particle density at the origin for a valence electron. Breit[4] has discussed the observed isotope shifts from the standpoint of the effect of departure from the Coulomb law associated with a change in nuclear radius for the different isotopes. The formulas occurring in that discussion also require a knowledge of $\psi^2(0)$ so we may use the values that he calculates to estimate how large K must be to explain the entire effect as due to electron-neutron interaction. Here the levels are observed to be raised in going to heavier isotopes indicating electron-neutron *repulsion* if this interaction is mainly responsible for the isotope shift. The sign of K is not determined by the scattering considerations so this is a new bit of information.

In the 6s term of Hg II there is a difference of 0.52 cm^{-1} between Hg^{204} and Hg^{202}, that is, 0.26 cm^{-1} per neutron assuming the effect on the lines is all due to a shift of the s term. Breit calculates $\psi^2(0)=1.45\times10^{26}$ cm^{-3} for the 6s electron. Writing $K=kmc^2(e^2/mc^2)^3$, the whole shift is accounted for if $k=20$, which is consistent with the upper limit obtained from consideration of the slow neutron cross sections. The same value is obtained for Tl I 7s using $\psi^2(0)=0.17\times10^{26}$ cm^{-3} and an observed $\Delta\nu=0.03$ cm^{-1} per neutron. The data for Hg I 7s indicate $k=5.5$ so that there is no quantitative consistency except as to order of magnitude.

In conclusion, the foregoing discussion shows that electron-neutron interaction if of the form $K\delta(\mathbf{r}_N-\mathbf{r}_e)$ must have $K<30mc^2(e^2/mc^2)^3$ to be in accord with slow neutron scattering data; and if K is about of this magnitude, say from $\frac{1}{6}$ to $\frac{2}{3}$ of this upper limit, and is positive, such interaction could be the main source of the isotope displacement of spectral lines.

[3] Dunning, Pegram, Fink and Mitchell, Phys. Rev. **48**, 265 (1935).

[4] Breit, Phys. Rev. **42**, 348 (1932).

Remarks on the Polarization Effects in the Positron Theory

W. PAULI AND M. E. ROSE, *Institute for Advanced Study, Princeton, New Jersey*

(Received January 30, 1936)

A simple method of obtaining the induced charge-density four vector on the basis of the subtraction formalism of the positron theory is given. Further, in the general case of time-dependent fields the result is calculated directly without use of the Lorentz invariance of the theory.

INTRODUCTION

IT is the purpose of the following paper to show that the integrals which determine the additional polarization density δj_0 and the corresponding current density $\delta\mathbf{j}$, produced by an original charge density j_0 and a current density $\mathbf{j}$ according to the positron theory, can be evaluated in a simpler way than has been done previously.[1] We shall consequently restrict ourselves, however, to the approximation in which effects proportional to powers of the fine structure constant $\alpha=e^2/\hbar c$ higher than the first will be neglected. Then the connection between δj_0 and $\delta\mathbf{j}$ with the scalar and vector potential A_0 and $\mathbf{A}$ of the original field is a linear one and therefore there is no loss of generality if we use plane waves

$$A_0=a_0\exp\,(i[(\mathbf{k}\cdot\mathbf{x})-k_0t])+\text{conj.},\qquad \mathbf{A}=\mathbf{a}\exp\,(i[(\mathbf{k}\cdot\mathbf{x})-k_0t])+\text{conj.} \tag{1}$$

for the potential field. In the following we employ $\hbar/mc$ as the unit of length, $\hbar/mc^2$ as the unit of time and the electron mass m as unit of mass.

For the sake of simplicity we shall treat explicitly the particular case in which $\mathbf{A}=0$ and we shall be interested only in the charge density j_0 not in the current density $\mathbf{j}$. According to Serber[1] it is then not difficult to treat also the general case characterized by (1). In the particular case

$$A_0=a_0\exp\,(i[(\mathbf{k}\cdot\mathbf{x})-k_0t])+\text{conj.},\quad \mathbf{A}=0 \tag{1a}$$

where according to Maxwell's equations one has

$$j_0=(k^2/4\pi)A_0, \tag{2}$$

one gets according to Heisenberg[2] for the difference between the density matrix in the cases of the presence and of the absence of the external field in the approximation in question, after multiplication by the electron charge e and summation over the spin index, the expression

$$e\sum_{\rho=1}^{4}(\mathbf{x}',\rho\,|\,\delta R\,|\,\mathbf{x}'',\rho)=-\frac{\alpha}{\pi}F(\mathbf{k},k_0,\mathbf{x})j_0, \tag{3}$$

where

$$\mathbf{x}=\mathbf{x}'-\mathbf{x}'' \tag{4}$$

and F is given by

$$F(\mathbf{k},k_0,\mathbf{x})=\frac{1}{\pi k^2}\int\frac{\epsilon\epsilon'-(q^2+1-k^2/4)}{\epsilon\epsilon'}\times\frac{\epsilon+\epsilon'}{(\epsilon+\epsilon')^2-k_0^2}\exp\,(i(\mathbf{q}\cdot\mathbf{x}))d\mathbf{q} \tag{5}$$

with

$$\epsilon=[1+(\mathbf{q}+\mathbf{k}/2)^2]^{\frac{1}{2}},\qquad \epsilon'=[1+(\mathbf{q}-\mathbf{k}/2)^2]^{\frac{1}{2}}. \tag{6}$$

For large values of q, or what turns out to be the same, for small values of k one has the expansion

$$\epsilon\sim\epsilon'\sim(1+q^2)^{\frac{1}{2}}$$

and more exactly

$$\epsilon\epsilon'\sim 1+q^2+k^2/4-\tfrac{1}{2}(\mathbf{q}\cdot\mathbf{k})^2(1+q^2)^{-1},$$

so that we can separate F into two terms.

$$F(\mathbf{k},k_0,\mathbf{x})=F_0(\mathbf{k},\mathbf{x})+F_1(\mathbf{k},k_0,\mathbf{x}) \tag{7}$$

with

$$F_0(\mathbf{k},\mathbf{x})=\frac{1}{4\pi}\int\left[1-\frac{q^2\cos^2\vartheta}{1+q^2}\right]\frac{\exp\,(i(\mathbf{q}\cdot\mathbf{x}))}{(1+q^2)^{\frac{1}{2}}}d\mathbf{q}, \tag{8}$$

[1] W. Heisenberg, Zeits. f. Physik **90**, 209 (1934); R. Serber, Phys. Rev. **48**, 49 (1935); E. A. Uehling, Phys. Rev. **48**, 55 (1935).

[2] W. Heisenberg, reference 1, p. 221, Eq. (34) and p. 222 below.

ϑ being the angle between the direction of $\mathbf{q}$ and $\mathbf{x}$ and where F_1 is finite for $x=0$ and has there the value

$$f(\mathbf{k}, k_0) \equiv F_1(\mathbf{k}, k_0, 0)$$
$$= \frac{1}{\pi k^2} \int \left\{ \frac{\epsilon\epsilon' - (q^2+1-k^2/4)}{\epsilon\epsilon'} \frac{\epsilon+\epsilon'}{(\epsilon+\epsilon')^2 - k_0^2} - \frac{k^2}{4}\left[1 - \frac{q^2\cos^2\vartheta}{1+q^2}\right]\frac{1}{(1+q^2)^{\frac{1}{2}}}\right\} d\mathbf{q}. \quad (9)$$

While each of the parts in the latter formula decreases like $|\mathbf{q}|^{-3}$ for large values of $|\mathbf{q}|$ and therefore the corresponding parts of the integral are logarithmically divergent, the difference in the integrand decreases with the higher order $|\mathbf{q}|^{-5}$ so that the total integral is convergent. On the contrary the integral (8) which can be expressed by means of cylindrical functions is of the order $\log|\mathbf{x}|$ +const. for small values of $\mathbf{x}$.

The formalism of the positron theory, which is accepted at present and which unfortunately is not yet substituted by a more satisfactory one, does not identify, however, the physical electric charge density with the value of the left side of (3) for $\mathbf{x}=0$ but introduces first properly chosen subtractive terms depending on $\mathbf{x}$ in such a way that the difference is finite for $\mathbf{x}=0$ ("subtraction-physics"). One remains in agreement with the more general prescription of Heisenberg if, in the case here considered and in the approximation in question (terms proportional to α), one identifies the subtraction terms with $F_0(\mathbf{k}, \mathbf{x})$ given by (8). Then one gets, according to (3),

$$\delta j_0 = -(\alpha/\pi) f(\mathbf{k}, k_0) j_0, \quad (10)$$

where the function f is given by (9).

The Evaluation of the Integral

While Serber evaluates the integral (9) only for the particular case of $k_0=0$ (time-independent fields) and uses the Lorentz invariance of the subtraction-formalism to get the result for the general case, we shall here directly compute the general integral (9). For this purpose we introduce, besides the azimuth φ around the coordinate axis parallel to $\mathbf{k}$ the variables v, w defined by

$$\tfrac{1}{2}(\epsilon-\epsilon') = v, \quad \tfrac{1}{2}(\epsilon+\epsilon') = w, \quad (11)$$

where ϵ and ϵ' are given by (6). From the latter equations one gets, by computing the functional determinant, for the volume element of the $\mathbf{q}$ space the simple expression

$$d\mathbf{q} = (2/k)\epsilon\epsilon' dv dw d\varphi = (1/\kappa)\epsilon\epsilon' dv dw d\varphi. \quad (12)$$

Here we introduced the convenient abbreviation

$$k/2 = \kappa. \quad (13)$$

From (6) we get further

$$\tfrac{1}{2}(\epsilon^2+\epsilon'^2) = v^2+w^2 = q^2+\kappa^2+1, \quad (14a)$$
$$\tfrac{1}{4}(\epsilon^2-\epsilon'^2) = vw = \tfrac{1}{2}(\mathbf{qk}). \quad (14b)$$

From these equations there follows the inequalities

$$v^2w^2 \leqq \kappa^2(w^2-\kappa^2-1+v^2), \quad v^2 \leqq \kappa^2\frac{w^2-\kappa^2-1}{w^2-\kappa^2}.$$

We get the whole $\mathbf{q}$ space if we first for a given value of w integrate over the surface $w=$const., where v runs through the interval

$$-\kappa\left(\frac{w^2-\kappa^2-1}{w^2-\kappa^2}\right)^{\frac{1}{2}} \leqq v \leqq \kappa\left(\frac{w^2-\kappa^2-1}{w^2-\kappa^2}\right)^{\frac{1}{2}}, \quad (15)$$

and after that w runs from $(\kappa^2+1)^{\frac{1}{2}}$ to ∞,

$$(\kappa^2+1)^{\frac{1}{2}} \leqq w \leqq \infty, \quad (16)$$

the point $v=0$, $w=(\kappa^2+1)^{\frac{1}{2}}$ corresponding to the origin $\mathbf{q}=0$.

Before we definitely compute the integral (9), we remark that it would not be convenient to use the variables v and w for the second (subtractive) part of (9) also. To avoid this we use the circumstance that for large values of W the surface $w=$const. $=W$ is nearly a sphere. More exactly we see from (14a) that the least and the largest values of q on this surface corresponding to $v=0$ and $v_{\max}$, given by

$$q_1^2 = W^2-\kappa^2-1,$$
$$q_2^2 = (W^2-\kappa^2-1)(1+\kappa^2/(W^2-\kappa^2))$$

have a quotient q_2/q_1 converging to unity as W approaches infinity. Now we should first integrate both parts of (9) over a volume limited by the same surface $w=$const. and then go to the limit $W\to\infty$. Instead of that we shall extend

the subtractive integral only over the sphere inscribed in the surface in question with the radius $q_1=(W^2-\kappa^2-1)^{\frac{1}{2}}$. The error caused by this procedure is certainly smaller than the subtractive integral extended over the spherical shell with the radii q_1 and q_2 given above, because its integrand does not change sign in the domain in question; and even the latter integral converges to zero for $W\to\infty$ because the subtractive integral diverges only logarithmically and lim $q_2/q_1=1$.

Performing the integration over the azimuth and introducing spherical polar coordinates in the subtractive integral, we now get from (9)

$$f(k,k_0)=\lim_{W\to\infty}[J_1(W)-J_2(W)], \tag{17}$$

where

$$J_1(W)=\frac{1}{2\kappa^3}\int_{(\kappa^2+1)^{\frac{1}{2}}}^{W}\frac{wdw}{w^2-k_0^2/4}\int_{-\kappa z}^{\kappa z}(\kappa^2-v^2)dv \tag{18}$$

and z is an abbreviation for

$$z=((w^2-\kappa^2-1)/(w^2-\kappa^2))^{\frac{1}{2}}; \tag{19}$$

and

$$J_2(W)=\int_0^{(W^2-\kappa^2-1)^{\frac{1}{2}}}\left[1-\frac{q^2/3}{1+q^2}\right]\frac{q^2dq}{(1+q^2)^{\frac{1}{2}}}. \tag{20}$$

Performing the integration over v in (18) and introducing z given by (19) instead of w as integration variable, one gets

$$w^2=\frac{1+\kappa^2(1-z^2)}{1-z^2},\quad wdw=\frac{zdz}{(1-z^2)^2},$$

$$J_1(Z)=\int_0^Z\frac{z^2-z^4/3}{1-z^2}\,\frac{dz}{1+(\kappa^2-k_0^2/4)(1-z^2)},$$

where Z is connected with the upper limit W in (18) analogous to (19).

$$Z=((W^2-\kappa^2-1)/(W^2-\kappa^2))^{\frac{1}{2}}, \tag{19a}$$

Z tending to unity when $W\to\infty$.

In (20) we substitute

$$q/(1+q^2)^{\frac{1}{2}}=z,\quad dq/(1+q^2)^{\frac{1}{2}}=dz$$

and then the upper limit of the integral (20) in the new variable z coincides exactly with Z given by (19a) and we get

$$J_2(W)=\int_0^Z\frac{z^2-z^4/3}{1-z^2}dz. \tag{20a}$$

The integrand of the difference J_1-J_2 is finite for $z=1$ and we can now easily perform the lim $Z\to1$ (corresponding to lim $W\to\infty$) and get the final result

$$f(k,k_0)=-\int_0^1\frac{(\kappa^2-k_0^2/4)(z^2-z^4/3)}{1+(\kappa^2-k_0^2/4)(1-z^2)}dz. \tag{21}$$

The most important fact is that f does not depend on k and k_0 separately but on the simple combination

$$L=\kappa^2-k_0^2/4=(k^2-k_0^2)/4, \tag{22}$$

$$f(k,k_0)=f(L)=-L\int_0^1\frac{z^2-z^4/3}{1+L(1-z^2)}dz. \tag{21a}$$

This result is a consequence of the Lorentz invariance of the formalism and was assumed by Serber with this argument without direct proof.[3]

For small values of L one can neglect the term proportional to L in the denominator and get at once

$$f(L)\cong-4L/15\quad\text{for}\quad|L|\ll1 \tag{23}$$

in accordance with Heisenberg's original result. Further one gets from (21a) for $f(L)$ a power series in L which converges for $|L|<1$.

The exact evaluation of (21a), which is elementary, leads to the following result:

$$f(L)=-\frac{1}{3}\left\{-\frac{5}{3}+\frac{1}{L}+\frac{(L+1)(2L-1)}{L}\varphi(L)\right\}, \tag{24}$$

where $$\varphi(L)=\int_0^1 dz[1+L(1-z^2)]^{-1}. \tag{25}$$

One has

$$\varphi[L)=[L(1+L)]^{-\frac{1}{2}}\log[(1+L)^{\frac{1}{2}}+L^{\frac{1}{2}}]$$
$$\text{for}\quad L>0, \tag{26a}$$

[3] In the particular case $k_0=0$ Serber gives for $f(k^2)$ (our function is connected with his function χ by $f=\chi/\pi k^2$) the formula (comp. his Eq. (7)),

$$f=-\frac{1}{2}\int_0^1(1-z^2)\log[1+(k^2/4)(1-z^2)]dz.$$

Using $(1-z^2)dz=d(z-z^3/3)$ and integrating by parts, one gets at once from it our expression (21) for $k_0=0$.

$$\varphi(L)=[|L|(1-|L|)]^{-\frac{1}{2}}\arcsin|L|^{\frac{1}{2}} \quad \text{for} \quad -1<L<0, \quad (26b)$$

$$\varphi(L)=-[|L|(|L|-1)]^{-\frac{1}{2}}\log[(|L|-1)^{\frac{1}{2}}+|L|^{\frac{1}{2}}] \quad \text{for} \quad L<-1. \quad (26c)$$

In the latter case the denominator in the integrand in (21a) and (25) becomes zero at one point of the integration path and one has there to take the principal value. For large positive values of L one gets the asymptotic expression

$$f(L)\leqq\frac{5}{9}-\frac{2}{3}\log(2L^{\frac{1}{2}}) \quad \text{for} \quad L\gg 1.^{4} \quad (27)$$

As far as the general case is concerned which we have mentioned in the beginning, where a vector potential given by (1) is also present, one can again check Serber's general result

$$\delta j_0=-(\alpha/\pi)f(L)j_0, \qquad \delta\mathbf{j}=-(\alpha/\pi)f(L)\mathbf{j}, \quad (28)$$

where f is again given by (21a), with the method here considered. Only the subtractive integrals due to the singularities, become more complicated in this case.[5]

The Function $U(r)$

We shall finally add some remarks concerning the function $U(r)$ defined by

$$\delta j_\lambda(\mathbf{x}')=(\alpha/4\pi^2)\int U(r)\Delta j_\lambda(\mathbf{x}'')d\mathbf{x}''; \qquad r=|\mathbf{x}'-\mathbf{x}''|. \quad (29)$$

This formula is valid for the case of the time independent j_λ. According to Uehling[6] this function also determines the interaction energy $V(r)$ of two particles with charges $Z'e$ and $Z''e$ separated by a distance r.

$$V(r)=Z'Z''e^2[1/r-(\alpha/\pi)U(r)].$$

From the definition (29) and (28) it follows that

$$U(r)=\frac{1}{2\pi^2}\int\frac{f(k^2)}{k^2}\exp(-i(\mathbf{k}\cdot\mathbf{x}))d\mathbf{k}=\frac{2}{\pi}\int\frac{f(k^2)}{k^2}\frac{\sin kr}{r}kdk. \quad (30)$$

If one now introduces the integral (21) (with $k_0=0$) for f the integral over k can be evaluated in an elementary manner and the remaining integral over z can, by the substitution $z=(q^2-1)^{\frac{1}{2}}/q$ and by partial integration, be reduced to the well-known integrals for the Bessel functions of the second kind,

$$K_0(x)=\int_1^\infty\frac{e^{-qx}}{(q^2-1)^{\frac{1}{2}}}dq,$$

$$K_1(x)=x\int_1^\infty e^{-qx}(q^2-1)^{\frac{1}{2}}dq$$

and an indefinite integral of K_0

$$B(x)=\int_x^\infty K_0(y)dy=\int_1^\infty\frac{e^{-qx}}{q(q^2-1)^{\frac{1}{2}}}dq.$$

The final result is

$$U(r)=-\frac{1}{3r}\left\{2\left(\frac{r^2}{3}+1\right)K_0(2r)-\frac{2r}{3}(2r^2+5)K_1(2r)+r\left(\frac{4r^2}{3}+3\right)B(2r)\right\}.$$

From this expression one can obtain easily the asymptotic forms for $U(r)$ for small and large values of r. These have been given by Uehling.[7]

[4] In the case $k_0=0$ one has $L=k^2/4$ and the formulas (24) and (26a) lead to the result

$$f=-\frac{1}{3}\left\{-\frac{5}{3}+\frac{4}{k^2}+2\frac{(k^2+4)^{\frac{1}{2}}(k^2-2)}{k^3}\log\frac{(k^2+4)^{\frac{1}{2}}+k}{2}\right\}.$$

This result is contained indirectly in Uehling's Eq. (22), p. 61, reference 1. Indeed, in order to calculate the scattering of two particles surrounded by a continuous charge distribution according to the Born approximation, one has to make the Fourier expansion of the electric density and to identify k with the difference of the wave-vector for the incident and the scattered beam of the particle (measured in the unit $mc/\hbar$).

[5] The fact that the polarization effects here considered do vanish for $L=0$ even if k and k_0 are different from zero, has the consequence that Heisenberg's conclusion about a correction of the relative order α to the Klein-Nishina formula for the scattering of light by free electrons (comp. Heisenberg, reference 1, p. 223) cannot be maintained. Indeed the effect considered by him vanishes because for the intensity of the scattered light only the terms with $L=0$ give any contribution. A definite answer to the question of the corrections to the Klein-Nishina formula in the approximation here considered needs however a more detailed investigation.

[6] Reference 1, Eq. (21).

[7] Uehling, reference 1, Eqs. (9) and (10).

A New Relativity

Paper II. Transformation of the Electromagnetic Field Between Accelerated Systems and the Force Equation

LEIGH PAGE AND N. I. ADAMS, JR., *Sloane Physics Laboratory, Yale University*

(Received February 3, 1936)

The transformation for **E** and **H** between equivalent Euclidean reference systems with constant relative acceleration is obtained, and the necessary modification of the classical equation of motion of the electron is deduced.

FURTHER KINEMATICAL CONSIDERATIONS

IN Eqs. (I–68) of Paper I[1] is given the space-time transformation between two equivalent, relatively accelerated, reference systems S and S' with Euclidean geometries and equal constant light velocities. At time $t=t'=0$ every point in either reference system is at rest relative to the other, the origin O of S being a point at infinity of S', and the origin O' of S' a point at infinity of S. With the exception of the origins O and O', the two reference systems are coextensive at this time. At a time t not zero, however, points lying inside the sphere $\rho^2=T^2$ about O as center in S are inaccessible to S'. Nevertheless, at any *finite* time t' in S', every point in S except its origin O is accessible to S', since $t'=\infty$ for $\rho^2=T^2$. Similar remarks apply to the region inside the sphere $\rho'^2=T'^2$ about O' as center in S'. Incidentally any fixed sphere in S with O as center is an expanding (or contracting) sphere in S' with O' as center. The sphere $\rho^2=T^2$ about O in S transforms into the sphere $\rho'^2=T'^2$ about O' in S'.

The velocity transformation for a particle having velocity **V** relative to S and **V**′ relative to S' is easily found to be

$$\begin{aligned}
\frac{\mathrm{B}_\rho'}{(1-\mathrm{B}'^2)^{\frac{1}{2}}}&=-\frac{\mathrm{B}_\rho-\beta}{(1-\beta^2)^{\frac{1}{2}}(1-\mathrm{B}^2)^{\frac{1}{2}}},\\
\frac{\mathrm{B}_\theta'}{(1-\mathrm{B}'^2)^{\frac{1}{2}}}&=\frac{\mathrm{B}_\theta}{(1-\mathrm{B}^2)^{\frac{1}{2}}},\\
\frac{\mathrm{B}_\psi'}{(1-\mathrm{B}'^2)^{\frac{1}{2}}}&=-\frac{\mathrm{B}_\psi}{(1-\mathrm{B}^2)^{\frac{1}{2}}},\\
\frac{1}{(1-\mathrm{B}'^2)^{\frac{1}{2}}}&=\frac{1-\beta\mathrm{B}_\rho}{(1-\beta^2)^{\frac{1}{2}}(1-\mathrm{B}^2)^{\frac{1}{2}}},
\end{aligned}\tag{1}$$

where $\mathbf{B}'\equiv\mathbf{V}'/c$, $\mathbf{B}\equiv\mathbf{V}/c$, $\beta\equiv v/c=2\rho T/(\rho^2+T^2)$. Here v represents the velocity relative to S of the point ρ in S' at time T. Although β is a function of ρ and T and therefore not constant, it is worthy of note that the transformations for the parallel and transverse components of velocity are identical in form with those for Euclidean reference systems moving with constant relative velocity such as are contemplated in the special relativity theory. In this connection it is easily shown that

$$\left(\frac{\rho'^2-T'^2}{1-\mathrm{B}'^2}\right)^{\frac{1}{2}}\frac{d}{dT'}=\left(\frac{\rho^2-T^2}{1-\mathrm{B}^2}\right)^{\frac{1}{2}}\frac{d}{dT}\tag{2}$$

is an invariant differential operator.

A photon describing a straight path in S with the constant velocity of light describes a straight path in S' with the same constant velocity. To prove this, take for the X Y plane in S the plane determined by the path of the photon and the origin O, and put $T\equiv\phi t/2c$, $\xi\equiv\phi X/2c^2$, $\eta\equiv\phi Y/2c^2$. Then the motion of the photon relative to S is given by the equations

$$\xi-a=lT,\quad \eta-b=mT;\quad l^2+m^2=1.\tag{3}$$

On transforming to S' by means of (I–68) these become

$$\xi'-a'=l'T',\quad \eta'-b'=m'T';\quad l'^2+m'^2=1,\tag{4}$$

where

$$\begin{aligned}
a'&\equiv\frac{a}{a^2+b^2},\qquad l'\equiv\frac{-(a^2-b^2)l-2abm}{a^2+b^2},\\
b'&\equiv\frac{b}{a^2+b^2},\qquad m'\equiv\frac{-2abl+(a^2-b^2)m}{a^2+b^2}.
\end{aligned}\tag{5}$$

[1] Page, Phys. Rev. **49**, 254 (1936).

With each of two equivalent, relatively accelerated, Euclidean reference systems S and S' may be associated a triple infinity of Euclidean reference systems moving with constant relative velocities for which the Lorentz transformation is valid. Each of these aggregates may be designated as a *Lorentz group*. Thus we have a Lorentz group G associated with S, and including S as one member of the group, and another Lorentz group G' associated with S' and including S'. Let S_1' be a member of G' which has the constant velocity v_1' relative to S'. Take as origin of S_1' the point coincident with O' when $t'=0$, and orient the X' axis of S' and the X_1' axis of S_1' in the direction of the velocity v_1' of S_1' relative to S'. The space-time transformation between S_1' and S is obtained by combining a Lorentz transformation with (I–68). If we take the X and X_1' axes antiparallel, the Y and Y_1' axes parallel, and the Z and Z_1' axes antiparallel, so that each set is right handed, and put $T\equiv\phi t/2c$, $\xi\equiv\phi X/2c^2$, $\eta\equiv\phi Y/2c^2$, $\zeta\equiv\phi Z/2c^2$, $\rho^2\equiv\xi^2+\eta^2+\zeta^2$, as before, this transformation is

$$T_1'=\frac{T-\beta_1'\xi}{(1-\beta_1'^2)^{\frac{1}{2}}(\rho^2-T^2)},\quad \eta_1'=\frac{\eta}{\rho^2-T^2},$$
$$\xi_1'=\frac{\xi-\beta_1'T}{(1-\beta_1'^2)^{\frac{1}{2}}(\rho^2-T^2)},\quad \zeta_1'=-\frac{\zeta}{\rho^2-T^2}, \tag{6}$$

giving $(\rho'^2-T'^2)(\rho^2-T^2)=1$. When $\beta_1'=0$ this reduces to (I–68).

Transformation of **E** and **H**

Now we are ready to consider the electromagnetic field. It was shown many years ago[2] that the four field equations, which represent kinematical relations between the moving lines of force of an electromagnetic field, assume the Maxwellian form in any reference system with Euclidean geometry and constant light velocity c. What remains is to find the transformation for **E** and **H** when we pass from S to S'.

First consider the radial component E_ρ of electric intensity. The transformation for an element ds of area at right angles to the radius vector is

$$ds'=\frac{4c^4}{\phi^2}\rho'^2\sin\theta'd\theta'd\psi'=-\frac{ds}{(\rho^2-T^2)^2}.$$

As T' is not a function of θ or ψ, all the dN tubes of force passing through this area at time T in S will pass through it at time T' in S'. Hence

$$E_\rho'=\frac{dN}{ds'}=-(\rho^2-T^2)^2\frac{dN}{ds}=-(\rho^2-T^2)^2E_\rho. \tag{7}$$

Having found the transformation for one component of **E**, the transformations for the other components are easily obtained as soon as we have found the relations between the direction of a line of force in S' and that in S. Let P'' and Q'' be two neighboring moving-elements on the same line of force. Since Q'' is moving with the velocity **c** of light its velocity components relative to S can conveniently be designated by c_ρ, c_θ, c_ψ. Let dR, $d\theta$, $d\psi$ be the coordinates of Q'' relative to P'' at time t in S and dR_1, $d\theta_1$, $d\psi_1$ its coordinates at time t' in S', where t and t' refer to the same event P''. Then

$$dR_1=dR+c_\rho dt_1,$$
$$d\theta_1=d\theta+(c_\theta/R)dt_1,$$
$$d\psi_1=d\psi+(c_\psi/R\sin\theta)dt_1,$$

where $dt_1=\beta dR_1/c$. Using the space-time transformation (I–68) we find

$$dR'=-\frac{(1-\beta^2)^{\frac{1}{2}}dR}{(\rho^2-T^2)(1-\beta c_\rho/c)},$$
$$R'd\theta'=\frac{Rd\theta}{\rho^2-T^2}+\frac{\beta(c_\theta/c)dR}{(\rho^2-T^2)(1-\beta c_\rho/c)},$$
$$R'\sin\theta'd\psi'=-\frac{R\sin\theta d\psi}{\rho^2-T^2}-\frac{\beta(c_\psi/c)dR}{(\rho^2-T^2)(1-\beta c_\rho/c)}.$$

Hence, remembering that $\mathbf{H}\equiv\mathbf{c}\times\mathbf{E}/c$, we obtain for the transformation of the electromagnetic field,

$$E_\rho'=-(\rho^2-T^2)^2E_\rho, \tag{8}$$
$$E_\theta'=\frac{(\rho^2-T^2)^2}{(1-\beta^2)^{\frac{1}{2}}}\left\{E_\theta+\frac{1}{c}(\mathbf{v}\times\mathbf{H})_\theta\right\}, \tag{9}$$
$$E_\psi'=-\frac{(\rho^2-T^2)^2}{(1-\beta^2)^{\frac{1}{2}}}\left\{E_\psi+\frac{1}{c}(\mathbf{v}\times\mathbf{H})_\psi\right\}, \tag{10}$$

[2] Page, *Introduction to Electrodynamics* (Ginn and Co., 1922).

$$H_\rho' = -(\rho^2 - T^2)^2 H_\rho, \tag{11}$$

$$H_\theta' = \frac{(\rho^2 - T^2)^2}{(1-\beta^2)^{\frac{1}{2}}}\left\{H_\theta - \frac{1}{c}(\mathbf{v}\times\mathbf{E})_\theta\right\}, \tag{12}$$

$$H_\psi' = -\frac{(\rho^2 - T^2)^2}{(1-\beta^2)^{\frac{1}{2}}}\left\{H_\psi - \frac{1}{c}(\mathbf{v}\times\mathbf{E})_\psi\right\}, \tag{13}$$

and we find the invariants

$$(\rho''^2 - T''^2)^2(E''^2 - H''^2) = (\rho^2 - T^2)^2(E^2 - H^2), \tag{14}$$

$$(\rho''^2 - T''^2)^2\mathbf{E}'\cdot\mathbf{H}' = (\rho^2 - T^2)^2\mathbf{E}\cdot\mathbf{H}. \tag{15}$$

It is interesting to note that this transformation, apart from the scale factor $(\rho^2 - T^2)^2$, is identical in form with that of the special relativity, where v is a constant.

As a simple example of the significance of these transformations, consider a *diverging* radial electrostatic field in S with center at the singular point O (Fig. I–6). Then $\boldsymbol{E}_\rho = a/\rho^2$ and (8) gives $\boldsymbol{E}_\rho' = -a/\rho''^2$. So the field in S' is a *converging* radial electrostatic field with center at O'.

Equation of Motion

If the distribution of charge of a finite electron is symmetrical with respect to its center and its rest-mass m' is constant relative to the Lorentz group G', its distribution of charge will be asymmetrical and its rest-mass m will be a function of position and time relative to any member of the Lorentz group G. We may express this asymmetry of charge distribution relative to G by saying that the electron has an *electric moment* relative to the reference systems in this group.

In the circumstances described we should expect the classical force equation to hold relative to any reference system of the Lorentz group G'. Denoting a unit vector along the time axis by $\mathbf{k}_t'$ the equation of motion relative to G' is given by the four-vector relation

$$\frac{d}{dt'}\left\{m'\frac{\mathbf{V}' + \mathbf{k}_t' ic}{(1-\mathbf{B}'^2)^{\frac{1}{2}}}\right\} = e\{\mathbf{E}' + \mathbf{B}'\times\mathbf{H}' + \mathbf{k}_t' i\mathbf{E}'\cdot\mathbf{B}'\}. \tag{16}$$

We shall take this to represent the equation of motion relative to the reference system S' with respect to which the electron has a symmetrical charge distribution and a constant rest-mass m'.

To find the equation of motion of an electron with an asymmetrical charge-distribution and a variable rest-mass all that is necessary is to transform this equation to the equivalent, relatively accelerated, reference system S. In addition to the transformations already given we need the transformation for the rest-mass. Since this is inversely proportional to the linear dimensions of the electron, we find from (I–68),

$$m = m'/(\rho^2 - T^2). \tag{17}$$

In carrying out the transformation we have treated each rectangular component of (16) separately. First we find that

$$\frac{e(\rho''^2 - T''^2)}{(1-\mathbf{B}'^2)^{\frac{1}{2}}}\{\mathbf{E}' + \mathbf{B}'\times\mathbf{H}' + \mathbf{k}_t' i\mathbf{E}'\cdot\mathbf{B}'\} = \frac{e(\rho^2 - T^2)}{(1-\mathbf{B}^2)^{\frac{1}{2}}}\{\mathbf{E} + \mathbf{B}\times\mathbf{H} + \mathbf{k}_t i\mathbf{E}\cdot\mathbf{B}\} \tag{18}$$

is an invariant four-vector for the transformation from S to S'. Next, if we put

$$\mathbf{R} \equiv \boldsymbol{\varrho} + \mathbf{k}_t iT, \quad \mathbf{Q} \equiv \frac{\mathbf{B}}{(1-\mathbf{B}^2)^{\frac{1}{2}}} + \frac{\mathbf{k}_t i}{(1-\mathbf{B}^2)^{\frac{1}{2}}},$$

$$\mathbf{G} \equiv m\{R^2\mathbf{Q} - 2\mathbf{Q}\cdot\mathbf{R}\mathbf{R}\},$$

$$\mathbf{F} \equiv (e/c)\{\mathbf{E} + \mathbf{B}\times\mathbf{H} + \mathbf{k}_t i\mathbf{E}\cdot\mathbf{B}\},$$

we find that (16) becomes

$$\frac{d\mathbf{G}}{dt} - \frac{2}{R^2}\mathbf{R}\cdot\frac{d\mathbf{G}}{dt}\mathbf{R} = R^2\mathbf{F}. \tag{19}$$

As $dm/dt = -(2m/R^2)\,\mathbf{R}\cdot d\mathbf{R}/dt$ this reduces easily to

$$m\left\{\frac{d\mathbf{Q}}{dt} + 2\left(\frac{1}{R^2}\mathbf{Q}\cdot\frac{d\mathbf{R}}{dt}\mathbf{R} - \frac{1}{R^2}\mathbf{Q}\cdot\mathbf{R}\frac{d\mathbf{R}}{dt}\right)\right\} = \mathbf{F}. \tag{20}$$

Let $\mathbf{Q}'$ be the velocity four-vector of the electron relative to S'. Then it is easily shown that

$$\mathbf{Q} = \mathbf{Q}' - (2/R^2)\mathbf{R}\cdot\mathbf{Q}'\mathbf{R}, \quad \mathbf{Q}\cdot\mathbf{R} = -\mathbf{Q}'\cdot\mathbf{R}. \tag{21}$$

Differentiating $\mathbf{Q}$ for constant $\mathbf{Q}'$ we get

$$\left(\frac{d\mathbf{Q}}{dt}\right)_{Q'} = -2\left(\frac{1}{R^2}\mathbf{Q}\cdot\frac{d\mathbf{R}}{dt} - \frac{1}{R^2}\mathbf{Q}\cdot\mathbf{R}\frac{d\mathbf{R}}{dt}\right), \tag{22}$$

and combining (22) with (20), we find for the equation of motion relative to S

$$m(d\mathbf{Q}/dt)-m(d\mathbf{Q}/dt)_{Q'}=\mathbf{F}. \qquad (23)$$

This can be written in the form, invariant for all members of the Lorentz group G,

$$\frac{d}{dt}\left\{m\frac{\mathbf{V}+\mathbf{k}_4 ic}{(1-\mathrm{B}^2)^{\frac{1}{2}}}\right\}-\left[\frac{d}{dt}\left\{m\frac{\mathbf{V}+\mathbf{k}_4 ic}{(1-\mathrm{B}^2)^{\frac{1}{2}}}\right\}\right]_{V'}$$
$$=e\{\mathbf{E}+\mathbf{B}\times\mathbf{H}+\mathbf{k}_4 i\mathbf{E}\cdot\mathbf{B}\}, \qquad (24)$$

the space component being the force equation and the time component the energy equation relative to any reference system of this group. Evidently the second term on the left of (24) is a measure of the electron's asymmetry or electric moment. The part of this term appearing in the force equation represents the time rate of decrease of momentum of an electron moving with the same velocity relative to S as the actual electron at the instant under consideration, but with zero acceleration relative to S'. The force equation states that the excess of the actual time rate of increase of momentum over that which the electron would have if its velocity relative to S' were constant, is equal to the electromagnetic force. If $\mathbf{E}$ and $\mathbf{H}$ are zero (and hence $\mathbf{E}'$ and $\mathbf{H}'$ are also zero) the actual time rate of increase of momentum is equal to that of an electron moving with constant velocity relative to S'.

There exist, then, two distinct agencies which may cause acceleration of an electron, (a) an external electromagnetic field, and (b) an asymmetry of charge distribution or electric moment. To observers in the Lorentz group G' the charge distribution of the electron under consideration is symmetrical and therefore an acceleration can be produced only by the application of a field, but to observers in the Lorentz group G the charge distribution is asymmetrical and the acceleration is attributable in part to the electric moment observed and only in part to the field.

Splitting off the time component of (24) we find for the energy equation

$$\frac{d}{dt}\left\{\frac{mc^2}{(1-\mathrm{B}^2)^{\frac{1}{2}}}\right\}-\left[\frac{d}{dt}\left\{\frac{mc^2}{(1-\mathrm{B}^2)^{\frac{1}{2}}}\right\}\right]_{V'}=e\mathbf{E}\cdot\mathbf{V}, \qquad (25)$$

the second term on the left representing the time rate of increase of kinetic energy of an electron moving with the same velocity relative to S as the actual electron, but with zero acceleration relative to S'. As in the case of the force equation, the excess of the actual time rate of increase of kinetic energy over that which the electron would have if its velocity relative to S' were constant, is equal to the rate at which work is done by the field. If the electron is permanently at rest in S' in the absence of a field, the energy equation relative to S assumes the significant form

$$\frac{d}{dt}\left\{\frac{mc^2}{(1-\mathrm{B}^2)^{\frac{1}{2}}}\right\}+\frac{d}{dt}\{mc^2\}=0, \qquad (26)$$

which shows that the kinetic energy increases at the expense of the mass, the sum of the two being conserved. This conversion of mass into energy was pointed out in Paper I.

The circumstances under which an electron may acquire an electric moment and move in an external field in accord with Eq. (24) relative to the observer's reference frame is a matter for speculation outside the scope of the present development of the theory. One might expect that in weak fields such as can be produced in the laboratory the electric moment represented by the second term on the left of (24) would be negligible, whereas in intensely converging fields such as exist inside the atom the electric moment produced might be sufficient to appreciably modify the equation of motion. Obviously, however, any electric moment produced must depend on the space rate of change of field rather than upon the field itself.

We are now investigating the possibility of equivalent Euclidean reference systems in relative rotation in the hope of finding the modification of the force equation necessary to account for the motions of electrons inside the atom.

Hindered Rotation in Liquid H_2O and D_2O

C. HAWLEY CARTWRIGHT, *Department of Physics, University of Michigan*

(Received March 2, 1936)

THE spectra of molecules in the liquid and vapor state are often so similar that one has often assumed the origin of the absorption to be the same, that is, due to characteristic intramolecular vibrations of the atoms and rotation of the molecules. The lack of fine structure in the part attributed to rotation in liquids was accounted for by a small free path of the translational motions. The absorption spectra of liquid water and water vapor from 1μ to 20μ [1] under low resolution are indeed strikingly similar. It is only as we proceed to longer wave-lengths that the differences become great both in absolute magnitude and the shape of the absorption curves; and these differences cannot be entirely accounted for by the influence of viscosity on an orientation of the permanent dipoles.

Recently it has been found that many properties of liquid could for the first time be successfully explained by assuming a liquid to be more nearly a solid than a dense gas. The molecules of a liquid are thought of as forming a quasi-crystalline structure in which there is no free path at all and the molecules vibrate about slowly displaced equilibrium positions, with a frequency which is about the same as that of the molecules in the solid state.[2] The concept of a quasi-crystalline structure in liquids however does not exclude the possibility of free rotation for, as Pauling has shown, the molecules rotate in certain solids. Whether free or hindered rotation occurs depends on the intermolecular field of potential energy. In the case of liquid water, Debye[3] has calculated from two different types of experimental data that an energy of $10kT$ is necessary to turn a water molecule through 90°. Bernal and Fowler[4] have been able to explain several physical properties of liquid water by assuming a tetrahedral quartz-like structure in which each water molecule is surrounded by four others. From calculating the intermolecular field of this model,[5,6] a characteristic frequency is predicted at 60μ due to a mutual vibration between water molecules and a frequency at 20μ due to hindered rotation. The 60μ band should appear only changed by $(20/18)^{\frac{1}{2}}$ in D_2O while the 20μ band should be shifted to longer wave-lengths by the factor $\sqrt{2}$.

We have observed the infrared absorption, reflection and dispersion of liquid H_2O and D_2O and have established the existence of two strong, rather broad bands, one at about 60μ and the other at about 20μ. The 60μ ($\nu = 5\times10^{12}$ sec.$^{-1}$ or 160 cm^{-1}) band[7] (1) is practically the same in H_2O and D_2O, (2) is very strongly absorbing (a thickness of 10μ transmits only 30 percent at $\lambda = 60\mu$), (3) is present in ice, (4) disappears for water dissolved in dioxane, (5) increases but slightly the reflecting power and the index of refraction and (6) is Raman active.[5] The 20μ ($\nu = 15\times10^{12}$ sec.$^{-1}$ or 500 cm^{-1}) band (1) is shifted by about $\sqrt{2}$ in D_2O, (2) is strongly absorbing, (3) greatly increases the reflecting power (both the absorbing and reflecting powers are much greater than for the fundamental intramolecular vibration bands at 3μ and 6μ), (4) causes anomalous dispersion and (5) is weakly Raman active.

These results are a striking confirmation of the theory by Bernal and Fowler on liquid water although there is a certain difficulty in explaining the strong infrared activity of the 60μ band of hindered translation unless we assume that the surrounding molecules are forced to turn to follow the characteristic intermolecular vibrational frequency.[7] The nature of the two frequencies predicted by Bernal and Fowler, and found experimentally to be strongly infrared active, can perhaps be understood by the following order of magnitude calculation. One may suppose the water molecule to be bound by an intermolecular field. The molecule will then execute vibrations which fall into two main types. One involving a large amplitude of motion of

[1] H. Rubens and E. Ladenburg, Le radium **6**, 33 (1909).
[2] E. N. da C. Andrade, Phil. Mag. **17**, 497 (1934).
[3] P. Debye, Physik. Zeits. **36**, 100, 193 (1935).
[4] J. D. Bernal and R. H. Fowler, J. Chem. Phys. **1**, 515 (1933); Trans. Faraday Soc. **29**, 1049 (1933).
[5] M. Magat, J. de phys. et rad. **5**, 347 (1934).
[6] J. D. Bernal and G. Tamm, Nature **136**, 229 (1935).
[7] C. H. Cartwright, Nature **136**, 181 (1935).

the hydrogen atoms and one involving a large amplitude of motion of the oxygen atom. These vibrations are of course in addition to the three interatomic oscillations which appear in the near infrared. Assuming harmonic oscillations of a water molecule about the axis of smallest moment of inertia ($I=0.998\times10^{-40}$; this would give the highest frequency, be infrared active and be practically only a motion of the hydrogen atoms), we obtain for the 20μ band in H_2O or the 28μ band in D_2O, according to the formula $\nu=1/2\pi(K/I)^{\frac{1}{2}}$, a value of $K=9\times10^{-13}$ dyne-cm or $22kT$. The water molecule would therefore be hindered from oscillating through an angle of about $\pm27°$. If we assume that the oxygen atoms vibrate in the same field as was found for the hydrogen atoms, the wave-length of the natural vibration period of the oxygen atoms would be 57μ, which agrees well with the experimental data. The amplitude of the vibrations of the oxygen atoms would be about 0.15A.

The results obtained experimentally when compounded with the Bernal and Fowler model of liquid water or when interpreted with an order of magnitude calculation show clearly that at room temperature the molecules in liquid water are hindered by a strong intermolecular field from executing a free rotational motion.

I am pleased to thank Professor Dennison for his helpful suggestions.

MARCH 15, 1936 PHYSICAL REVIEW VOLUME 49

A Method for the Determination of the Selective Absorption Regions of Slow Neutrons

D. F. WEEKES, M. STANLEY LIVINGSTON AND H. A. BETHE, *Department of Physics, Cornell University*

(Received March 4, 1936)

FERMI and Amaldi[1] and Szilard[2] have demonstrated that each element which shows a strong capture absorption of slow neutrons absorbs neutrons of a characteristic energy. These bands of selective absorption were originally assumed to be in the thermal or near-thermal region. Rasetti and Fink[3] have shown, however, that there is no temperature effect on these bands except for cadmium.

According to the Wigner-Breit[4] theory the selective absorption is explained as a resonance phenomenon. It is assumed that the nucleus which is formed by the capture of the neutron has some excited level whose energy is equal to that of the original nucleus plus a neutron of a certain energy E_0. If a neutron of this energy falls on the nucleus there may be a nonradiative transition (inverse "Auger-effect") into the above-mentioned excited state. This excited state will then, after a certain time, go over into the ground state with the emission of radiation rather than disintegrate again with the emission of a neutron. The theory, therefore, explains also the large observed ratio of capture to scattering in strongly absorbing elements.

The probability of capture of a neutron of energy E is, according to this theory, given by:

$$\sigma_c=(a/E^{\frac{1}{2}})\cdot(\gamma/((E-E_0)^2+\gamma^2), \qquad (1)$$

where γ is the natural breadth of the energy level at E_0 as determined by its lifetime against radiation, and a, E_0 and γ are constants characteristic of the element. γ is estimated to be of the order 1 to 50 volts and E_0 of from 0 to 1000 volts. The capture cross section has, according to Eq. (1), two maxima, one at a very low energy (thermal) and one near E_0.

It is obvious that the velocity selectors for neutrons of thermal energies in use at present[5] cannot be readily extended to this energy region. We wish to propose here a simple experiment designed to measure these energies, which depends on a few relatively safe assumptions. The main assumption is that in certain elements (e.g., B and Li) the absorption is inversely propor-

[1] Amaldi and Fermi, Ricerca Scientifica **VI–II**, Nos. 9–10 (1935).
[2] Szilard, Nature **136**, 950 (1935).
[3] Rasetti and Fink, Bull. Am. Phys. Soc., New York Meeting, Vol. **11**, Nos. 1, 28 (Feb., 1936).
[4] Wigner and Breit, Bull. Am. Phys. Soc., New York Meeting, Vol. **11**, No. 30 (Feb., 1936).
[5] Fink, Dunning, Pegram and Mitchell, Phys. Rev. **49**, 103 (1936).

tional to the neutron velocity, which follows from the elementary theory of slow neutron absorption.[6] The elementary theory can be expected to hold for reactions between neutrons and nuclei which lead to the emission of alpha-particles because such processes are very probable *a priori* as compared to radiative processes, and it is therefore not necessary to assume resonance effects in order to explain the observed cross sections of these processes. Furthermore, B is a very light nucleus which cannot be expected to have the great number of closely-spaced energy levels which should occur in heavier nuclei, and therefore probably does not have an energy level for neutrons anywhere near this region. *The absorption coefficient of neutrons in B should therefore be a good measure of the energy of the neutrons absorbed.*

In order to separate the two absorption regions for an element such as Ag we may use Cd thick enough to absorb all neutrons in the low energy region. This is justified because the velocity selector experiments show practically a Maxwellian distribution of the neutrons absorbed by Cd, and furthermore, this distribution is influenced by temperature changes.[5] The resonance level of Cd seems, therefore, to lie in or near the thermal region, which is also in accord with experiments of Rasetti[7] on the dependence of the absorption coefficient of Cd on the velocity of the neutrons absorbed.

One should, therefore, measure the activity produced in some detector for which the resonance level E_0 is to be determined (e.g., Ag) with four experimental arrangements:

(1) Ag detector acitvated directly by a source of slow neutrons;
(2) same with B absorber interposed;
(3) with Cd absorber, but without B;
(4) with both Cd and B absorbers.

The difference of the measured activities of (1) and (3) should then be attributed to thermal neutrons. (2)−(4) gives the effect of thermal neutrons reduced by the B absorption. From the ratio (1)−(3)/(2)−(4) we can therefore determine the absorption coefficient of B for thermal neutrons. Similarly from the ratio (3)/(4) the absorption coefficient in B for the resonance neutrons can be determined. Since it is to be expected that the absorption coefficient is much larger in the first case it is advantageous to use different thicknesses of B for the determination of the two ratios.

TABLE I.

RUN	DETECTOR	ABSORBER	B(g/cm²)	TOTAL COUNTS	BACKGROUND	ACTIVITY
(1)	Ag	——	——	1309	231	1078
(2)	Ag	B	0.050	863	269	594
(3)	Ag	Cd	——	580	306	274
(4)	Ag	Cd+B	0.050	576	335	241
(3a)	Ag	Cd	——	649	363	286
(4a)	Ag	Cd+B	0.80	508	363	145

Ratios:

R_1(slow neutrons) $=\frac{(1)-(3)}{(2)-(4)}=\frac{804}{353}=2.28$: Abs. Coef. $=16.5/\text{g cm}^{-2}$.

R_2(fast neutrons) $=\frac{(3a)}{(4a)}=\frac{286}{145}=1.97$: Abs. Coef. $=0.85/\text{g cm}^{-2}$.

In our experiments a Ag detector of 5×6 cm, which could be rolled into a cylinder and placed around a thin-walled tube counter, was placed 2 cm above the surface of a paraffin block 12 cm on a side. A Rn-Be source of neutrons (*cà.* 400 mc) was placed 10 cm below the upper surface of the paraffin. The B absorber was powdered boron carbide spread in a uniform layer in a box made of 9-mil aluminum sheet of dimensions 7×8 cm and 2 cm deep. A similar Al box, without B, was used in the experiments (1) and (3). The Cd absorber was 0.85 mm thick and covered the paraffin surface. In all experiments a Cd shield surrounded the absorber and detector to protect from stray neutrons.

The ratio of these two absorption coefficients is 19.4, from which we deduce that the energy of the resonance absorption in Ag is $(19.4)^2$ or 375 times the thermal energy, that is, nearly 10 volts. In these preliminary data of Table I the experimental arrangement was somewhat unsatisfactory, requiring the application of certain corrections. Firstly, an estimated 10 percent of the slow neutrons could reach the detector around the edges of the thin B absorber. Applying this correction increases the coefficient from R_1 to 19.4/g cm^{-2}, corresponding to a cross section of about 450×10^{-24} cm² as compared with Dunning's[8] value of 600×10^{-24} cm². The corresponding correction for the thick B absorber is

[6] Bethe, Phys. Rev. **47**, 747 (1935).
[7] Rasetti, Segrè, Fink, Dunning and Pegram, Phys. Rev. **49**, 104 (1936).
[8] Dunning, Pegram, Fink and Mitchell, Phys. Rev. **47**, 417 (1935).

probably small. Secondly, the absorption coefficient for fast neutrons should be corrected for scattering. Estimating the cross section for scattering to be about 3×10^{-24} cm^2, which is the average value for nonabsorbing light elements, and considering that only scattering of greater than about 90° reduces the intensity of the neutron beam, we get a correction of about 10 percent for the coefficient from R_2, which is thereby reduced to 0.77/g cm^{-2}. The ratio of the absorption coefficients now gives 25, resulting in a resonance energy E_0 for Ag of about 16 volts. This numerical value may no doubt be made more accurate with improved data.

MARCH 15, 1936 PHYSICAL REVIEW VOLUME 49

Variations of Properties of Cosmic Shower Radiations with Altitude

J. C. STEARNS, *Department of Physics, University of Denver*

(Received March 2, 1936)

PRODUCTION OF SHOWER RADIATIONS

AN investigation of some of the properties of cosmic and shower radiations was initiated during the summer of 1935.

The first experimental work was the determination of the optimum thickness of lead for producing showers at altitudes 120, 5300, 10,800 and 14,200 feet, respectively. Three Geiger counters arranged in the form of a triangle as indicated in Fig. 1a, were connected in a circuit which recorded triple coincidences. The counter voltage and temperature were held constant.

In the first experiment there was no lead in position B. N/N_0, where N and N_0 are the respective counts per minute with and without the lead at A, was determined for each thickness of lead utilized. This provided a constant check on the operation of the apparatus and determined the thickness for the maximum shower production independent of any slow changes in the efficiency of the counters.

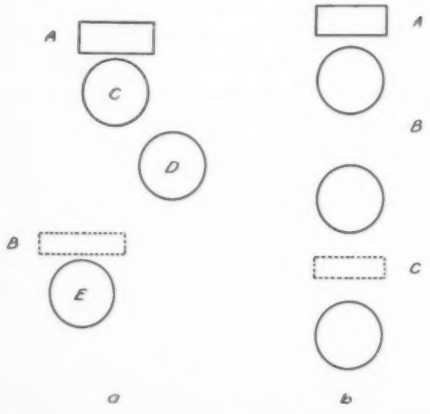

FIG. 1. Arrangement of Geiger counters.

In the second method the counters were arranged in a vertical line (Fig. 1b). Coincidences per minute were determined with the lead block in respective positions A and C. The absorption of the primary rays is the same with the block in either position. The accidentals, which were less than two percent of the smallest count, were practically constant, since the individual counting rate of the several counters was approximately the same with the lead block in either position. This was tested by placing the lead block in position B, and determining the triples per minute which were found to be the same as with the block in the C position. The increased counting rate with the block in position A may be due to one or more ionizing particles ejected from the lead plate by

1. Incident nonionizing rays.
2. Incident ionizing rays moving in a direction not included within the solid angle defined by the counters.
3. Incident ionizing rays moving in a direction within the solid angle defined by the counters but incident on the portion of the lead plate external to the area subtended by this solid angle.

The results of the two methods are shown in Fig. 2.

It will be seen that the shape of the curves is independent of altitude, as is the optimum thickness for shower production, but that both the shape and maximum vary with the method used.

ABSORPTION OF SHOWER RADIATION

To measure the absorption of shower radiation the arrangement shown in Fig. 1a was used. The showers are produced in a lead scatterer, A, and

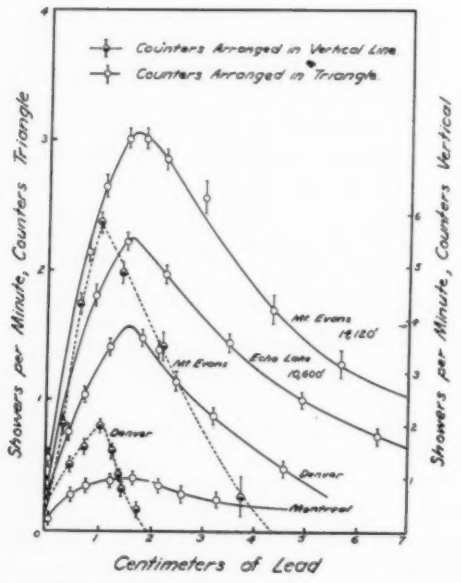

FIG. 2. Rates of shower detection with the two arrangements of counters.

the shower radiation actuating the lower counter absorbed in lead block B. A charged particle may eject another charged particle from A, which will penetrate counters C and D, while the original ray passes through counter E. In such cases, B is absorbing the shower producing radiation. The influence of this is believed to be small because:

1. The chance of such an event occurring is relatively small.
2. The shower producing rays are hard compared to the shower radiation.

The coincidence rates with and without lead of different thicknesses at B were determined. In Fig. 3a the ratio of the coincidence rate with lead at B to the rate with no lead at B is plotted against the thickness of the absorber. In Fig. 3b the logarithm of 10 times this ratio is plotted against the thickness of the absorbing block.

There are two points of significance. First, the curves appear to have a plateau in the region of 2 cm of lead. While the probable errors are large enough to permit the drawing of a curve with no inflection points, the general shape of both curves, and the careful checking of points in this region is strong evidence that such a plateau does exist. This would be expected if shower

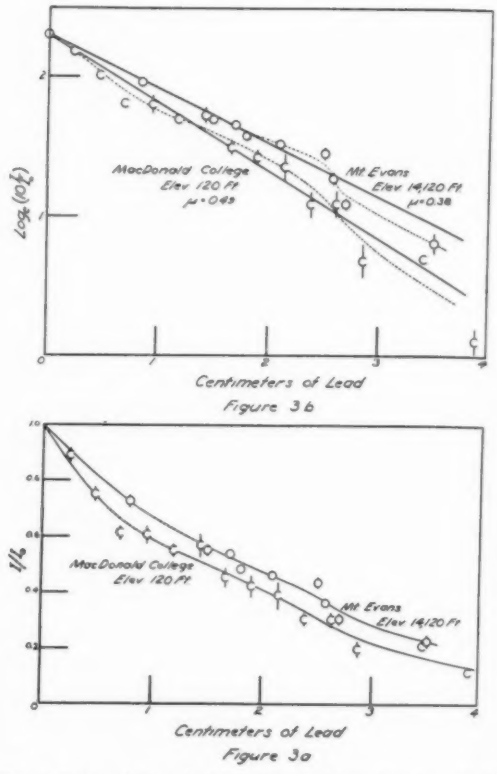

FIG. 3. Ratio of the coincidence rate with and without lead at B in the arrangement shown in Fig. 1a.

radiation can eject one or more charged particles from material which it traverses, for then E would be actuated by rays ejected from block B by shower radiation which itself would not have passed through E. Evidence that such a process may occur is shown by the work of O. Zeiller,[1] and E. C. Stevenson and J. C. Street.[2]

This work was made possible by grants from the National Research Council, the Rumford Committee, and the American Association for the advancement of Science. We wish to acknowledge the cooperation of Mr. George Cranmer, Superintendent of Mountain Parks, City of Denver, for providing electric power and transportation, and the Garden City Press, Ste. Anne de Bellevue, who kindly furnished laboratory space and electric power.

[1] O. Zeiller, Zeits. f. Physik **96**, 121 (1935).
[2] E. C. Stevenson and J. C. Street, Phys. Rev. **48**, 464 (1935).

LETTERS TO THE EDITOR

Prompt publication of brief reports of important discoveries in physics may be secured by addressing them to this department. Closing dates for this department are, for the first issue of the month, the twentieth of the preceding month; for the second issue, the fifth of the month. The Board of Editors does not hold itself responsible for the opinions expressed by the correspondents.

Communications should not in general exceed 600 words in length.

Beta-Activity Induced by Gamma-Rays

A nucleus, which is not naturally β-active, may be stimulated to emit a β^- or β^+-particle under the influence of a γ-ray. We may visualize the β^--emission as a double process. First, the nucleus emits an electron into a virtual energy state. Second, if sufficient energy is transmitted to the electron from the absorption or scattering of the γ-ray, the electron is freed. Likewise, the β^+-process can be considered as an interaction of the γ-quantum with a negative energy electron followed by absorption of the electron into the nucleus.

The virtual emission is taken as that given by the Fermi[1] theory of β-decay.

The cross section σ_a for electron or positron emission with absorption of γ-rays is found to be

$$\sigma_a = 4.2\times10^{-4}\alpha G^2\Lambda^2 |M|^2 (K+\Delta)^6 \log_\epsilon (2K)/K^4$$
$$(K+\Delta)\gg 1,\ \Delta<1.$$

K is the energy of the γ-ray, Δ is the change in energy of the nucleus from original to final state. Both quantities are in mc^2 units. α is fine-structure constant $2\pi e^2/hc = 1/137$. Λ is Compton wave-length $h/2\pi mc$. G, a dimensionless constant[2] characteristic of the theory of β-decay, is given by $g/\Lambda^3 mc^2 = 9\times10^{-13}$, M is the matrix element of β-decay theory.[3]

The cross section σ_s for electron or positron emission with scattering of γ-ray is given by

$$\sigma_s = 1.7\times10^{-5}\alpha^2 G^2\Lambda^2 |M|^2 (K+\Delta)^7/K^3$$
$$(K+\Delta)\gg 1,\ \Delta<1.$$

Thus $\sigma_s \ll \sigma_a$ for $K<50$.

The cross section σ_Z for electron or positron emission with the scattering of a charge Ze was calculated by the Weizsäcker[4] method from σ_a.

$$\sigma_Z = 6.7\times10^{-5}\times Z^2\alpha^2 G^2\Lambda^2 |M|^2 [\log_\epsilon (2\epsilon)-1]\epsilon^2$$
$$\epsilon\gg 1,\ \Delta=0.$$

ϵ is the energy of the charged particle Ze in mc^2 units.

For energy of intense Th C'' γ-rays with $\Delta=1$, $\sigma_a = 6.4\times10^{-49}$ cm^2 an extremely small value. Similar results are obtained if the Konopinski-Uhlenbeck modification of the β-theory is used.

We wish to thank Dr. Irving Lowen for suggestions and discussions.

WILLIAM RARITA

Department of Physics,
Columbia University,
February 27, 1936.

[1] E. Fermi, Zeits. f. Physik **88**, 161 (1934).
[2] Wolfe and Uhlenbeck, Phys. Rev. **46**, 234 (1934).
[3] Konopinski and Uhlenbeck, Phys. Rev. **48**, 7 (1935).
[4] Weizsäcker, Zeits. f. Physik **88**, 612 (1934).

A Very Accurate Experimental Verification of the Inverse Square Law of Electrical Attraction

This law was tested by Coulomb with his torsion balance and much more precisely by Maxwell using a modification of a method invented by Cavendish. Maxwell used a spherical air condenser consisting of two insulated spherical shells ("globes"), the outer having a small hole in it so that the inner could be tested for charge by inserting an electrode from an electrometer. This hole was closed by a small lid carrying an inward projection which simultaneously connected the two shells together. A charge of high potential V was then applied to the outer shell, the lid and connector removed by a silk thread and the outer shell earthed. If the exponent in the inverse square law it written $2\pm q$, the potential remaining on the inner sphere v and the radii of the spheres a and b, then $q<v/VF(a, b)$ where $F(a, b)$ is a known function. Maxwell obtained the result $q<1/21{,}600$.

Professor A. W. Duff has called the attention of the writers to the possibility of greatly improving the accuracy of this test if a way could be found of using the extremely sensitive electrometers now available.

Because of the disturbing effects of spontaneous ionization and contact potential gradients, we have found it necessary to replace the static method by a quasi-static method, as follows. A "resonance electrometer" consisting of an FP-54 tube, amplifier and galvanometer is placed permanently within the spherical shells, the high input-grid resistor forming the link connecting them. The galvanometer is observed through a small window at the top made conducting by covering it with a transparent electrolytic solution. No effect is observed when a harmonically alternating high potential, at the resonance frequency of the galvanometer, is applied to the outer sphere. This high potential V is obtained from a specially designed generator, through a filter to prevent the passage of any frequency high enough to affect the electrometer by electromagnetic induction. The smallest potential v detectable by the electrometer is determined by coupling it to the same generator through a potentiometer and a small air condenser. In this way it is found that the exponent in Coulomb's law does not differ from 2 by more than one part in one hundred million ($1/10^8$). The apparatus is being redesigned with the expectation of a very considerable improvement in accuracy.

S. J. PLIMPTON
W. E. LAWTON

Worcester Polytechnic Institute,
February 26, 1936.

Remarks on Measurements in Quantum Theory

Since the completion of my note[1] on a paper of Einstein, Podolsky and Rosen,[2] there have appeared two articles by Schrödinger[3] on the same subject. Mathematically the content of Schrödinger's papers and mine is essentially the same, although the emphasis is quite different. The interpretations given are exact opposites. I wish here to add a few words to the discussion.

Bohr[4] has emphasized that the essential difficulty with the argument of EPR lies in the assumption that whenever a system is not in mechanical interaction with other systems it may be regarded as having independently real properties. This assumption depends on the ascription of an undue significance to the fact that the systems are not connected in any way which finds a reflection in our description of the situation by means of a model. If it were tenable, it would provide an easy solution, quite acceptable to our habitual ways of thinking, of the problem of the relation of subject and object. In fact, however, the difficulties of this problem as they appear in quantum theory are not to be resolved by any such facile bit of analysis.

To make this assumption a definite basis for arguments, one must add some assertion as to the nature of the "real" properties of the "free," system. Being in agreement with Bohr's point of view, and wishing only to make clearer an interesting characteristic of quantum mechanics, I took as my additional assumption one which suggests itself from the content and manner of the usual discussions of the theory of measurement. My "Assumption A" is that a "free" system which was formerly coupled to an instrument is "really" in some one of a certain set of quantum-mechanical states, which are the eigenstates of the observable which the instrument is suited to measure. Assumption A has three important properties:

(1) The corresponding picture of the situation is in full accord with our habitual attitudes, and is the one we use in ordinary practice.

(2) The predictions derived from Assumption A for the sorts of cases which *actually occur* agree exactly with those of quantum mechanics.

(3) In more general cases, *realizable in principle* according to the postulates of the theory, there is flat contradiction between the formulas given by Assumption A and those of quantum mechanics. Therefore Assumption A is actually untrue.

The corresponding postulate chosen by Schrödinger is altogether different, on account of his different point of view. Since he agrees with the underlying assumption of EPR, he is careful to introduce no *a priori* "doubtful" element into his thesis. Thus he rejects (N, p. 827) Assumption A, and ends with taking as his criterion of "reality" just that of EPR: The "real" properties of the "free" system are the values of those observables whose values could be predicted "without in any way disturbing the system." On this basis one can give interesting considerations only about certain degenerate situations, such as that chosen as an example by EPR. Schrödinger accordingly devotes most of his mathematical discussion to a complete elaboration of this example. As was to be expected on general principles (F, footnote 11), the resulting picture of the situation is much more complicated than that originally drawn by EPR, and could scarcely be traced to so simple a source as an "incompleteness" of the theory; Schrödinger implies that it indicates some serious defect.

We may note two properties of this assumption:

(1′) It is, in the opinion of EPR and of Schrödinger, indisputably true *a priori*.

(2′) None of its assertions—it is innocent of actual predictions—ever comes into direct contradiction with the results of quantum mechanics; hence it cannot be either proved or disproved objectively.

According to the prevailing attitude in theoretical physics, (2′) is enough to consign all such assertions to the limbo of "meaningless statements."[5] Against this verdict (1′) is of no avail; for, as asserted already in the second paragraph of this letter, the assumption underlying such an opinion is definitely untenable: it is not correct to assume that the only physically significant relations are those which are directly obvious from a classical model. One striking experimental example is the collision of two similar particles. No matter how far apart the particles are when we try to collect one of them, the relative probabilities of finding it in different places are strongly affected by the "interference term" in the cross section; it is not really "free." (In this case, as in the one under consideration, there is of course nothing "magical" about the affair. The interference effect does not come in unless there has been an actual opportunity for the two particles to get interchanged,[6] just as in the case in hand there is never any relation between the systems without the existence of an actual dynamical interaction to start it.)

Thus there can be no doubt that quantum mechanics requires us to regard the realistic attitude as in principle inadequate. But it need not disturb at all our habit of taking such an attitude as a matter of practical convenience in the interpretation of experiments. In any measuring process actually used the "biorthogonal" expansion (F, Eq. (3)) is unique, and the experimenter concerns himself only with the observable and "pointer reading" which belong to this expansion. Thus Assumption A is a perfectly safe working hypothesis.

Schrödinger's misgivings (C, p. 555) about the fact that measurement involves actually a chain of object-instrument relations accordingly seem groundless. This question was discussed in full detail some years ago by Neumann,[7] and in my opinion his treatment is altogether adequate.

W. H. Furry

Department of Physics,
Harvard University,
March 2, 1936.

[1] W. H. Furry, Phys. Rev. **49**, 393 (1936). Referred to as F.
[2] A. Einstein, B. Podolsky and N. Rosen, Phys. Rev. **47**, 777 (1935). Referred to as EPR.
[3] E. Schrödinger, Proc. Camb. Phil. Soc. **31**, 555 (1935) (referred to as C); and Naturwiss. **23**, 807–812, 823–828, 844–849 (1935) (referred to as N).
[4] N. Bohr, Phys. Rev. **48**, 696 (1935).
[5] Cf. W. Heisenberg, *The Physical Principles of the Quantum Theory*, p. 15, footnote.
[6] W. Pauli, *Handbuch der Physik* **24/1**, pp. 192–193.
[7] J. v. Neumann, *Mathematische Grundlagen der Quantenmechanik*, Chapter VI.

Beta-Rays of High Energy

The primary β-rays of a radioactive substance form, in general, a continuous spectrum with a definite upper limit to the energy or velocity. Some experimenters, however, using the method of direct magnetic deviation have obtained evidence of the emission of weak bands of much greater average energy. In particular Curie and d'Espine[1] reported in 1925 that radium E emitted a band of β-rays with values of $H\rho$ between 7000 and 10,000 whereas the main spectrum ends in the neighborhood of $H\rho$ 5500.

To test this result, the following experiment was performed. Radium (D+E) was deposited on a watch glass and placed 3 cm below an electroscope lined with cardboard except for the window which consisted of 0.200 Al, 0.200 Al signifying a sheet of aluminum of mass/cm^2=0.200 g. Above the active material was placed 0.200 cardboard +0.212 Pb. The rays coming through this absorber were tested by sheets of graphite (0.85 C) of mass/cm^2=0.85 g. The results are shown in Table I.

TABLE I.

	Absorber	Intensity
1	0.200 Cbd +0.212 Pb +0.200 Al	10.0
2	0.200 Cbd +0.212 Pb +0.85 C +0.200 Al	9.3
3	0.200 Cbd +0.212 Pb +1.70 C +0.200 Al	8.64

With this initial intensity of 10 divisions a minute, the intensity of the β-rays, allowing for absorption was 1,000,000 divisions a minute. In the first absorber the function of the cardboard was to prevent production of x-rays in the lead, of the lead to absorb the γ-rays from the source, and of the aluminum to absorb the characteristic L radiation which is produced in the lead by the γ-rays. This absorber has a total mass/cm^2=0.612 g which is necessary to ensure the total absorption of the β-rays in the main spectrum, permitting at the same time a considerable number of the high energy β-rays to pass through it.

It will be noticed that the first sheet of graphite causes a reduction in intensity of seven percent, as also does the second sheet. The first sheet of graphite is thick enough to absorb all high energy β-rays passing through the first absorber. If any do pass through absorber number 1, then the second sheet of graphite should cause a reduction in intentity of less than seven percent. This is not the case, so that this experiment affords no evidence whatever of the emission of β-rays of high energy from radium E.

We are certain that we could have detected these β-rays quite easily if of the ten divisions a minute due to rays passing through absorber number 1, 0.1 had been due to β-rays of high energy. Assuming for the moment that they have this intensity, it is easy to show that only one β-ray in 2,000,000 disintegrations can be a β-ray of high energy.

J. A. Gray

Queen's University,
Kingston, Ontario,

W. J. Henderson

Princeton University,
March 3, 1936.

[1] Curie and d'Espine, Comptes rendus **181**, 31 (1925).

The Gamma-Rays of Radium E

As a result of some experiments carried out several years ago by W. J. Henderson and J. A. Gray, the latter came to the provisional conclusion that the γ-rays of radium E were not primary rays but were x-rays excited by β-rays in the atoms from which these β-rays are emitted.

To test this view, some pure radium E was deposited on paper of mass/cm^2=0.0033 g. This source was placed 20 cm from an ionization chamber the window of which consisted of two sheets of cellophane. β-rays were deflected from this chamber by means of a magnetic field, so that only γ-rays or x-rays produced near the source on substances placed close to it, could enter the ionization chamber. The absorption of the γ-rays was first found in aluminum. The first curve obtained could be represented approximately by the equation

$$I = 19.3^{-136m} + 40^{-31m} + 18.4^{-5.22} + 22.3^{-0.303m},$$

where m is the mass per unit area of absorbing screen and the numbers such as 136, mass absorption coefficients.

A mass absorption coefficient in aluminum of 136 corresponds to a wave-length of 2.2A and an energy of 5600 ev, so that there is some very soft radiation present. To see whether soft x-radiation was produced in other substances filter paper, aluminum and gold were used. The results obtained with gold of mass/cm^2=0.00328 g are given in Table I, the absorber being aluminum. The

TABLE I.

Absorber (g/cm^2)	Intensity γ-rays	Intensity x-rays	Absorber (g/cm^2)	Intensity γ-rays	Intensity x-rays
0.000	100	100	0.0329	49	47
0.00656	80	77	0.073	34.7	33
0.0164	64.5	66	0.1744	22.6	20
0.0230	57	57	0.294	18.4	16.8

x-ray intensities were found by first placing the foil near the source and then near the ionization chamber and taking the differences of the readings.

The first column shows how the γ-rays are absorbed, the second how the x-rays excited in the gold foil are, and a glance at the figures show that in both cases the rays are of the same type. The intensities are given in arbitrary units, the initial intensity of the x-rays being about 35 percent that of the γ-rays.

We have also examined the x-rays produced in thick foils of cardboard, aluminum, copper, tin and lead and have found that up to a thickness of 2 cm of lead the absorption of the x-rays is almost identical with that of the γ-rays. We conclude therefore that the γ-rays of radium E are really x-rays produced by β-rays in escaping from the atoms in which they are produced. Whether the very soft rays found are due to slow β-rays we are not prepared to say.

J. A. Gray
J. F. Hinds

Queen's University,
Kingston, Ontario,
March 3, 1936.

Anomalous Secondary Electron Emission
A New Phenomenon

Aluminum, oxidized electrolytically in a bath of borax and boric acid, is made the target of an electron gun. Caesium is introduced into the tube which is then baked at 200°C for ten minutes after which the tube is flushed with oxygen.

If a collector—electrode adjacent to the target is maintained at a positive potential with respect to the former, it is found that an electron beam from the gun impinging upon the target causes a current to the collector which, in certain cases, may be several thousand times greater than the primary beam. Over a considerable range of collector voltage and primary beam current density, it is found that

$$J_c = a e^{\beta V_c} J_B^{\gamma},$$

where J_c is the collector current divided by the area of the primary beam, V_c is the collector potential, and J_B is the primary beam current density.

The collector current decays slowly after the removal of the primary beam and has been detected even after twenty-four hours. Similar time lag effects occur when the beam is first turned on, particularly if the beam has previously been permitted to fall upon the target with the collector potential reversed.

White light from a tungsten filament produces a marked drop in J_c as well as a more rapid change in the decay and building up characteristics.

Apparently, the treatment outlined above produces a surface on a resistive film which has a high emission coefficient for secondary electrons. Since the primary beam causes an emission of true secondary electrons greater in number than those in the primary beam, the surface becomes positively charged resulting in the establishment of an intense potential gradient through the resistive oxide film. This gradient is responsible for the enhanced secondary emission. This type of "secondary electron emission" is referred to as "anomalous secondary electron emission."

A complete report of this work will be published shortly.

The author wishes to express his thanks to Dr. V. K. Zworykin for extending to him the facilities of the Electronic Research Laboratory of the RCA Manufacturing Company, Inc. where some of this work was done.

LOUIS MALTER

Cornell University,
February 24, 1936.

Can Protons Represent the Primary Cosmic Rays at Sea Level?

Analyses of the cosmic-ray intensity-altitude curves have appeared to suggest the conclusion that the primary cosmic radiation in the vicinity of the earth is composed exclusively of protons.[1] The purpose of this letter is to point out certain difficulties inherent in this view.

A charged particle is characterized by the fact that its ionization increases enormously towards the end of its range, so that, in the case of protons and alpha-particles large and measurable spurts of ionization should be produced in relatively short distances by those rays which are ending their journeys.

Let r be the distance from the end of the range to the point where the ionization per centimeter of path is σ. Then all rays producing more ions per centimeter than σ will be absorbed within the distance r; and, on a view which considers the rays as the observed entities disappearing according to an exponential law of absorption, the fraction disappearing within the distance r is $(1-e^{-\mu r})$ where μ is the observed absorption coefficient. This is the fraction of the rays which would produce at the point considered more than σ ions per centimeter of path at atmospheric pressure, and so, more than $Lp\sigma$ ions in a distance L at a pressure p. If we assign 54,000 ions as the lower limit of a spurt which is to be considered in the measurements the corresponding value of σ is $\sigma = 54{,}000/Lp$. In a vertical cylinder of length L and cross-sectional area a, the number of spurts greater than 54,000 ions should consequently be, with sufficient approximation, S, where,

$$S = (Na^2/L^2)(1-e^{-\mu r}). \qquad (1)$$

N is here the number of rays per square centimeter per second per unit solid angle at the vertical and is equal to 0.013. The value of r is that corresponding to the above value of σ and must be obtained by extrapolation of the experimental data through the aid of Bethe's formula for energy loss.[2] Thus we find for a case where $L = 15.2$ cm and $p = 10$ atmospheres, the value $r = 2700$ cm. Compton quotes $\mu = 0.08$ per meter of water for proton cosmic rays, so that, with proper adjustments of units, (1) gives, for a cylinder with $L = 15.2$ cm and $a = 45.6$ cm^2, a value $S = 1.2$ spurts per hour greater than 54,000 ions.

At my suggestion, an experiment of the above type, later to be described in detail, has been performed by C. G. and D. D. Montgomery, W. E. Ramsey, and myself. The measured value of S was found to be less than 0.11 spurt per hour. It will suffice to say that alpha-particles were eliminated by observing only coincident spurts in the upper and lower halves of the vessel, and "showers" were detected and eliminated by Geiger-counter devices.

In view of the above considerations it would seem that if protons are to be admitted at all they must function in some such manner as that implied in the writer's theory,[3] through the production of secondary rays which then become the entities actually observed by our counters.

W. F. G. SWANN

Bartol Research Foundation
of the Franklin Institute,
February 20, 1936.

[1] A. H. Compton and H. Bethe, Nature **134**, 734 (1934); also A. H. Compton, Rev. Sci. Inst. **7**, 71 (1936).
[2] H. Bethe, Zeits. f. Physik **76**, 293 (1932); see also P. M. S. Blackett, Proc. Roy. Soc. **A135**, 132 (1932). Extrapolation of the experimental results by aid of the theory is enhanced in validity by the fact that experiments have checked the theory for electrons, for the range of velocity contemplated in the calculations for protons. Ionization per centimeter of path has been obtained from energy loss on the assumption that 30 volts corresponds to one ion.
[3] W. F. G. Swann, Phys. Rev. **48**, 641 (1935).

Proceedings of The New England Section of the American Physical Society

Minutes of the Cambridge Meeting February 1, 1936

THE eighth regular meeting of the New England Section was held in Cambridge, Massachusetts, on Saturday, February first, at Harvard University. The presiding officers for the morning sessions for contributed papers were Professor R. B. Lindsay, Chairman of the Section, and Dr. F. V. Hunt. The presiding officer at the afternoon session was Professor Lindsay. After the morning sessions the Harvard Physics Laboratories were open for inspection. Luncheon was served at the Harvard Faculty Club.

The afternoon session consisted of two invited papers, one on "Radioactivity and Geology" by Professor R. D. Evans of Massachusetts Institute of Technology and the other on "New Measurements at High Pressures" by Professor P. W. Bridgman of Harvard.

At the meeting of the Program Committee it was decided that the next October Meeting would be held at Bowdoin College, probably on the 17th of October.

85 members attended the morning sessions and 140 members the afternoon session.

The program of the Section consisted of 15 papers, the abstracts of which are given below.

PHILIP M. MORSE, *Secretary-Treasurer*
New England Section

Abstracts

1. Thermal Conductivity of Rocks. FRANCIS BIRCH AND HARRY CLARK, *Harvard University.*—Apparatus is described for the routine measurement of thermal conductivities of rocks and other poor conductors at temperatures up to 500°C. Specimens are in the form of small flat circular disks with carefully planned surfaces. Errors due to imperfect contact with metal surfaces are eliminated by extrapolation from measurements made in atmospheres of helium and hydrogen. A guard ring prevents leakage from edges of specimen. Results on several rocks and glasses are presented.

2. The Determination of Frequency Distribution Characteristics with a Photoelectric Integrator. IRVING J. SAXL, *The Waypoyset Manufacturing Company.*—A photoelectric device has been developed with which it is possible to measure automatically the relative times of exposure of a photo-cell put in the path of a moving beam of light. When the photo-cell is illuminated, a relay is activated which closes contacts for an electrical stopwatch. Accordingly this clock runs only when the beam of light is projected upon the photoelectric cell. By adjusting the position of this cell upon a graduated upright or within a predetermined area, it is possible to read on the stopwatch directly the time during which the photo-cell was exposed to illumination at a given location. Frequency distribution curves obtained in this manner were analyzed and have been found valuable in the analysis of filamentous materials such as textile yarns and metal wires.

3. Magnetic Field Control by Circular Coils. L. W. MCKEEHAN, *Yale University.*—The general expressions for the magnetic field due to any combination of circular current loops having a common axis and a plane of symmetry (or a center of inversion) can be expressed, as is well known, in a series of zonal harmonics. Particular arrangements with from one to eight such loops have been proposed for producing a relatively large region of uniform magnetic field. These are critically compared and the errors arising from the finite cross section of actual current coils are analyzed. Arrangements of two and of four loops for producing relatively large regions of uniform field gradient are similarly treated.

4. Low Pressure Arc Characteristics. J. D. COBINE, *Harvard University.*—The results of an oscillographic study of the short a.c. arc between pure graphite electrodes show that the reignition potential is a linear function of the gas pressure for air, nitrogen, oxygen, and carbon dioxide. The relation is expressed by $V_r = A + Bp$. The constant A follows the minimum sparking potential of the gas, increases with the rate of rise of the impressed voltage, and is independent of the arc current, except for carbon dioxide. The constant B depends on the gas, arc current, and rate of rise of impressed voltage. The reignition potential is closely related to the glow discharge and is shown to approach the sparking potential of the gas as the r.m.s. value of the current approaches zero. The factors that affect reignition are indicated, and a reasonable mechanism of the phenomenon is stated.

5. Metal-Rare Gas Spectra. W. M. PRESTON, *Harvard University.*—A study has been made of the metal-rare gas spectra of the type investigated by Oldenberg,[1] which occur in the neighborhood of the line Hg 2536.5 in the presence of a rare gas. In particular, it was desired to ascertain whether similar bands appear with comparable intensity by all metal lines, in a discharge through a metal vapor with a moderate pressure of a rare gas added. Bands of various shape and extent were indeed found by many strong lines of Hg, Cd, and Tl with A or He added; their intensity relative to the lines which they accompany was always of the same order of magnitude. There is no evidence that similar bands do not occur by *all* lines, but because they are relatively very faint, they are difficult to demonstrate experimentally unless they extend some distance from the associated line. These spectra originate in the emission from excited metal atoms perturbed by the very close approach of a colliding normal rare gas atom; their shape and location is determined by the relative positions of the potential curves representing the interaction between metal atoms and rare gas atoms; their low relative intensity indicates that collision induced emission[2] is not an important factor.

[1] Oldenberg, Zeits. f. Physik **47**, 184 (1928); **55**, 1 (1929); and Phys. Rev. **41**, 72 (1932).
[2] W. M. Preston, Phys. Rev. **49**, 140 (1936).

6. On the Kinetics of Hydroxyl Radicals. A. A. FROST AND O. OLDENBERG, *Harvard University.*—In order to analyze elementary processes in rapid gas reactions, the concentration of OH radicals is traced by the intensity of their absorption spectrum photographed in the second order of a 21-foot grating by snapshots. While after interrupting an electric discharge through H_2O vapor the OH radicals persist over as long a time interval as 0.4 sec., they disappear in the discharge through new H_2O_2 at a very much higher rate. In the same experiment, the large intensity of the emission spectrum indicates that they are formed probably even at a higher rate than in water vapor. This result suggests a bimolecular reaction of OH with H_2O_2. The abnormal rotation observed in the emission spectrum of OH, is even stronger in new H_2O_2 than in H_2O indicating that OH radicals are produced with energy exceeding the thermal value. Since no other gases are present, providing for rapid dissipation of this energy, the reaction $OH+H_2O_2$ might be favored by this energy over the rate observed when all degrees of freedom are at room temperature. The rapid decomposition of H_2O_2 by effect of an electric discharge is probably explained by decomposition into $OH+OH$ [1] and the subsequent reaction between OH and H_2O_2.

[1] Urey, Dawsey and Rice, J. Am. Chem. Soc. **55**, 62 (1933).

7. Biological Effects of Slow Electrons. F. S. COOPER AND S. H. HUTNER, *Massachusetts Institute of Technology.*—Experiments are in progress to determine the gross biological effects following electron bombardment and the probability of a particular effect as a function of electron energy and of total dosage. Such data should help to clarify the mechanism of gene mutations and to make possible a more direct attack on the x-ray dosage problem than can be made by the use of x-rays themselves. Present plans are to use electron energies from 10 to 7500 volts and the spores of *Penicillium* sp. and *Aspergillus niger* as target material. These spores withstand evacuation to about 10^{-5} mm for one hour without noticeable effect although twenty-four-hour evacuation leads to retarded germination and 90–95 percent killing. Preliminary work with *Neurospora* spores showed almost complete killing following rapid evacuation to 10^{-3} mm. However, gradual evacuation for thirty minutes, retention at 10^{-5} mm for sixty minutes, and a slow return to atmospheric pressure lasting thirty minutes was followed by only 50–60 percent killing. Spores of *Nephrolepis*, *Polypodium*, and *Scolopendrium* behaved quite differently, showing 90–100 percent germination after rapid evacuation to 10^{-3} mm for several hours, but almost complete killing following even slow evacuation to 10^{-6} mm for forty-five minutes. Preliminary rayings indicate that heat radiation from the filament may also be a troublesome factor.

8. A Method of Determining the Ranges of Charged Corpuscles. GLADYS A. ANSLOW, *Smith College.*—When a charged particle is scattered by atomic or molecular collisions, the mean thickness of the absorbing layer of matter, its effective range, is considerably less than the length of path traversed, its actual range. A statistical relation between the mean values of the two quantities may be obtained by equating the components of the effective range, R_e, and of the actual range, R, in the initial direction of the charged corpuscle. Expressions for scattering may be obtained from Bethe's theory, in which K was used to indicate the initial wave number of the electron, and q the change in this number due to a collision. By using a mean value of the q's for all n collisions, the equation desired is

$$R_e\left(1-\frac{q^2}{2K^2}\right)=R-\frac{q^2}{2K^2}\sum_{r=1}^{n-1}r-\frac{q^4}{4K^4}\sum_{r=1}^{n-1}\frac{r(r-1)}{2}.$$

By using the mean value of $q^2/2K^2$ as $-E_{n1}/2T$, where T is the initial energy of the electron and $-E_{n1}$ is its most probable ionization energy, values of the actual ranges have been calculated from determinations of the effective ranges of low energy electrons in nitrogen, and agree well with values calculated from an equation for the range obtained by integration of the Bethe equation for the rate of loss of energy of electrons as they pass through matter.

9. Electron Temperatures and Mobilities. HARRIET W. ALLEN, *Massachusetts Institute of Technology.*—If the free electrons in a gas discharge are assumed to have a Maxwell distribution, the computed temperatures and mobilities are widely different from the experimental values. Starting with the distribution derived by Morse, Allis, and Lamar, "temperatures" and mobilities have been calculated for electrons in rare gases and for small values of E/p, and good agreement with experiment found. The difference between "temperatures" measured by the Townsend method and by the Langmuir probe method are due to the concept of temperature being invalid for a non-Maxwellian distribution. In the case of argon, it is found necessary to take fully into account the variation of the cross section with electronic energy.

10. Nuclear Potential Fields. J. B. FISK, WM. SHOCKLEY, L. I. SCHIFF AND PHILIP M. MORSE, *Massachusetts Institute of Technology.*—Assumption that the neutron-proton interaction potential has the form

$$V_{\sigma\tau} = D_0(e^{-4r/r_0} - 2e^{-2r/r_0})P_{\sigma\tau},$$

where P is the Majorana operator, allows the H^2 problem to be solved exactly. If one assumes a trial wave function for H^3 of the form

$$\exp[-\mu(r_{12}+r_{13})-\mu\sigma r_{23}],$$

where particle 1 is the proton, the energy variation can be carried out. Tests on the H^2 problem seem to show that the resulting energy should be at least 75 percent of the correct energy. Using only neutron-proton interaction, the computed binding energy of H^3 turned out only a little greater than 50 percent of the experimental value, for reasonable values of r_0. Assuming a neutron-neutron interaction similar to $V_{\sigma\tau}$, only omitting $P_{\sigma\tau}$ and using a new depth, D_1; and a proton-proton interaction equal to the neutron-neutron function plus the Coulomb term; gave satisfactory results. The values $D_0 \leq 200mc^2$, $D_1 \leq 50mc^2$, $r_0 \leq 1.5\times10^{-13}$ give binding energies for H^2, H^3 and He^3 which check the experimental data within the probable error. The scattering cross section for fast neutrons or protons checks experiment, but further refinements must be added to $V_{\sigma\tau}$ in order to check the slow neutron cross section.

11. Voltage Sources and Amplifiers for Geiger-Müller Tube Counters. N. S. GINGRICH, *Massachusetts Institute of Technology.*—Voltage for Geiger counters is commonly supplied by some form of a.c. operated rectifier-filter-stabilizer circuit. The most common of these use a 45-v battery for constant bias of one of the stabilizing tube elements. In the present work, complete a.c. operation is obtained through use of a neon lamp in place of the single battery in Evans' [1] pentode circuit. Stabilization similar to that in Evans' circuit is obtained and the neon lamp modification is more flexible. In addition to this circuit, a very simple, inexpensive circuit, using a bank of neon lamps in series with a ballast resistance, has operated successfully for some time. A new amplifier circuit is described in which the tube counter-pulse is impressed upon the grid of a 57 tube, whose plate pulse trips a small neon lamp which acts as a thyratron, passing current for a short time to the grid system of a 46 tube. The time constant of the 46 grid system determines the length of the 46 plate pulse, which can be made sufficiently long to operate a Western Electric Message Register. In addition to this circuit, description will be given of the use of a strobotron tube, which was developed by Germeshausen and Edgerton for use in their "Strobotak." The tube counter pulse will operate this tube directly, though more positive action is achieved by using a single stage of amplification before it.

[1] R. D. Evans, Rev. Sci. Inst. **5**, 371 (1934).

12. Radioactivity in Rocks. WM. D. URRY, *Massachusetts Institute of Technology.*—(*Introduced by R. D. Evans.*) The presence of minute traces of radioactivity in nearly all common rocks affords a means to the physicist of converting the qualitative geological study of the history of the Earth into a time function based on an actual physical unit, e.g., the year. The theoretical assumptions of a constant disintegration rate and stability of the end-products of the radioactive series under all possible terrestrial conditions are well proven. On the basis of present available data the time function is a self-consistent record and the correctness of the absolute magnitude supported by semi-independent evidence.

13. The Rotation-Vibration Energy Levels of Asymmetric Top Molecules. E. BRIGHT WILSON, JR. AND J. B. HOWARD, *Harvard University.*—The usual method of treating the rotational fine structure of the rotation-vibration bands of asymmetric polyatomic molecules has not previously been justified rigorously. In this paper such a justification is given. The classical kinetic energy and the corresponding quantum-mechanical Hamiltonian operator are obtained for a molecule considered as a system of point atoms. A perturbation method is used to obtain approximations to the energy levels of this Hamiltonian more accurate than the usual rigid rotator approximation. It is found that when centrifugal stretching effects are neglected and when no near-by vibrational state perturbs the level in question, the Wang secular equation for the rigid asymmetric top gives the correct energy levels if three "effective moments of inertia" are used. These three quantities, however, are not in general merely moments of inertia averaged over the vibrational motion but are somewhat more complicated quantities.

14. Radioactivity and Geology. R. D. EVANS, *Massachusetts Institute of Technology.*

15. New Measurements at High Pressures. P. W. BRIDGMAN, *Harvard University.*